axioms

MDPI

Article

Geometric and Topological Analysis of Financial Market Structure: Evidence from Turkish Markets and the 2022–2023 Structural Break

Larissa Margareta Batrancea [1], Mehmet Ali Balcı [2], Ömer Akgüller [2,*] and Lucian Gaban [3,*]

[1] Department of Business, Babeş-Bolyai University, 7 Horea Street, 400174 Cluj-Napoca, Romania; larissa.batrancea@ubbcluj.ro
[2] Department of Mathematics, Faculty of Science, Mugla Sitki Kocman University, Muğla 48000, Turkey; mehmetalibalci@mu.edu.tr
[3] Faculty of Economics, "1 Decembrie 1918" University of Alba Iulia, 510009 Alba Iulia, Romania
* Correspondence: oakguller@mu.edu.tr (Ö.A.); lucian.gaban@uab.ro (L.G.)

Abstract

The financial market correlation structure exhibits dynamic evolution with implications for systemic risk and diversification benefits; yet, conventional approaches using correlation magnitude monitoring may miss fundamental organizational changes. This study develops an integrated geometric–topological framework synthesizing Riemannian manifold geometry with discrete network topology to characterize market structure transformations, applying the methodology to Turkish financial markets spanning May 2015–May 2025. The analysis employs intrinsic dimensionality estimation, curvature tensor computation, and Forman–Ricci curvature calculation alongside correlation network topology measures across seventeen variables, including sectoral equity indices and macroeconomic indicators. The results document an extraordinary mid-2022 structural break featuring dimensional collapse from 2.4 to 0.43 dimensions, network density surge to 0.97, and Ricci curvature spike to 16.0, establishing a persistent hypersynchronized regime evident through 2024–2025 with density elevated by 44% and the Ricci curvature being amplified 258% above the baseline. A comparative crisis analysis reveals heterogeneous structural signatures distinguishing COVID-19 geometric vulnerability from currency crisis modular reorganization. Macro-financial linkages identify credit growth as primary structural driver, achieving $r = 0.504$ correlation with geometric resilience. The findings demonstrate that markets undergo permanent structural transformations responding systematically to monetary–credit conditions, with implications for surveillance frameworks, stress testing design, and macroprudential policy.

Keywords: financial networks; Riemannian geometry; market microstructure; systemic risk; structural breaks

MSC: 53C23; 55N31; 91G45

Check for updates

Academic Editors: Xu Liu and Feipeng Zhang

Received: 11 November 2025
Revised: 25 December 2025
Accepted: 28 December 2025
Published: 1 January 2026

Copyright: © 2026 by the authors. Licensee MDPI, Basel, Switzerland. This article is an open access article distributed under the terms and conditions of the Creative Commons Attribution (CC BY) license.

1. Introduction

The intricate dynamics of financial markets in emerging economies are profoundly shaped by recurrent macroeconomic instabilities, policy shifts, and external shocks, often leading to abrupt reorganizations in asset co-movements and systemic interdependencies. Turkey, as a prototypical emerging market, has experienced a series of profound episodes

including the 2018 currency crisis, the 2020 COVID-19 pandemic, and the unconventional monetary policy regime of 2021–2022, followed by orthodox normalization in 2023, that have repeatedly tested the resilience of its financial system [1–3]. These events highlight the limitations of conventional econometric tools, such as vector autoregressions or simple correlation matrices, which typically capture linear dependencies but overlook the higher-order geometric configurations and topological connectivity that govern collective market behavior during transitions between regimes.

Recent advances in econophysics have introduced powerful geometric and topological frameworks that treat multivariate financial time series as point clouds embedded in high-dimensional manifolds or as evolving complex networks. Topological data analysis through persistent homology has proven effective in detecting latent structural shifts and identifying early-warning signals of financial crises [4,5]. Complementarily, manifold learning techniques combined with local principal component analysis enable estimation of intrinsic dimensionality and curvature invariants, revealing how markets collapse onto low-dimensional attractors during stress episodes [6,7]. Discrete curvature measures, particularly Forman–Ricci curvature applied to correlation graphs, have further illuminated network fragility by distinguishing redundant connectivity from bottleneck structures prone to contagion [8,9]. Applications in emerging markets have documented modular reorganizations and curvature anomalies during volatility spikes [10,11], while studies of Turkish markets specifically have employed Forman–Ricci curvature to map dynamic interdependencies among sectoral indices [12].

Despite these advances, critical gaps persist. Most studies adopt either purely geometric or topological perspectives, rarely integrating Riemannian manifold invariants with discrete graph curvatures in a unified multiscale framework. Long-horizon analyses spanning multiple regimes that are essential for distinguishing transient perturbations from permanent structural breaks remain scarce, particularly in emerging contexts where policy endogeneity complicates causal inference. Furthermore, comprehensive geometric–topological investigations of macro-financial linkages across sectoral and macroeconomic variables over extended periods are notably absent from the literature on the Turkish market.

This paper addresses these gaps through four principal contributions. First, we develop an integrated multiscale geometric–topological methodology that synthesizes Riemannian manifold geometry including Gaussian and mean curvature computation, intrinsic dimensionality estimation, and tangent space analysis with discrete network topology incorporating Forman–Ricci curvature and centrality measures, providing complementary perspectives on correlation structure evolution. Second, we document and characterize an unprecedented mid-2022 structural break in Turkish financial markets featuring the following events: intrinsic dimensionality collapse from 2.4 to 0.43 dimensions; network hyperdensification to 97% connectivity; Forman–Ricci curvature amplification to maximum values of 16.0 (with this elevation proving persistent rather than transient as the 2024 post-transition period exhibits network density elevated 44% above baseline); Ricci curvature amplified to 258%; dimensionality remaining 24% suppressed. Third, we demonstrate crisis heterogeneity through a comparative analysis, revealing that COVID-19 produced unique geometric vulnerability via Ricci curvature suppression; moreover, the 2021–2022 currency crisis exhibited modular reorganization with elevated local clustering but reduced global density, while the 2022–2023 transition constituted permanent hypersynchronization. These observations establish that different stress types produce qualitatively distinct structural signatures requiring crisis-specific monitoring approaches. Fourth, we identify monetary–credit policy variables as primary structural drivers, with credit growth achieving correlation of 0.504 with geometric resilience and explaining approximately 25% of variance in network topology; this substantially exceeds the explanatory power of

exchange rates, inflation, or commodity prices. Meanwhile, a centrality analysis establishes banking, inflation, and sovereign credit default swap spreads as the most systemically important variables based on combined degree, betweenness, and closeness centrality.

Our analysis employs daily observations spanning 30 May 2015–1 May 2025, encompassing 3617 observations across seventeen variables including ten Borsa Istanbul sectoral equity indices and seven macroeconomic indicators, with rolling window methodology generating 178 temporal segments enabling characterization of both stable baseline regimes and acute crisis periods.

The remainder of this paper is organized as follows. Section 2 provides a comprehensive review of the existing literature on geometric and topological methods in financial markets, applications to emerging economies, and positions our study relative to prior research. Section 3 details the dataset, which covers Turkish financial markets from 2015 to 2025, and elaborates on the multiscale geometric–topological methodology used in this study. This includes the frameworks for computing manifold properties such as Gaussian and mean curvature, intrinsic dimensionality, and the construction of correlation networks with their associated Forman–Ricci curvature. Section 4 presents the core empirical findings, meticulously tracking the temporal evolution of these geometric and network measures, with a specific focus on the unprecedented structural break observed in mid-2022. This section also analyzes sectoral centrality, macro-financial linkages, and provides a comparative analysis of market structure across different crisis regimes. Section 5 discusses the broader implications of these results, interpreting the 2022–2023 transition, the heterogeneous signatures of different crises, and the policy relevance for systemic risk, while also addressing the study's limitations. Finally, Section 6 concludes with a summary of the key contributions.

2. Literature Review

The application of advanced mathematical frameworks to financial market analysis has evolved substantially over the past decade, with geometric and topological methods emerging as powerful complements to traditional econometric approaches. This section synthesizes recent developments across topological data analysis, Riemannian geometry, network curvature measures, and their specific applications to emerging market contexts, positioning our study relative to existing research and articulating the contributions made.

2.1. Topological Data Analysis and Persistent Homology in Financial Markets

Topological data analysis has demonstrated remarkable effectiveness in detecting latent structural shifts and identifying early-warning signals of financial crises through persistent homology, a technique that captures multiscale topological features of data across varying resolutions. The foundational work in Gidea and Katz [4] established that L^p-norms of persistence landscapes exhibit strong growth approximately 250 trading days before major market crashes, providing actionable early-warning signals for the 2000 technology bubble and the 2007–2009 financial crisis. This seminal contribution demonstrated that topological features capture market instability dynamics invisible to conventional volatility or correlation magnitude monitoring, as persistence diagrams quantify the births and deaths of topological structures, including connected components, loops, and voids in the point cloud representation of financial time series.

Recent extensions have validated and refined these methodologies across diverse market contexts. The authors of Ismail et al. [13] combined L^1-norm time series of persistence landscapes with critical slowing down indicators including autocorrelation, variance, and mean power spectrum at low frequencies, achieving 46.15% predictive success across correlation tests in US, Singapore, and Malaysian markets. The robustness was validated

through significance, structural break, and sensitivity analyses, establishing persistent homology as a reliable crisis detection framework. The authors of Akingbade et al. [14] provided crucial theoretical justification by linking topological data analysis to the Log-Periodic Power Law Singularity model; they demonstrated that, when LPPLS conditions hold, persistent homology generates consistent early-warning signals, thereby establishing a theoretical bridge explaining why topological methods succeed in bubble detection.

Methodological innovations have expanded the practical applicability of TDA frameworks. The authors of Yen et al. [9] demonstrated that Betti numbers measuring the number of connected components, loops, and voids, along with Euler characteristics and persistent entropy, exhibit consistent crash signatures in Singapore and Taiwan equity markets, with homology groups becoming systematically less persistent during market crashes. The authors of Baitinger and Flegel [15] developed a persistent homology-based turbulence index that outperforms the VIX volatility index in forecasting adverse market regimes across multiple asset classes. The authors of de Jesus Jr. et al. [16] integrated TDA-derived features into neural forecasting models, achieving superior performance across 32 datasets for mean absolute percentage error, mean absolute error, and root mean square error metrics, establishing that topological features enhance predictive accuracy when combined with contemporary machine learning architectures.

The continental-scale analysis by Rai et al. [10] represents the most comprehensive empirical validation, examining multiple Asian markets and establishing that extreme events coincide with L^1 and L^2 norms, exceeding the $\mu + 4\sigma$ thresholds during the 2008 financial crisis and COVID-19 pandemic. This work demonstrates the robustness of topological signatures across heterogeneous market structures and crisis types, validating persistent homology as a universal early-warning framework rather than it being a methodology specific to particular markets or episodes.

2.2. Riemannian Geometry and Manifold Learning Approaches

Information geometry and manifold learning techniques offer complementary perspectives by characterizing the intrinsic geometric structure of financial data through differential geometric invariants, treating multivariate time series as trajectories on curved manifolds rather than linear vector spaces. The seminal contribution by Sandhu et al. [17] established that Ollivier–Ricci curvature exhibits negative correlation with network fragility, with financial crashes preceded by system-level curvature changes serving as geometric hallmarks of instability. This foundational work demonstrated that geometric curvature measures capture fundamental properties of correlation structure evolution, with curvature reduction indicating increased vulnerability to cascading failures through bottleneck edges connecting sparsely overlapping network communities.

Recent advances have integrated entropy theory with Riemannian geometry to analyze global stock market complexity. The authors of Shu et al. [18] modeled stock markets as submanifolds on Riemannian manifolds, employing the Laplace–Beltrami operator to analyze risk aggregation and diffusion processes. The research found that emerging markets including Argentina exhibit lower entropy and higher independence in correlation structure, while developed economies (including the United States and United Kingdom) demonstrate higher entropy and complexity, reflecting more intricate interdependencies. This finding suggests that geometric complexity measures capture fundamental differences in market organization between developed and emerging contexts, with implications for diversification strategies and contagion vulnerability.

The application of Fisher information metric as a Riemannian metric on probability distribution manifolds has proven particularly fruitful for financial risk analysis. The authors of Taylor [19] demonstrated that Fisher geodesic distances, which measure the

intrinsic distance between probability distributions accounting for manifold curvature, outperform Kullback–Leibler divergence for risk-based clustering of NASDAQ 100 and S&P 500 stocks. The superiority of information geometric approaches stems from their capacity to capture the natural geometry of statistical manifolds, with Fisher distances respecting the intrinsic structure of probability spaces rather than imposing arbitrary Euclidean geometry.

Manifold learning techniques have demonstrated capacity to extract intrinsic structure from high-dimensional financial time series. The authors of Huang et al. [6] developed information metric-based manifold learning to extract intrinsic manifolds of financial dynamic systems for crisis early warnings, establishing connections between information geometry and dimensionality reduction frameworks. The authors of Xu et al. [20] created a manifold feature index using the Laplace–Beltrami operator eigen problem for Shanghai stock market analysis, demonstrating that manifold-based indicators capture market uncertainty dynamics invisible to conventional measures.

The authors of Khashanah and Yang [21] introduced the evolution index (EI) as a measure of systemic risk using the Fisher information metric applied to financial time series. They were the first to apply the Fisher information metric to a set of financial time series for systemic risk measurements. The authors demonstrated this approach on concrete networks with actual data from several stock markets. These information geometric approaches establish that the intrinsic geometry of financial data contains rich information about market state and stability, justifying geometric frameworks as fundamental rather than merely auxiliary analytical tools.

2.3. Network Curvature Measures and Systemic Risk Assessment

Discrete Ricci curvatures, particularly Forman–Ricci and Ollivier–Ricci formulations adapted from differential geometry to graph structures, have proven highly effective for characterizing financial network fragility and systemic risk transmission. The comprehensive empirical study by Samal et al. [8] compared four discrete curvature measures across 32 years of S&P 500 and Nikkei 225 data, establishing that Forman–Ricci curvature correlates most strongly with traditional market indicators and serves as an excellent indicator for system-level fear and fragility. This finding validates Forman–Ricci curvature as the preferred measure for large-scale financial network analysis, balancing predictive power with computational efficiency.

The foundational methodological work by Sreejith et al. [22] adapted Forman's discretization of Ricci curvature to undirected networks, establishing computational advantages over Ollivier–Ricci curvature that requires optimization procedures for computing optimal transport distances. The authors of Samal et al. [23] validated that Forman–Ricci curvature empirically correlates with Ollivier–Ricci despite being purely combinatorial, defined through degree sequences and neighborhood overlap without reference to metric structures, while requiring significantly faster computation time for large-scale networks. This computational efficiency enables real-time monitoring of evolving correlation networks, a practical advantage over computationally intensive alternatives.

Applications to specific market contexts have demonstrated robustness across diverse settings. The authors of Wang et al. [24] conducted the first systematic application of discrete Ricci curvature to China's stock market using CSI 300 index constituents from 2005 to 2020, developing a hybrid forecasting model combining curvature analysis with machine learning algorithms. The methodology accurately captured systemic stability transitions and identified major market events including the 2015 Chinese stock market crash, validating that network curvature measures generalize beyond Western developed markets to capture instability in emerging Asian contexts.

Recent methodological advances include the introduction of Ricci flow techniques with surgery for handling singularities in dense correlation networks. The authors of Srinivasan [25] developed discrete Ollivier–Ricci graph curvature with Ricci flow and a novel surgery technique for handling neckpinch singularities in NASDAQ 100 correlation graphs, enabling topological structure discovery through hidden hierarchy and community detection in networks exhibiting near-complete connectivity. This advancement addresses a critical limitation wherein traditional community detection algorithms fail in dense networks, providing tools for analyzing hypersynchronized market states.

The integration of discrete Ricci curvatures with topological data analysis represents a promising frontier. The authors of Kulkarni et al. [11] combined network curvature measures with persistent homology for Indian stock market analysis, demonstrating that persistent entropy proves more robust than L^2-norm persistence landscapes as a stability indicator, and that TDA captures higher-order interactions while eliminating noisy correlations more effectively than network-only approaches. This integrated framework exemplifies the complementary nature of geometric and topological perspectives, with curvature capturing local network properties while persistent homology characterizes the global topological structure.

2.4. Applications to Emerging Asian Markets

Research on Asian financial markets has revealed both shared characteristics with developed markets and unique structural features reflecting regional economic integration patterns and institutional differences. The authors of Guo et al. [26] applied topological data analysis with persistence landscapes to 100 Chinese stocks over 17 years spanning 2005 to 2022, successfully detecting critical dates corresponding to the 2008 financial crisis, the 2015 stock market crash, the China–US trade war, and the COVID-19 pandemic. The methodology revealed heterogeneous impacts of different events across industry sectors, with the technology and finance sectors exhibiting distinct topological signatures during trade tensions, while industrial sectors showed stronger responses to global financial shocks.

For Indian markets, Kulkarni et al. [11] performed comparative analysis of geometry-inspired measures and TDA methods on National Stock Exchange and Bombay Stock Exchange constituents, establishing that network analysis exhibits high sensitivity to threshold construction methodology while persistent homology provides more robust results across different threshold specifications. The authors of Bhattacharjee and Maiti [27] examined BSE 500 stocks using disparity filtering and minimum spanning tree analysis, revealing high sector-specific dominance in healthcare and technology sectors, with fast-moving consumer goods and healthcare demonstrating elevated eigenvector centrality indicating structural importance in correlation networks.

Southeast Asian market integration patterns have been characterized through network topological analysis. The authors of Wu [28] employed minimum spanning tree analysis on ASEAN5 plus four markets, finding that Singapore serves as the gatekeeper for Asian markets, with interconnectedness falling substantially after filtering global influences. The authors of Huang et al. [29] demonstrated that, during the 2008 financial crisis and 2015 Chinese stock market turbulence, the average network degree and giant component size increased significantly, indicating crisis-induced integration amplification consistent with contagion theories.

Cross-country wavelet coherence analysis by Younis et al. [30] using MSCI indices for China, India, Pakistan, Malaysia, Singapore, and Indonesia found that co-movement patterns intensify during crisis periods, with China showing high correlation with other Asian emerging markets in both high-frequency and low-frequency spectra. This finding suggests that Chinese market dynamics increasingly drive regional correlation structure,

reflecting China's growing economic dominance in Asia. The authors of Das et al. [31] found that, across emerging market regions, non-financial firms show higher systemic risk exposure than banks in network-based risk measures, with network connectedness increasing with corporate leverage, challenging conventional wisdom that banks dominate systemic risk in all contexts.

2.5. Turkish Financial Market Studies

Research on Turkish financial markets represents methodologically advanced applications of geometric–topological methods to emerging market analysis, with particular focus on sectoral dynamics and crisis transmission mechanisms. The authors of Işlak and Temoçin [32] analyzed BIST 100 network dynamics for crisis precursors using both correlation-based and causality-based network constructions, identifying network characteristics measuring uniformity among nodes as potential early-warning indicators. The comparative analysis of correlation versus causality networks revealed that Granger causality networks capture directional information flow absent from symmetric correlation networks, with centrality measures in causal networks identifying systemically important stocks whose distress predicts broader market deterioration.

Crisis-period analyses have documented substantial network reorganization during stress episodes. The authors of Şükrüoğlu [33] showed that COVID-19 effects multiplied BIST 100 interconnectedness by factors of three in Granger causality networks and eight in contemporaneous correlation networks, representing dramatic integration amplification far exceeding the typical developed market responses. The authors of Derindere Köseoğlu [34] identified private banks including Garanti, Akbank, İş Bank, and Yapı ve Kredi as major systemic risk sources using Component Expected Shortfall and quantile spillover analysis, establishing that Turkish banking sector concentration produces systemic vulnerability through dominant institution failures.

Methodological contributions from Turkish market studies include Kuzubaş et al. [35] validation of network centrality measures for detecting systemically important financial institutions during the 2000 Turkish financial crisis, confirming Demirbank's central role consistent with ex-post regulatory assessments. The authors of Hadi et al. [36] documented significant anti-phase movements between the Turkish lira and Turkish equity indices during currency crises using wavelet coherence, establishing that currency depreciation episodes produce negative correlation regimes wherein traditional diversification across domestic asset classes fails.

2.6. Research Gaps and Study Positioning

Despite substantial progress across topological data analysis, Riemannian geometry, and network curvature applications to financial markets, several critical gaps persist that this study addresses. First, most existing studies adopt either purely geometric perspectives focusing on manifold invariants or purely topological approaches emphasizing persistent homology and network structure, rarely integrating Riemannian manifold curvatures with discrete graph curvatures in a unified multiscale framework. The complementary information content of continuous geometric measures like Gaussian and mean curvature versus discrete topological measures like Forman–Ricci curvature remains underexplored, with few studies systematically comparing or combining these approaches to leverage their respective strengths.

Second, long-horizon analyses spanning multiple distinct market regimes that are essential for distinguishing transient perturbations from permanent structural breaks remain scarce, particularly in emerging market contexts where policy endogeneity and frequent macroeconomic instability complicate causal inference. Existing TDA and network

studies typically focus on single crisis episodes or short windows, limiting capacity to characterize baseline structural properties, assess regime persistence, or differentiate crisis-specific signatures. The decade-long observation periods necessary to observe multiple complete cycles of crisis, recovery, and renewed stability have rarely been examined with geometric–topological methods in emerging markets.

Third, comprehensive investigations of macro-financial linkages connecting geometric–topological structural measures to specific macroeconomic drivers including monetary policy variables, credit conditions, exchange rate dynamics, and external shocks remain notably absent from the literature, particularly for Turkish markets, while studies document structural changes coinciding with crises, systematic quantification of which macroeconomic factors drive geometric reorganization, the magnitude and timing of structural responses to policy interventions, and the relative importance of domestic versus external drivers remains underdeveloped. Understanding these linkages proves essential for translating geometric–topological findings into actionable policy frameworks.

Fourth, the Turkish financial market literature, while pioneering in certain methodological applications, lacks comprehensive long-horizon geometric–topological analysis integrating sectoral equity indices with macroeconomic indicators across extended periods encompassing multiple crisis episodes and policy regime transitions. Existing studies focus on specific methodologies applied to limited time windows or particular crisis events, without synthesizing geometric manifold properties, discrete network curvature, topological complexity, and macro-financial drivers into an integrated framework characterizing the full structural evolution spanning pre-crisis baselines through post-crisis new equilibria.

This study bridges these gaps by developing an integrated multiscale geometric–topological methodology that synthesizes Riemannian manifold invariants including Gaussian curvature, mean curvature, intrinsic dimensionality, and tangent space smoothness with discrete network topology incorporating Forman–Ricci curvature and comprehensive centrality measures, applied to Turkish financial markets over nearly a decade from May 2015 to May 2025. This extended temporal coverage enables characterization of baseline structural properties during stable periods, identification and differentiation of crisis-specific signatures across COVID-19, currency crisis, and the unprecedented 2022–2023 geometric transition, assessment of structural break persistence versus transience through post-transition observation extending into 2024–2025, and systematic quantification of macro-financial linkages connecting credit growth, monetary policy, and other drivers to geometric network reorganization. The integration of ten Borsa Istanbul sectoral equity indices with seven macroeconomic indicators provides comprehensive coverage of market segments and policy-relevant drivers, while the methodological pluralism leveraging complementary geometric and topological perspectives enables robust structural characterization validated across multiple analytical frameworks.

3. Materials and Methods

3.1. Dataset

The empirical analysis employs daily time series data spanning 30 May 2015–1 May 2025, encompassing 3617 observations across a nearly decade-long period characterized by multiple macroeconomic stress episodes including the COVID-19 pandemic, Turkish currency crises, and significant monetary policy regime transitions. Raw data acquisition was conducted through Investing.com, a comprehensive financial data aggregation platform providing standardized access to equity indices, macroeconomic indicators, and global financial market variables. The extended temporal coverage enables characterization of both stable baseline regimes and acute crisis periods, providing sufficient

variation to identify structural transformations distinguishing transient volatility from permanent reorganizations.

The dataset comprises seventeen variables partitioned into two principal categories reflecting distinct but interconnected aspects of Turkish financial market dynamics. Table 1 presents the complete variable set with symbols, measurement units, observational frequencies, and data sources. The first category encompasses ten sectoral equity indices drawn from the Borsa Istanbul (BIST) classification system: Banking (XBANK), Electricity (XELKT), Holding Companies (XHOLD), Chemical (XKMYA), Finance (XUMAL, non-bank financial institutions), Insurance (XSGRT), Raw Materials (XMANA), Technology (XUTEK), Trade (XTRZM, retail and wholesale), and Transportation (XULAS). Each index aggregates constituent firm equity prices within the respective sector, providing summary measures of sectoral performance and enabling analysis of correlation structure across the economy's major segments.

Table 1. Variable definitions, data sources, and frequency structure. Monthly indicators (*) are forward-filled to daily frequency.

Variable	Symbol	Unit	Frequency	Source
Sectoral Equity Indices (Borsa Istanbul)				
Banking	XBANK	Index points	Daily	BIST
Electricity	XELKT	Index points	Daily	BIST
Holding Companies	XHOLD	Index points	Daily	BIST
Chemical	XKMYA	Index points	Daily	BIST
Finance (non-bank)	XUMAL	Index points	Daily	BIST
Insurance	XSGRT	Index points	Daily	BIST
Raw Materials	XMANA	Index points	Daily	BIST
Technology	XUTEK	Index points	Daily	BIST
Trade (retail/wholesale)	XTRZM	Index points	Daily	BIST
Transportation	XULAS	Index points	Daily	BIST
Macroeconomic and Financial Market Indicators				
CDS Spread	CDS5Y	Basis points	Daily	Bloomberg
Inflation *	CPI_YoY	% year-over-year	Monthly	TURKSTAT
Policy Interest Rate	CBRT_Rate	% per annum	Daily	CBRT
Credit Growth *	Credit_YoY	% year-over-year	Monthly	CBRT
Exchange Rate	USDTRY	TRY per USD	Daily	CBRT
Oil Price	Brent	USD per barrel	Daily	Bloomberg
Volatility Index	VIX	Index points	Daily	CBOE

Note: All data accessed via Investing.com (accessed on 9 November 2025) aggregation platform. Sample period: 30 May 2015–1 May 2025 (3617 daily observations). BIST = Borsa Istanbul; CBRT = Central Bank of the Republic of Turkey; TURKSTAT = Turkish Statistical Institute; CBOE = Chicago Board Options Exchange.

The tripartite financial sector decomposition distinguishes banking (capturing commercial bank equity performance and institutions dominating Turkish financial intermediation) from finance (encompassing non-bank institutions including investment firms and leasing companies) and insurance (tracking property, casualty, and life insurance providers). Real economy sectors span diverse activities with heterogeneous macroeconomic exposures: trade exhibits high sensitivity to domestic consumption and currency fluctuations; transportation depends on both domestic activity and international trade volumes; raw materials demonstrates commodity price sensitivity and export orientation; chemical shows energy price exposure; technology represents knowledge-intensive activities with distinct growth dynamics; electricity includes regulated utilities with stable cash flows; and holding companies serve as proxies for broad market exposure across multiple industries.

The second data category comprises seven macroeconomic and financial market indicators spanning domestic policy levers, external price pressures, inflation outcomes,

sovereign risk perceptions, and international risk sentiment. Turkish sovereign credit default swap (CDS) spreads on five-year debt provide market-based sovereign risk measures. Consumer price Inflation rates capture price level changes affecting real returns and policy responses. Policy interest rates set by the Central Bank of the Republic of Turkey represent the primary monetary policy instrument. Credit growth rates measure year-over-year banking sector loan expansion, capturing financial conditions and credit cycle dynamics. The USD/TRY exchange rate quantifies lira depreciation pressure and balance of payments dynamics. Brent crude oil prices represent energy import costs for Turkey's net importing economy. The CBOE VIX volatility index captures global equity market uncertainty, enabling assessment of international volatility transmission to Turkish markets.

The dataset combines variables observed at heterogeneous frequencies, as detailed in Table 1. Fifteen variables including all sectoral equity indices, CDS spreads, exchange rates, oil prices, VIX, and policy interest rates are available at daily frequency, while consumer price inflation and credit growth rates are reported monthly by TURKSTAT and the Central Bank of the Republic of Turkey, respectively. To generate a coherent multivariate time series suitable for correlation analysis and geometric–topological computation, monthly indicators undergo forward-filling to daily frequency, wherein each month's reported value is replicated across all trading days within that month. Specifically, for the monthly indicator, M_t, observed at the month-end, t, we assign $M_t^{(d)} = M_t$ for all trading days, d, falling within month t. This methodology preserves actual reported values without introducing interpolation artifacts that would generate spurious intra-month variation, and accurately reflects the information set available to market participants at each point in time.

All variables undergo z-score standardization prior to geometric–topological analysis, transforming each time series to zero mean and unit variance via $z_{it} = (x_{it} - \bar{x}_i)/\sigma_i$ where x_{it} denotes the raw observation, $\bar{x}_i$ represents the full-sample mean, and σ_i denotes the full-sample standard deviation. This standardization eliminates scale differences across variables exhibiting intrinsically different units and magnitudes, proving essential for geometric analysis as Euclidean distance computations in manifold embedding and correlation matrix construction require commensurable scales across dimensions. The standardized data matrix $\mathbf{Z} \in \mathbb{R}^{3617\times17}$ serves as input for all subsequent geometric–topological computations including rolling window correlation estimation, UMAP manifold embedding, local PCA tangent space estimation, curvature tensor computation, and correlation network construction.

Data completeness proves exceptional, with zero missing values across the 3617 observation–17 variable matrix, eliminating interpolation or imputation complications that could introduce artifacts in correlation structure estimation. The continuous daily coverage captures major Turkish economic episodes including the 2018 currency crisis, the 2019 post-crisis normalization, the 2020 COVID-19 pandemic disruption, the 2021–2022 unconventional monetary policy period with negative real interest rates, the extraordinary mid-2022 market structure transformation (documented extensively in this study), the subsequent 2023 normalization attempts, and the 2024–2025 post-transition regime establishment. The temporal coverage extends sufficiently far preceding the 2022 structural break to establish robust baseline characterization while extending far enough beyond to assess persistence versus transience of observed transformations.

The variable set's dual structure combining sectoral equity indices with macroeconomic indicators enables integrated analysis of correlations within the equity market and linkages between market structure and economic conditions. The sectoral indices provide the primary data for geometric manifold construction and correlation network analysis, with their co-movements defining the state space geometry and topological connectivity patterns investigated throughout this study. The macroeconomic indicators serve dual

roles: first as additional correlation network nodes enabling assessment of macro-financial linkages and variable centrality, and second as explanatory variables in analyses examining relationships between geometric network properties and economic conditions. The Investing.com platform provides standardized formatting and vendor-consistent calculation methodologies across the variable set, utilizing official exchange data for BIST indices, central bank sources for policy rates and credit aggregates, recognized benchmark indices for oil and VIX, and established financial data providers for CDS spreads, ensuring data quality consistent with academic research standards.

3.2. Multiscale Geometric Analysis

This study employs a multiscale geometric framework to characterize the dynamical properties of Turkish financial markets through state space reconstruction, differential geometric analysis, and network topology. The methodology integrates curvature estimation on high-dimensional manifolds with temporal network analysis to reveal structural transitions and systemic dependencies across market regimes.

Let $\mathcal{D} = \{x_1, x_2, \ldots, x_T\}$ denote the multivariate time series comprising T temporal observations across d financial variables, where each observation $x_t \in \mathbb{R}^d$ represents a vector of standardized returns. The dataset encompasses ten sectoral indices from Borsa Istanbul (BIST), specifically the banking, electricity, holding, chemical, finance, insurance, raw materials, technology, trade, and transportation sectors, alongside seven macroeconomic indicators including Brent crude oil prices, credit default swap spreads, inflation rates, interest rates, credit growth, the USD/TRY exchange rate, and the VIX volatility index. All variables undergo Z-score normalization to ensure commensurability across disparate scales, yielding standardized observations $z_t = (x_t - \mu)/\sigma$ where μ and σ denote the empirical mean and standard deviation vectors, respectively.

To capture temporal evolution of geometric properties, we partition the time series into overlapping windows $\mathcal{W}_i = \{z_t : t \in [t_i, t_i + w]\}$, where w denotes the window width and consecutive windows are separated by step size $s < w$. This sliding window approach generates $N_w = \lfloor (T - w)/s \rfloor + 1$ temporal segments, each representing a local snapshot of market geometry. The choice of window size $w = 60$ and step $s = 20$ balances temporal resolution against statistical stability, ensuring sufficient observations for robust geometric estimation while maintaining sensitivity to regime transitions.

For each temporal window $\mathcal{W}_i$, we construct a point cloud $\mathcal{P}_i = \{p_1, p_2, \ldots, p_n\} \subset \mathbb{R}^d$, where $n = |\mathcal{W}_i|$ represents the number of observations within the window. Under the manifold hypothesis, we assume these points lie on or near a lower-dimensional smooth manifold $\mathcal{M} \subset \mathbb{R}^d$ with intrinsic dimension $m < d$. This assumption reflects the notion that high-dimensional financial data exhibits latent structure arising from underlying economic factors.

The local geometry at each point $p_j \in \mathcal{P}_i$ is characterized by examining its k-nearest neighborhood $\mathcal{N}_k(p_j) = \{q_1, \ldots, q_k\}$, where neighbors are identified via Euclidean distance $\|p_j - q_\ell\|_2$. The neighborhood size, k, is adaptively chosen to satisfy $k \geq 2m + 1$ to ensure adequate sampling of the local tangent space, typically setting $k \in [20, 30]$ based on the estimated intrinsic dimensionality. For each neighborhood, we compute the centered point cloud $\tilde{\mathcal{N}}_k = \{q_\ell - \bar{q} : q_\ell \in \mathcal{N}_k\}$, where $\bar{q} = k^{-1} \sum_{\ell=1}^{k} q_\ell$ represents the neighborhood centroid.

The Gaussian curvature, a fundamental invariant characterizing the intrinsic geometry of a manifold, quantifies the degree to which the manifold deviates from flatness. For a two-dimensional surface embedded in three-dimensional space, Gaussian curvature K is defined as the product of principal curvatures κ_1 and κ_2. In higher dimensions, we adopt a generalized measure based on the local covariance structure.

For each point, p_j, we construct the empirical covariance matrix of its centered neighborhood

$$\mathbf{C}_j = \frac{1}{k-1} \sum_{\ell=1}^{k} (q_\ell - \bar{q})(q_\ell - \bar{q})^\top \in \mathbb{R}^{d \times d}. \tag{1}$$

The local covariance structure and eigenvalue spectrum are derived following the point-set surface analysis framework established by Pauly et al. [37].

Performing eigen decomposition yields $\mathbf{C}_j = \mathbf{U}_j \mathbf{\Lambda}_j \mathbf{U}_j^\top$ where $\mathbf{U}_j$ contains orthonormal eigenvectors and $\mathbf{\Lambda}_j = \text{diag}(\lambda_1, \lambda_2, \ldots, \lambda_d)$, with $\lambda_1 \geq \lambda_2 \geq \cdots \geq \lambda_d \geq 0$ representing the spectrum of eigenvalues. These eigenvalues quantify the variance explained along principal directions, with larger eigenvalues corresponding to directions of greatest variation.

We define a logarithmic curvature measure to capture geometric complexity while ensuring numerical stability

$$\kappa_G(p_j) = \log_{10}\left(\frac{\lambda_d}{\lambda_1} + \epsilon\right), \tag{2}$$

where $\epsilon = 10^{-10}$ prevents the numerical underflow. This quantity is consistently negative, with values closer to zero indicating approximately flat local geometry (similar variance across all directions), while increasingly negative values signify high curvature corresponding to manifold regions where data concentrates along fewer dimensions. The window-level Gaussian curvature statistics are computed as $\bar{\kappa}_G = n^{-1} \sum_{j=1}^{n} \kappa_G(p_j)$ and $\sigma_{\kappa_G} = \sqrt{n^{-1} \sum_{j=1}^{n} (\kappa_G(p_j) - \bar{\kappa}_G)^2}$.

We define a logarithmic curvature measure in Equation (2), adapted from the surface variation index [37], to capture geometric complexity while ensuring numerical stability in the context of high-volatility financial data.

Complementing the Gaussian curvature, we estimate mean curvature to characterize the average bending of the manifold. For an m-dimensional manifold embedded in $\mathbb{R}^d$, the mean curvature H represents the trace of the shape operator, corresponding to the arithmetic mean of principal curvatures. We approximate this through variance ratios in the principal component spectrum.

Following the eigen decomposition of $\mathbf{C}_j$, we identify the effective tangent space dimension by retaining components explaining a cumulative variance threshold of 95%. Let m_j denote the number of such components. The mean curvature approximation is then defined as

$$\kappa_H(p_j) = \frac{1}{m_j} \sum_{i=1}^{m_j} \frac{\lambda_i}{\lambda_{\max} + \epsilon}, \tag{3}$$

where $\lambda_{\max} = \max\{\lambda_1, \ldots, \lambda_d\}$. This normalized measure quantifies how variance is distributed among the principal tangent directions, with values approaching unity indicating relatively uniform variance distribution (lower mean curvature) and smaller values suggesting concentrated variance (higher mean curvature). Window-level statistics $\bar{\kappa}_H$ and σ_{κ_H} are computed analogously to the Gaussian curvature case.

Euclidean distances in the ambient space $\mathbb{R}^d$ generally overestimate true distances along the manifold. To obtain more faithful distance measures, we compute geodesic distances approximating shortest paths constrained to the manifold structure. This is achieved through a graph-based approach where the data manifold is approximated by a k-nearest neighbor graph $\mathcal{G} = (\mathcal{V}, \mathcal{E})$, with vertices $\mathcal{V} = \mathcal{P}_i$ and edges $\mathcal{E}$ connecting each point to its k nearest neighbors.

Edge weights are assigned as Euclidean distances $w(p_j, p_\ell) = \|p_j - p_\ell\|_2$ for $(p_j, p_\ell) \in \mathcal{E}$. The geodesic distance between points p_a and p_b is then approximated by the shortest path distance on $\mathcal{G}$

$$d_{\mathcal{M}}(p_a, p_b) \approx \min_{\gamma \in \Gamma(a,b)} \sum_{(p_j, p_\ell) \in \gamma} w(p_j, p_\ell), \tag{4}$$

where $\Gamma(a, b)$ denotes the set of all paths connecting p_a and p_b in $\mathcal{G}$. We employ Dijkstra's algorithm to efficiently compute shortest paths, yielding a geodesic distance matrix $\mathbf{D}_{\text{geo}} \in \mathbb{R}^{n \times n}$ [38].

From this matrix, we extract summary statistics characterizing the manifold's global connectivity: the average geodesic distance $\bar{d}_{\text{geo}} = \frac{2}{n(n-1)} \sum_{a<b} d_{\mathcal{M}}(p_a, p_b)$ and the geodesic diameter $d_{\max} = \max_{a,b} d_{\mathcal{M}}(p_a, p_b)$. Increases in these quantities indicate manifold expansion or regime divergence, while decreases suggest convergence toward concentrated market states.

The intrinsic dimension, m, quantifies the minimum number of parameters required to describe the manifold locally, providing insight into the effective degrees of freedom in the financial system. We employ the maximum likelihood estimator developed by Levina and Bickel [39], which leverages the distribution of distances to nearest neighbors.

For each point, p_j, let $r_{j,1} \leq r_{j,2} \leq \cdots \leq r_{j,k}$ denote the sorted distances to its k nearest neighbors. The local intrinsic dimension estimate is given by

$$\hat{m}_j = \left(\frac{1}{k-1} \sum_{\ell=1}^{k-1} \log \frac{r_{j,k}}{r_{j,\ell}} \right)^{-1}. \tag{5}$$

This estimator is derived from the principle that, near a point on an m-dimensional manifold, the volume of a ball of the radius, r, scales as r^m. The global intrinsic dimensionality for window $\mathcal{W}_i$ is obtained as the median $\tilde{m}_i = \text{median}\{\hat{m}_1, \ldots, \hat{m}_n\}$, which proves robust to outliers and local irregularities. Temporal variations in $\tilde{m}_i$ indicate changes in the effective complexity of market dynamics, with dimension increases suggesting enhanced independent factors and decreases implying increased coordination or constraint.

To assess the regularity of the data manifold, we quantify how smoothly the tangent space varies across the manifold. This is accomplished by examining the consistency of principal directions in local neighborhoods. For a sub-sample of N_s points, drawn uniformly from $\mathcal{P}_i$, we perform principal component analysis on each neighborhood $\mathcal{N}_k(p_j)$ to obtain the first principal component eigenvector $v_j^{(1)} \in \mathbb{R}^d$ with $\|v_j^{(1)}\|_2 = 1$.

The smoothness measure is defined as the average variance explained by the first principal component [40]

$$S_{\text{tangent}} = \frac{1}{N_s} \sum_{j=1}^{N_s} \frac{\lambda_j^{(1)}}{\sum_{\ell=1}^{d} \lambda_j^{(\ell)}}. \tag{6}$$

Values approaching unity indicate that local neighborhoods are well-approximated by linear subspaces with a dominant direction, characteristic of smooth manifolds. Lower values suggest more complex local geometry with variance distributed across multiple directions, potentially indicating turbulent or irregular market regimes. This measure complements curvature by capturing the alignment and stability of tangent spaces.

The volume occupied by the point cloud in state space provides a measure of market dispersion and diversity. We estimate this through the generalized variance, defined as the determinant of the covariance matrix. For the entire window point cloud, $\mathcal{P}_i$, we compute

$$\mathbf{\Sigma}_i = \frac{1}{n-1} \sum_{j=1}^{n} (p_j - \bar{p})(p_j - \bar{p})^\top, \tag{7}$$

where $\bar{p} = n^{-1} \sum_{j=1}^{n} p_j$ is the centroid. The volume measure is then

$$V_i = \sqrt{\det(\mathbf{\Sigma}_i)}. \tag{8}$$

This quantity scales with the geometric mean of the principal axis lengths of the hyperellipsoid characterizing the data distribution. Larger volumes indicate greater market dispersion with diverse sectoral behaviors, while volume contraction suggests convergent dynamics or synchronized movements. The square root transformation ensures the measure scales appropriately with dimension.

To study interdependencies among financial variables, we construct temporal correlation networks for each window $\mathcal{W}_i$. The Pearson correlation coefficient between variables X_a and X_b within window i is computed as

$$\rho_{ab}^{(i)} = \frac{\sum_{t \in \mathcal{W}_i} (x_{at} - \bar{x}_a)(x_{bt} - \bar{x}_b)}{\sqrt{\sum_{t \in \mathcal{W}_i} (x_{at} - \bar{x}_a)^2} \sqrt{\sum_{t \in \mathcal{W}_i} (x_{bt} - \bar{x}_b)^2}} \tag{9}$$

yielding a correlation matrix: $\mathbf{R}^{(i)} \in [-1, 1]^{d \times d}$. We construct an undirected weighted network $\mathcal{G}_i = (\mathcal{V}, \mathcal{E}_i, W_i)$ where vertices $\mathcal{V}$ represent the d financial variables, edges $(a, b) \in \mathcal{E}_i$ exist if $|\rho_{ab}^{(i)}| \geq \theta$ for a threshold $\theta \in (0, 1)$, and edge weights are given by $w_{ab} = |\rho_{ab}^{(i)}|$. The threshold $\theta = 0.5$ filters weak correlations while retaining significant relationships. Importantly, self-loops are explicitly excluded by construction, ensuring $\mathcal{E}_i \cap \{(a, a) : a \in \mathcal{V}\} = \emptyset$.

The topological structure of $\mathcal{G}_i$ is characterized through several graph-theoretic measures [41]. Network density, defined as

$$\delta_i = \frac{2|\mathcal{E}_i|}{d(d-1)} \tag{10}$$

quantifies the proportion of potential edges realized in the network, with $\delta_i = 1$ indicating complete connectivity and $\delta_i \to 0$ suggesting sparse interactions.

Node importance is assessed via multiple centrality measures. Degree centrality for node v is given by $C_D(v) = \deg(v)/(d-1)$ where $\deg(v) = |\{u : (v, u) \in \mathcal{E}_i\}|$ counts adjacent nodes. Betweenness centrality quantifies the extent to which a node lies on shortest paths between other nodes

$$C_B(v) = \sum_{s \neq v s. \neq t} \frac{\sigma_{st}(v)}{\sigma_{st}}, \tag{11}$$

where σ_{st} denotes the number of shortest paths from s to t, and $\sigma_{st}(v)$ counts those passing through v. High betweenness identifies nodes serving as critical information conduits or structural bridges. Closeness centrality measures the average distance from a node to all others

$$C_C(v) = \frac{d-1}{\sum_{u \neq v} d_{\mathcal{G}}(v, u)}, \tag{12}$$

where $d_{\mathcal{G}}(v, u)$ represents the shortest path distance in the network.

The clustering coefficient quantifies local interconnectedness. For node v with degree $\deg(v) = k_v$, it is defined as

$$c(v) = \frac{2|\{(u, w) \in \mathcal{E}_i : u, w \in \mathcal{N}(v)\}|}{k_v(k_v - 1)}, \tag{13}$$

where $\mathcal{N}(v)$ denotes the neighborhood of v. The network-averaged clustering coefficient $\bar{c}_i = d^{-1} \sum_{v \in \mathcal{V}} c(v)$ indicates the prevalence of triangular motifs and local cohesion.

We compute the Forman–Ricci curvature to characterize the discrete geometric properties of correlation networks. For an edge $(v, w) \in \mathcal{E}_i$, the Forman–Ricci curvature is defined as

$$\mathcal{F}(v, w) = 4 - \deg(v) - \deg(w) + 3|\mathcal{N}(v) \cap \mathcal{N}(w)|. \tag{14}$$

This discrete curvature measure generalizes Ricci curvature from differential geometry to graph structures [23,42]. Positive curvature indicates that the neighborhoods of adjacent nodes have substantial overlap, suggesting redundant connectivity and network robustness. Negative curvature corresponds to bottleneck edges connecting sparsely overlapping communities, potentially representing vulnerability points or intermodular bridges. The network-averaged Forman–Ricci curvature

$$\bar{\mathcal{F}}_i = \frac{1}{|\mathcal{E}_i|} \sum_{(v,w)\in\mathcal{E}_i} \mathcal{F}(v, w) \tag{15}$$

provides a global geometric descriptor of network resilience. Temporal evolution of $\bar{\mathcal{F}}_i$ reveals structural transitions, with decreasing curvature often preceding network fragmentation or systemic stress.

The geometric and network measures are integrated into a unified temporal framework. For each window $\mathcal{W}_i$, we construct a feature vector

$$\phi_i = (\bar{\kappa}_G, \sigma_{\kappa_G}, \bar{\kappa}_H, \sigma_{\kappa_H}, \bar{d}_{\text{geo}}, d_{\max}, \bar{m}_i, S_{\text{tangent}}, V_i, \delta_i, \bar{c}_i, \bar{\mathcal{F}}_i)^\top. \tag{16}$$

This comprehensive representation captures both intrinsic manifold geometry and extrinsic network topology. Temporal trajectories $\{\phi_1, \phi_2, \ldots, \phi_{N_w}\}$ characterize the evolution of market structure, enabling identification of regime transitions, crisis periods, and structural breaks.

To study macro-financial linkages, we compute correlations between geometric features and macroeconomic indicators. For each window, we calculate the mean values of macroeconomic variables $\bar{M}_i = (M_1^{(i)}, \ldots, M_7^{(i)})^\top$ where $M_j^{(i)}$ represents the average of the j-th macro indicator within window $\mathcal{W}_i$. Cross-correlation analysis between components of ϕ_i and $\bar{M}_i$ reveals how external economic conditions influence the geometric organization of financial markets.

All geometric and network measures are subject to statistical validation to ensure robustness. For curvature estimates, we assess stability across varying neighborhood sizes $k \in \{15, 20, 25, 30\}$ through coefficient of variation analysis. Intrinsic dimensionality estimates are validated against theoretical bounds and compared with results from alternative estimators including correlation dimension and maximum likelihood approaches.

Network measures are tested for significance against appropriate null models. We employ configuration models preserving the degree sequence to assess whether observed centrality distributions and clustering coefficients exceed those expected under random rewiring. Statistical significance of temporal changes in geometric measures is evaluated using sliding window hypothesis tests, comparing consecutive windows via Mann–Whitney U tests for non-parametric assessment of distributional shifts.

The temporal stability of findings is verified through sensitivity analysis with respect to window parameters. By systematically varying window width $w \in \{45, 60, 75\}$ and step size $s \in \{15, 20, 25\}$, we confirm that qualitative patterns persist across reasonable parameter choices, ensuring that observed phenomena reflect genuine market dynamics rather than methodological artifacts.

3.3. Summary of Geometric–Topological Indicators

Table 2 summarizes the geometric and network measures employed as structural indicators throughout this study. These measures serve dual purposes: characterizing baseline market organization during stable periods and identifying early-warning signals of structural transitions during crisis episodes. The threshold values represent empirically-derived critical levels based on the 2015–2019 baseline period, with exceedances indicating heightened structural risk. Multiple simultaneous threshold breaches across independent indicators signal elevated probability of fundamental market reorganization rather than transient volatility.

Table 2. Geometric–topological early-warning indicators. Thresholds represent $\pm 2\sigma$ deviations from 2015 to 2019 baseline except where theoretical limits exist. Simultaneous threshold breaches across multiple indicators signal heightened structural risk.

Indicator	Definition	Interpretation	Threshold
Manifold Geometric Measures			
Intrinsic Dimensionality	MLE from k-NN distances	Effective degrees of freedom	<1.5 dimensions
Gaussian Curvature	$\log_{10}(\lambda_d/\lambda_1)$ via local covariance	Eigenvalue concentration	Std. $>3 \times 10^{-7}$
Mean Curvature	$m^{-1}\sum \lambda_i/\lambda_{\max}$ from PCA spectrum	Average manifold bending	<0.65
Tangent Smoothness	Var. explained by first PC	Local linearity (univariate signal)	>0.80
Avg Geodesic Distance	Mean shortest path on k-NN graph	Manifold compactness	>7.8
Max Geodesic Distance	Maximum shortest path (diameter)	Overall manifold span	>20.0
State Space Volume	$\sqrt{\det(\Sigma)}$ (generalized var.)	Hypervolume occupation	$>10^{-15}$
Network Topology Measures			
Network Density	$2\|E\|/(\|V\|(\|V\|-1))$ with $\|\rho\| \geq 0.5$	Proportion of realized correl.	>0.65
Clustering Coefficient	Triangle closure rate	Local cohesion (core–periphery)	>0.85
Forman–Ricci Curvature	$4 - \deg(v) - \deg(w)$ $+3\|N(v) \cap N(w)\|$	Geometric resilience	<0 (vuln.) >8 (hyper.)
Edge Count	Total edges in correlation network	Absolute connectivity	>80 edges
Centrality Measures (Node-Specific)			
Degree Centrality	$\deg(v)/(\|V\|-1)$	Local connectivity	Top 3 nodes
Betweenness Centrality	$\sum \sigma_{st}(v)/\sigma_{st}$	Structural bridge importance	>0.05
Closeness Centrality	$(\|V\|-1)/\sum d(v,u)$	Access efficiency	>0.42

Table 2 notation: MLE—maximum likelihood estimation; k-NN—k-nearest neighbors; PCA—principal component analysis; PC—principal component; $|E|$—edge count; $|V|$—

the number of nodes, fixed at seventeen in this study; $N(v)$—neighborhood of node v; $\deg(v)$—degree of node v; σ_{st}—number of shortest paths between nodes s and t; $d(v,u)$—shortest path distance between nodes. The baseline period for threshold calibration spans 2015–2019, representing pre-crisis market conditions. Critical threshold breaches during the 2022 structural break include intrinsic dimensionality collapsing to 0.43 dimensions in August 2022, network density surging to 0.97 in July 2022, and Forman–Ricci curvature peaking at 16.0 in September 2022, providing coordinated early-warning signals across multiple independent analytical frameworks.

The geometric measures capture manifold properties reflecting correlation structure complexity and organization. Intrinsic dimensionality quantifies effective degrees of freedom, with low values indicating markets operate under dominant common factors eliminating independent variation. Curvature measures characterize local and global geometric properties, with Gaussian curvature capturing eigenvalue concentration, mean curvature quantifying average bending, and tangent smoothness measuring local linearity. Geodesic distances and state space volume characterize manifold connectivity and dispersion, respectively.

Network topology measures quantify correlation structure from graph-theoretic perspectives. Density and edge count provide global connectivity indicators, while clustering coefficient captures local cohesion patterns. Forman–Ricci curvature serves as the primary network geometric resilience measure, with positive values indicating redundant robust connectivity and negative values signaling bottleneck vulnerability. Centrality measures identify systemically important variables whose dynamics disproportionately influence broader market behavior.

Computational Implementation

All empirical analyses were implemented in Python 3.10.12, leveraging the scientific computing ecosystem for geometric–topological calculations, network analysis, statistical computation, and visualization. This subsection details the specific software packages, algorithmic implementations, parameter selections, and computational procedures employed to ensure full methodological transparency and replicability.

The computational pipeline integrates specialized libraries for distinct analytical components. Geometric manifold analysis employs scikit-learn 1.3.0 for k-nearest neighbor graph construction, local principal component analysis, covariance matrix eigen decomposition, and standardization procedures. The k-NN implementation utilizes ball tree data structures for efficient nearest neighbor queries in high-dimensional spaces, with Euclidean distance metric applied to standardized data. UMAP manifold embedding utilizes the umap-learn 0.5.4 package implementing the uniform manifold approximation and projection algorithm for nonlinear dimensionality reduction, though primary results rely on correlation-based analysis rather than embedded coordinates.

Network topology computation leverages NetworkX 3.1 for correlation network construction, centrality measure calculation including degree, betweenness, and closeness centralities, clustering coefficient computation, and shortest path algorithms. The igraph 0.10.6 package provides supplementary network analysis capabilities and validation of centrality measures, with results cross-verified between implementations to ensure consistency. Forman–Ricci curvature calculation employs the GraphRicciCurvature 0.5.3 package, implementing the discrete curvature formulation for undirected networks with edge-level curvatures computed as $\mathcal{F}(v,w) = 4 - \deg(v) - \deg(w) + 3|\mathcal{N}(v) \cap \mathcal{N}(w)|$ and network-level measures obtained through arithmetic averaging over all edges.

Numerical computation and data manipulation utilize NumPy 1.24.3 for array operations, linear algebra routines, and eigenvalue decomposition, SciPy 1.11.1 for statistical func-

tions including correlation coefficient computation and hypothesis testing, and Pandas 2.0.3 for time series handling, rolling window operations, and data frame manipulation.

4. Results

4.1. Temporal Evolution of Manifold Geometry

The temporal analysis of manifold geometric properties encompasses 178 overlapping windows spanning May 2015 to April 2025, with window size $w = 60$ and step $s = 20$ yielding sufficient temporal resolution to capture regime transitions while maintaining statistical stability. Table 3 presents summary statistics for all geometric measures across the full observation period.

The Gaussian curvature $\kappa_G = \log_{10}(\lambda_d/\lambda_1 + \epsilon)$ exhibits remarkable stability from May 2015 to mid-2022, maintaining values between -10.000000 and -9.999999 with within-window standard deviation consistently below 3×10^{-7}. This persistent near-constancy indicates local neighborhoods consistently span the full ambient dimensionality with uniform variance distribution across principal components. A dramatic structural transition emerges in October 2022, where mean Gaussian curvature experiences an unprecedented shift from approximately -10.0 to values approaching -0.2 by early 2023, representing nearly ten orders of magnitude change in the underlying eigenvalue ratio. This transition indicates fundamental manifold reorganization wherein local neighborhoods concentrate variance along fewer principal directions. The transition proves transient, with partial recovery to intermediate levels around -0.5 by mid-2023, though exhibiting greater variability than pre-crisis periods. Curvature standard deviation during transition increases by more than two orders of magnitude to 6×10^{-8}, suggesting heterogeneous geometric properties across manifold regions.

The mean curvature, κ_H, demonstrates greater temporal variability, oscillating within $0.64 \leq \bar{\kappa}_H \leq 0.90$ with no systematic pre-2022 trend. Notable fluctuations occur during 2016–2017 and 2019–2020 with local maxima near 0.85. The late 2022 transition produces the most dramatic disruption, with mean curvature declining to a minimum of 0.55 in August 2022, representing 27% reduction and 4.1 standard deviations below pre-transition mean. This sharp reduction indicates disproportionate variance concentration in leading principal components. Recovery proceeds gradually throughout 2023, stabilizing near 0.75 by mid-2024 with elevated standard deviation of 0.059 compared to pre-2022 baseline.

Geodesic distance analysis reveals substantial temporal variation. Average geodesic distance $\bar{d}_{\text{geo}}$ fluctuates between 5.2 and 8.6 with time-averaged value near 6.5. Notable spikes appear in late 2021 ($\bar{d}_{\text{geo}} > 8.5$) and mid-2022 ($\bar{d}_{\text{geo}} \approx 8.6$), indicating manifold elongation or bottleneck development. Geodesic diameter $d_{\max}$ ranges from 10.9 to 23.8, with elevated values coinciding with increased average distances. The 2023 post-transition period shows reduced geodesic distances ($\bar{d}_{\text{geo}} \approx 5.3$), indicating a more compact manifold structure.

Intrinsic dimensionality $\tilde{m}$ exhibits considerable variability spanning the 1.1–3.0 dimensions. The 2015–2019 period shows dimensionality fluctuating between 1.5 and 2.7 with median near 2.2, suggesting the seventeen-dimensional ambient space reduces to roughly two–three independent factors. Sustained peaks occur during 2020–2021, with multiple windows near or exceeding 2.8 dimensions. The most dramatic collapse coincides with late 2022 transition, where $\tilde{m}$ plummets to 0.6 dimensions, indicating near-univariate dynamics with all variables moving in highly coordinated fashion. Recovery sees dimensionality returning to 1.2–2.6 by 2024, though remaining suppressed relative to pre-2022 baseline.

Tangent space smoothness S_{tangent} clusters between 0.40 and 0.60 for 2015–early 2022, indicating moderate local alignment. Late 2022 produces striking transition to values near 0.90, indicating local neighborhoods become nearly collinear with first principal component

explaining vast majority of local variance. Smoothness gradually declines throughout 2023–2024, stabilizing at 0.50–0.65, slightly elevated relative to pre-transition baseline.

State space volume $V = \sqrt{\det(\boldsymbol{\Sigma})}$ remains at negligibly small values (10^{-34} to 10^{-22}) for most windows, consistent with concentration on lower-dimensional manifolds. Three exceptional episodes show explosive expansion: early 2020 reaching 10^{-12}, mid-2021 near 4×10^{-12}, and late 2021 exceeding 4×10^{-12}. These represent transient extreme market stress episodes. Notably, late 2022 transition maintains baseline volume levels, indicating geometric reorganization without substantial dispersion magnitude increase.

Figure 1 presents complete temporal trajectories, revealing coordinated evolution and distinct regime character. The synchronized disruption across multiple indicators in late 2022 stands out as unique, characterized by simultaneous shifts in curvature, dimensionality, smoothness, and connectivity without accompanying volume expansion, suggesting qualitative change in market dynamics rather than merely increased volatility.

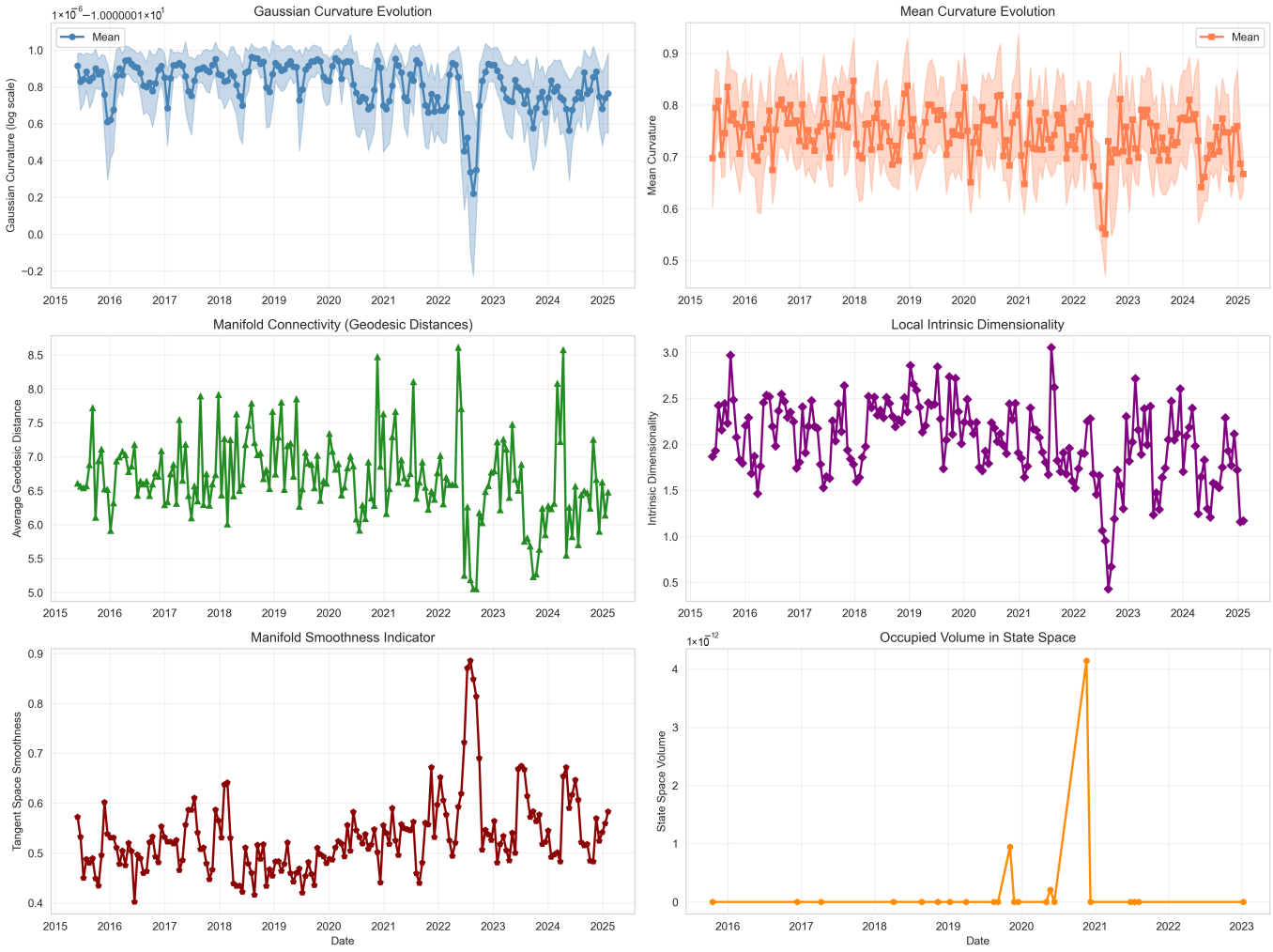


Figure 1. Temporal evolution of manifold geometric properties from May 2015 to April 2025. **Top row**: Gaussian curvature (**left**, logarithmic scale) showing stable period followed by dramatic 2022–2023 transition, and mean curvature (**right**) exhibiting moderate fluctuations with coincident 2022 minimum. **Middle row**: Average geodesic distance (**left**) indicating manifold connectivity with notable 2021–2022 peaks, and local intrinsic dimensionality (**right**) revealing dimensional collapse during late 2022. **Bottom row**: Tangent space smoothness (**left**) demonstrating late 2022 spike to extreme values, and state space volume (**right**) showing three episodic expansions during 2020–2021. Shaded regions in curvature panels indicate plus/minus one standard deviation from the mean.

Table 3. Summary statistics for manifold geometric measures across 178 temporal windows (May 2015–April 2025). Gaussian curvature presented in logarithmic scale. All measures computed from overlapping 60-period windows with 20-period step size.

Measure	Mean	Std. Dev.	Min	Max	Median
Gaussian Curvature (log)	-9.532	1.525	-10.000	-0.204	-10.000
Gaussian Curvature Std	1.44×10^{-7}	5.90×10^{-8}	5.81×10^{-8}	3.93×10^{-7}	1.35×10^{-7}
Mean Curvature	0.747	0.046	0.549	0.945	0.748
Mean Curvature Std	0.076	0.021	0.032	0.159	0.077
Avg Geodesic Distance	6.532	0.670	5.232	8.576	6.514
Max Geodesic Distance	16.756	2.782	10.886	23.775	16.211
Intrinsic Dimensionality	1.968	0.454	0.578	3.035	2.017
Tangent Smoothness	0.532	0.058	0.402	0.899	0.521

4.2. Gaussian and Mean Curvature Dynamics

Figure 2 presents curvature evolution with crisis periods demarcated, enabling direct visual assessment of geometric responses to market shocks. Table 4 provides quantitative characterization across major regimes.



Figure 2. Detailed curvature analysis with crisis period demarcation. Panel (**a**) displays Gaussian curvature evolution in logarithmic scale with shaded bands indicating plus/minus one standard deviation, revealing sustained baseline stability punctuated by elevated variance during the 2022 transition. Panel (**b**) presents mean curvature temporal trajectory, exhibiting greater short-term variability and a dramatic minimum of 0.552 during August 2022. Crisis periods are highlighted: COVID-19 pandemic (red, March–June 2020), currency crisis (orange, December 2021–March 2022), and geometric transition (purple, October 2022–March 2023). The transition period uniquely produces synchronized disruptions across both curvature measures.

Gaussian curvature exhibits sustained stability from mid-2015 to early 2022, with approximately 160 windows maintaining remarkably consistent values and window-to-window variations at scales of 10^{-7}. Within-window standard deviation averages 1.12×10^{-7} during the pre-crisis period, signifying homogeneous curvature distribution across manifold regions.

Table 4. Curvature measure statistics across market regimes. Gaussian curvature values represent logarithmic scale. Standard deviations computed from window means across each period.

Period	Mean Curvature (κ_H)		Within-Window Std		N
	Mean	Std	Gaussian ($\times 10^{-7}$)	Mean	Windows
Pre-Crisis (2019)	0.755	0.033	1.12	0.073	18
COVID-19 (2020)	0.755	0.032	0.93	0.074	6
Currency Crisis (2021–2022)	0.733	0.026	2.08	0.068	6
Geometric Transition (2022–2023)	0.740	0.044	1.29	0.080	9
Post-Transition (2024)	0.738	0.059	1.59	0.087	9
Full Period (2015–2025)	0.745	0.048	1.49	0.076	178

The COVID-19 pandemic (March–June 2020) and currency crisis (December 2021–March 2022) periods produce no discernible Gaussian curvature disruptions, with values indistinguishable from baseline regime. These observations suggest that while these events impact market valuations and volatility, they do not fundamentally reorganize manifold geometric structure at the scale captured by Gaussian curvature.

The geometric transition beginning October 2022 sharply contrasts with prior crises. Within-window curvature variance reaches maximum 4.47×10^{-7} during August 2022, representing fourfold increase over baseline. This surge indicates different manifold regions simultaneously exhibit disparate geometric properties. Peak curvature variance slightly precedes most dramatic manifestations in other geometric measures, suggesting increased spatial heterogeneity serves as early reorganization indicator. By mid-2023, within-window variance returns toward baseline though remaining modestly elevated, implying new equilibrium with greater geometric heterogeneity.

Mean curvature demonstrates substantially greater temporal variability, oscillating within $0.55 \leq \bar{\kappa}_H \leq 0.85$ with no systematic pre-2022 trend. Pre-crisis period (2019) exhibits mean curvature averaging 0.755 ± 0.033 with quasi-periodic oscillations potentially reflecting seasonal factors or policy cycles.

The COVID-19 period produced a transient response, with values reaching 0.80 in early 2020 before rapidly reverting to baseline by mid-2020, suggesting heightened but concentrated volatility rather than fundamental geometric reorganization. The geometric transition period produces the most dramatic disruption: mean curvature declines from 0.75 to minimum 0.552 in August 2022 (27% decrease, 4.1 standard deviations below pre-transition mean). This sharp reduction indicates disproportionate variance concentration in leading modes, with local neighborhoods temporarily collapsing toward lower-dimensional subspaces.

Recovery extends across multiple months, with values gradually returning toward historical norms throughout latter 2023. By early 2024, mean curvature stabilizes at 0.70–0.80 with elevated variability (standard deviation 0.059), suggesting post-transition regime operates with less consistent local geometric structure. Post-transition level of 0.738 remains slightly suppressed relative to pre-crisis 0.755.

Within-window standard deviation of mean curvature averages 0.073 during stable pre-2022 period. During geometric transition, this increases to 0.080, persisting into post-transition period where it reaches 0.087. This sustained 10%+ elevation implies more spatially irregular market geometric structure with distinct manifold regions exhibiting divergent local properties, potentially corresponding to reduced correlation synchronization or emergence of distinct simultaneous market regimes.

Crisis comparison reveals differential signatures: COVID-19 produced transient volatility effects with full recovery within months; currency crisis manifested through elevated Gaussian curvature variance without systematic mean shifts; while 2022–2023 transition constituted qualitatively distinct phenomenon with synchronized anomalies across mul-

tiple measures, persistent structural changes, and fundamental geometric reorganization rather than mere volatility amplification.

4.3. Intrinsic Dimensionality and Effective Degrees of Freedom

The intrinsic dimensionality estimates, obtained through maximum likelihood analysis of nearest-neighbor distance distributions, reveal substantial temporal variation in the effective complexity of Turkish financial market dynamics. Figure 3 presents both the temporal evolution and distributional properties of intrinsic dimensionality across the 178 temporal windows, while Table 5 provides quantitative characterization across major market regimes.

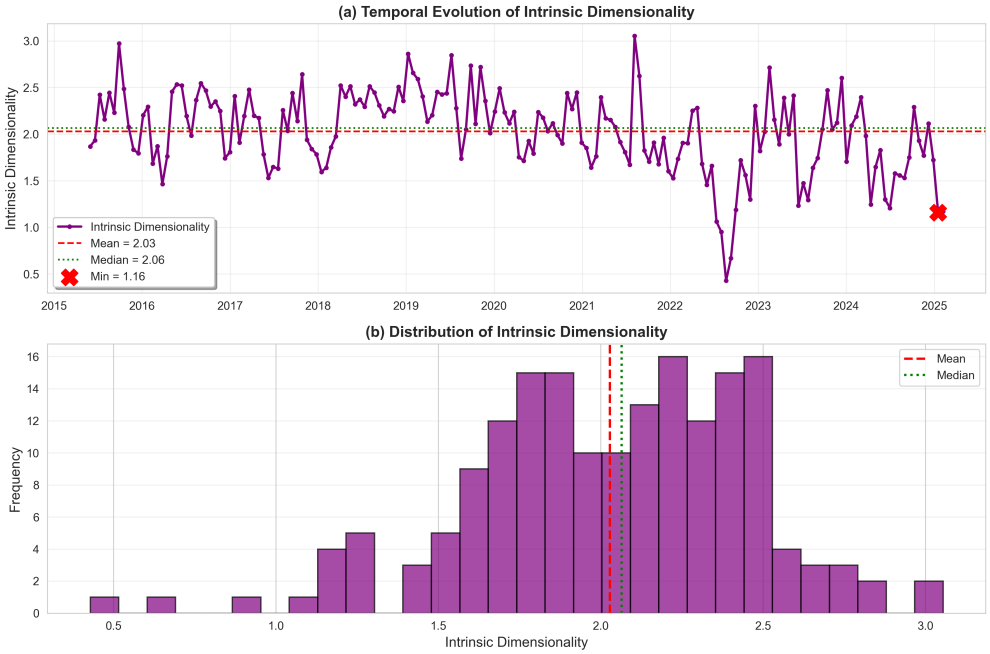


Figure 3. Intrinsic dimensionality evolution and distribution. Panel (**a**) displays temporal trajectory with mean (dashed red, 2.03) and median (dotted green, 2.06) reference lines, revealing substantial variation from approximately 1.5 to 3.0 dimensions across most periods, punctuated by dramatic collapse to 0.43 dimensions (marked with red X) during August 2022. The 2019 pre-crisis period exhibits consistently elevated dimensionality near or above 2.5 dimensions, while post-2022 values remain persistently suppressed below 2.5 dimensions. Panel (**b**) presents the frequency distribution across all 178 windows, showing modal concentration near 2.0 dimensions with negative skew and isolated low-dimensionality outliers corresponding to the 2022 collapse. The bimodal character reflects distinct high-complexity (pre-2022) and reduced-complexity (post-2022) market regimes.

Across the full observation period, the intrinsic dimensionality exhibits a mean of $\tilde{m} = 2.03$ dimensions with standard deviation 0.43 dimensions, indicating that despite the seventeen-dimensional ambient space comprising ten sectoral indices and seven macroeconomic indicators, the data manifold possesses effective dimensionality corresponding to approximately two independent factors. This substantial dimensional reduction from $d = 17$ to $\tilde{m} \approx 2$ reflects a strong coordination and correlation structure within the financial system, wherein most observed variation can be decomposed into a small number of underlying latent factors. The median intrinsic dimensionality of 2.07 dimensions closely matches the mean, suggesting an approximately symmetric distribution absent substantial skewness, though the range spanning from 0.43 to 3.05 dimensions indicates episodic excursions to extreme values.

Table 5. Intrinsic dimensionality statistics across market regimes. Values represent effective manifold dimensions estimated via maximum likelihood from nearest-neighbor distance distributions. Standard deviations computed across windows within each period.

Period	Mean	Std.	Min	Max	*N* Windows
Pre-Crisis (2019)	2.39	0.31	1.74	2.86	18
COVID-19 (2020)	1.92	0.21	1.71	2.24	6
Currency Crisis (2021–2022)	1.77	0.18	1.53	1.96	6
Geometric Transition (2022–2023)	1.94	0.42	1.30	2.72	9
Post-Transition (2024)	1.82	0.39	1.25	2.39	9
Full Period (2015–2025)	2.03	0.43	0.43	3.05	178

Figure 3a displays the temporal trajectory of intrinsic dimensionality, revealing distinct epochs characterized by varying effective complexity. The pre-crisis period from 2015 to 2019 demonstrates relatively elevated dimensionality, with annual means ranging from 2.15 to 2.39 dimensions and frequent excursions above 2.5 dimensions. During 2019, the intrinsic dimensionality achieves its highest annual average of 2.39 ± 0.31 dimensions, with multiple windows exceeding 2.8 dimensions and a maximum value of 3.05 dimensions observed in August 2021. These elevated dimensionality periods indicate epochs where market dynamics exhibit greater independence across variables, potentially reflecting reduced correlation synchronization or the simultaneous operation of multiple distinct economic factors. The pre-crisis regime's higher effective dimensionality suggests a market structure wherein sectoral and macroeconomic variables maintain relatively autonomous dynamics rather than moving in lockstep.

The COVID-19 pandemic period produces a measurable but moderate reduction in intrinsic dimensionality, with mean values declining to 1.92 ± 0.21 dimensions during the March–June 2020 window. This dimensional contraction reflects increased correlation across previously independent factors as the pandemic shock produces synchronized responses across sectors and macroeconomic variables. The magnitude of reduction proves modest relative to subsequent events, and dimensionality partially recovers in the post-pandemic months of late 2020 and early 2021, suggesting that the pandemic's dimensional impact manifested primarily through transient correlation amplification rather than persistent structural change.

The most dramatic dimensional collapse occurs during the geometric transition period of late 2022–early 2023, reaching an absolute minimum of $\tilde{m} = 0.43$ dimensions in August 2022. This extreme value stands 3.7 standard deviations below the overall mean and represents a reduction of approximately 83% relative to typical pre-crisis levels. The interpretation of such low intrinsic dimensionality proves striking: the seventeen-dimensional financial state space temporarily collapsed onto a near-univariate manifold, with essentially all observed variation explainable by movement along a single dominant direction. This geometric configuration corresponds to perfect correlation synchronization, wherein all sectoral indices and macroeconomic indicators move in highly coordinated fashion with minimal independent variation. The physical interpretation suggests that diverse economic factors temporarily lost their autonomy and responded in unison to a single dominant forcing mechanism.

The dimensional collapse proves neither instantaneous nor isolated to a single window. A total of sixteen temporal windows exhibit intrinsic dimensionality below 1.5 dimensions, with ten of these concentrated in the July–October 2022 period. The progression reveals a multi-month descent from typical values near 2.3 dimensions in early 2022, declining through intermediate values of 1.5 to 1.8 dimensions during mid-2022, before reaching the nadir of 0.43 dimensions in late August 2022. This gradual dimensional reduction suggests

a progressive loss of degrees of freedom rather than an abrupt phase transition, potentially corresponding to sequential elimination of independent factors as correlations strengthen across the system.

Recovery from the dimensional minimum extends across the remainder of 2022 and throughout 2023, exhibiting a trajectory characterized by substantial volatility. Following the August 2022 minimum, dimensionality rapidly rebounds to approximately 1.3 dimensions by October 2022, then continues irregular ascent reaching values near 2.7 dimensions by early 2023. However, this recovery proves incomplete and unstable, with intrinsic dimensionality continuing to exhibit large amplitude fluctuations throughout 2023 and 2024. The post-transition mean dimensionality of 1.82 dimensions remains significantly suppressed relative to the pre-crisis baseline of 2.39 dimensions, representing a persistent reduction of approximately 24%. This sustained dimensional deficit indicates that the market has not returned to its pre-crisis structural configuration, instead operating with reduced effective degrees of freedom corresponding to stronger systematic correlations.

The year 2022 emerges as uniquely anomalous in the temporal trajectory, exhibiting an annual mean intrinsic dimensionality of 1.53 dimensions with standard deviation 0.53 dimensions. The standard deviation value represents the highest temporal variability across any year in the observation period, exceeding the typical annual standard deviation by a factor of approximately two. This elevated volatility reflects the dramatic within-year excursion from near-baseline values in early 2022, through the extreme minimum in mid-2022, to partial recovery in late 2022. The combination of depressed mean and elevated variance uniquely characterizes 2022 as a year of dimensional instability, wherein the effective complexity of market dynamics underwent rapid and substantial fluctuations.

Figure 3b presents the distribution of intrinsic dimensionality across all temporal windows, revealing a roughly uni-modal structure centered near 2.0 dimensions with substantial spread. The modal bin encompasses values between 2.0 and 2.2 dimensions, containing approximately 16 windows and representing the most frequently observed dimensionality regime. The distribution exhibits modest negative skewness, with a longer tail extending toward lower dimensionality values, corresponding to the episodic dimensional collapse events. Notably, the distribution contains isolated observations at very low values below 1.0 dimensions, representing extreme anomalies that stand well separated from the main body of the distribution. These outliers correspond primarily to the 2022 geometric transition period and demonstrate that dimensional collapse represents a rare but distinctive dynamical regime qualitatively distinct from typical market behavior.

The temporal patterns in intrinsic dimensionality provide insight into the varying nature of market coordination. High-dimensionality periods correspond to regimes where sectoral performance and macroeconomic conditions exhibit substantial independence, potentially driven by idiosyncratic factors or distinct policy environments affecting different market segments differentially. The pre-2020 market operated predominantly in this high-dimensionality mode, consistent with a relatively liberalized market structure with multiple autonomous dynamics. Conversely, low-dimensionality periods indicate epochs of strong correlation synchronization, where common factors dominate variation across all variables. The extreme dimensional collapse of 2022 suggests a market temporarily operating under a single dominant constraint or forcing mechanism that eliminated independent variation across sectors and indicators.

The persistent suppression of post-transition dimensionality relative to pre-crisis levels constitutes an important structural finding. Mean dimensionality during 2024 of 1.78 dimensions represents a reduction of 0.61 dimensions relative to the 2019 baseline, despite occurring nearly two years after the acute transition episode. This sustained dimensional deficit implies fundamental changes in market correlation structure rather

than merely transient stress responses. Possible interpretations include increased policy coordination across sectors, enhanced financial integration reducing independent dynamics, or systematic shifts in investor behavior producing greater correlation in asset movements. The failure of dimensionality to recover to historical levels suggests the 2022–2023 transition constituted a structural break rather than a temporary perturbation.

4.4. Network Topology Evolution

The temporal analysis of correlation network topology reveals substantial variation in market interconnectedness across the observation period, with distinct epochs characterized by differing levels of integration and local cohesion. All networks comprise seventeen nodes representing the ten Borsa Istanbul sectoral indices and seven macroeconomic indicators, constructed via thresholding absolute correlation coefficients at the level $\theta = 0.5$. Figure 4 presents the evolution of four key topological measures across 178 temporal windows, while Table 6 provides quantitative characterization across major market regimes.

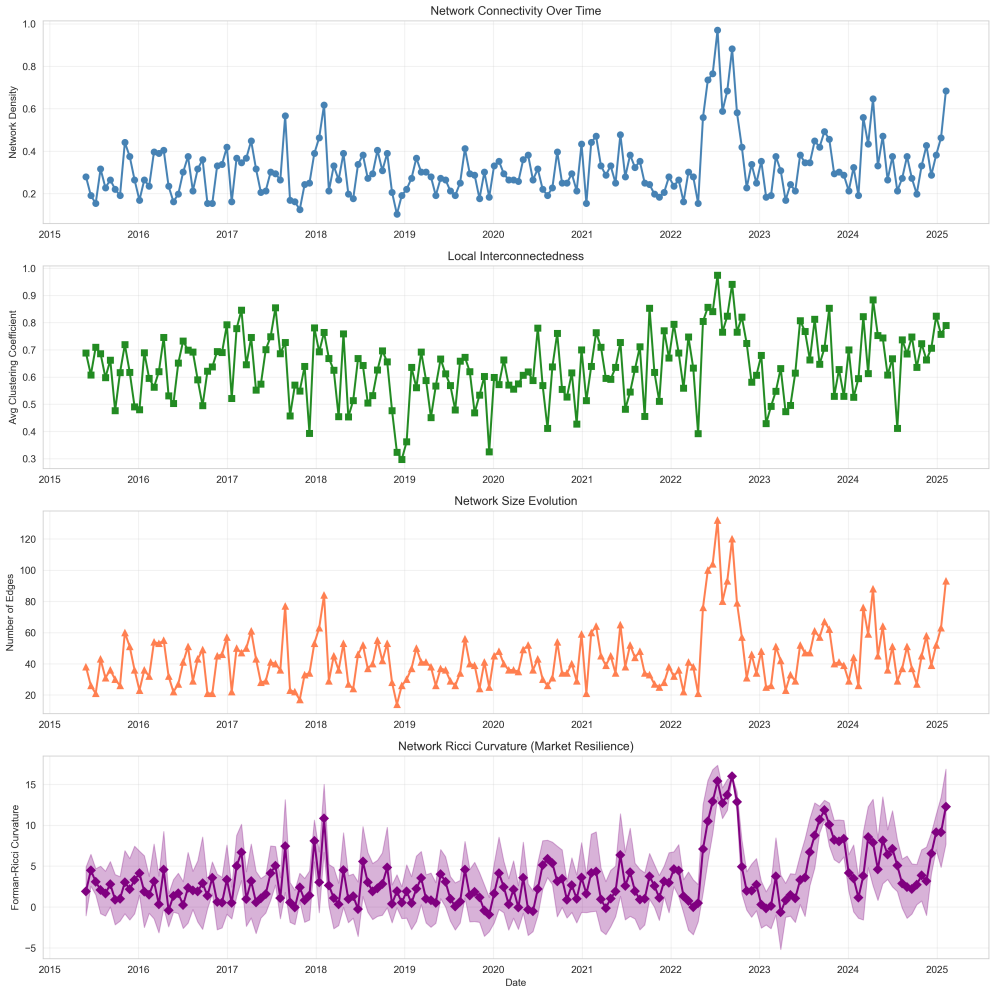


Figure 4. Network topology evolution across four key measures from May 2015 to April 2025. **Top panel**: Network density exhibits extended baseline stability between 0.15 and 0.45 punctuated by extraordinary spike to 0.97 during July 2022. **Second panel**: Average clustering coefficient demonstrates high values typically between 0.50 and 0.80, with extreme elevation to 0.97 coincident with density spike. **Third panel**: Edge count evolves from typical baseline of 30 to 50 edges to exceptional peak of 132 edges (97% of maximum possible 136) during mid-2022. **Bottom panel**: Forman–Ricci curvature discussed in subsequent subsection. The synchronized extrema across all measures during mid-2022 indicate fundamental network reorganization rather than independent fluctuations. Shaded region indicates plus/minus one standard deviation of Forman-Ricci curvature across network edges.

Table 6. Network topology statistics across market regimes. Density represents fraction of realized connections; clustering coefficient measures local interconnectedness; edge count indicates absolute network size. Standard deviations computed across windows within each period. All networks contain $|V| = 17$ nodes with maximum possible 136 edges.

Period	Density	Clustering	N Edges	N Edges (Std.)	N Windows
Pre-Crisis (2019)	0.266	0.559	36.1	8.6	18
COVID-19 (2020)	0.299	0.586	40.7	7.7	6
Currency Crisis (2021–2022)	0.241	0.705	32.8	7.0	6
Geometric Transition (2022–2023)	0.294	0.612	40.0	11.5	9
Post-Transition (2024)	0.382	0.694	51.9	21.3	9
Full Period (2015–2025)	0.319	0.635	43.4	18.5	178

Network density, defined as $\delta = 2|E|/(|V|(|V|-1))$ where $|E|$ denotes edge count and $|V| = 17$ represents node count, quantifies the proportion of potential connections realized in the network. Across the full observation period, density exhibits a mean of $\delta = 0.319$ with standard deviation 0.136, indicating that on average approximately one-third of possible correlations exceed the threshold magnitude. The temporal trajectory of density, displayed in the top panel of Figure 4, reveals extended periods of relative stability punctuated by dramatic excursions. From mid-2015 to early 2022, density fluctuates within a relatively constrained range, typically between 0.15 and 0.45, with transient elevations reaching 0.55 to 0.65 during brief episodes.

The pre-crisis period from 2019 demonstrates baseline network connectivity characterized by mean density $\delta = 0.266 \pm 0.063$, corresponding to an average of approximately 36 edges among the 136 possible connections in the seventeen-node network. This regime reflects moderate interconnectedness wherein roughly one-quarter of variable pairs exhibit correlations sufficiently strong to exceed the threshold. The COVID-19 pandemic produces a modest density increase to $\delta = 0.299 \pm 0.057$, representing approximately 13% elevation relative to the pre-crisis baseline. This amplification indicates that the pandemic shock strengthened correlations across the system, increasing the number of variable pairs exhibiting synchronized behavior. However, the magnitude of increase proves moderate and density returns toward baseline levels during late 2020 and 2021.

The most dramatic network densification occurs during mid-2022, reaching an extraordinary peak density of $\delta = 0.971$ in July 2022, corresponding to 132 realized edges among the 136 possible connections. This extreme value represents near-complete network saturation, wherein virtually all variable pairs exhibit correlations exceeding the threshold magnitude. The interpretation proves striking: the financial system temporarily evolved toward a state of universal correlation, with sectoral indices and macroeconomic indicators moving in highly synchronized fashion across nearly all pairings. This network hypersynchronization coincides temporally with the intrinsic dimensionality collapse and geometric transition documented in prior subsections, reinforcing the interpretation of mid-2022 as a period of fundamental structural reorganization characterized by elimination of independent dynamics.

The density spike proves neither instantaneous nor isolated to a single window. Five consecutive windows during June–September 2022 exhibit densities exceeding 0.68, with four surpassing 0.75 and two achieving values above 0.88. This sustained period of hyperdensity spanning multiple months indicates persistent rather than transient network saturation. The peak density window of July 2022 contains only four unrealized edges, implying that among 136 possible variable pairs, all but four exhibited correlations exceeding the 0.5 threshold. Following the September 2022 peak, density undergoes rapid decline,

returning to values near 0.30 by late 2022, though exhibiting continued elevated volatility throughout 2023.

The year 2022 emerges as uniquely anomalous in network topology, exhibiting annual mean density of $\delta = 0.467$ with standard deviation 0.259. The mean value represents a 76% elevation relative to the pre-crisis baseline, while the standard deviation exceeds typical annual values by a factor of approximately four. This combination of elevated mean and extreme variance characterizes 2022 as a year of topological instability, wherein network structure underwent rapid and substantial fluctuations between near-baseline configurations and states of extreme hypersynchronization. Notably, the post-transition period from 2024 exhibits mean density of $\delta = 0.382$, remaining elevated 44% above pre-crisis levels despite occurring nearly two years after the acute transition. This persistent density elevation suggests lasting structural changes in correlation patterns rather than merely transient stress responses.

The clustering coefficient, quantifying local interconnectedness through the prevalence of triangular motifs, provides complementary insight into network organization. Formally defined as $c(v) = 2|\{(u,w) \in E : u,w \in \mathcal{N}(v)\}|/(k_v(k_v-1))$ for node v with degree k_v, the clustering coefficient measures the probability that two neighbors of a given node are themselves connected. The network-averaged clustering coefficient evolves as shown in the second panel of Figure 4, exhibiting mean value $\bar{c} = 0.635$ across all windows with standard deviation 0.124. These relatively high clustering values indicate strong tendency toward local cohesion, wherein connected variable pairs typically share multiple common neighbors, forming tightly interconnected communities rather than dispersed tree-like structures.

The clustering coefficient trajectory demonstrates moderate positive correlation with density ($r = 0.66$), though the relationship proves imperfect, indicating that global and local connectivity measures capture partially independent aspects of network organization. Throughout most of the observation period, clustering fluctuates between 0.50 and 0.80, occasionally reaching values near 0.85 during brief episodes. The pre-crisis regime exhibits mean clustering $\bar{c} = 0.559$, increasing to $\bar{c} = 0.586$ during COVID-19 and reaching substantially elevated levels of $\bar{c} = 0.705$ during the currency crisis period of late 2021–early 2022.

The mid-2022 density spike coincides with extreme clustering coefficient elevation, achieving a maximum value of $\bar{c} = 0.975$ during the July 2022 hyperdensity episode. This near-unity clustering implies that the network approached a complete graph structure wherein virtually all nodes connect to all others, eliminating any community structure or modularity. Such extreme local cohesion typically emerges only in fully connected or near-fully connected networks, consistent with the observed density of 0.971 during this window. Following the mid-2022 peak, clustering gradually declines but stabilizes at somewhat elevated levels relative to historical baselines, with post-transition mean clustering of $\bar{c} = 0.694$ exceeding the pre-crisis value by 24%.

Network size, quantified by edge count, evolves as depicted in the third panel of Figure 4. Given the fixed node count of $|V| = 17$ and maximum possible edge count of 136, the realized edge count directly scales with density. Across the full period, networks contain an average of 43.4 edges with standard deviation 18.5 edges, reflecting substantial temporal variation. The pre-crisis regime exhibits mean edge count of 36 edges, corresponding to approximately 26% of maximum capacity. Edge count increases modestly to 41 edges during COVID-19 and declines to 33 edges during the currency crisis, before undergoing explosive growth during mid-2022.

The July 2022 network contains 132 edges, representing 97% of theoretical maximum and corresponding to the highest network size across the entire observation period. This extreme edge proliferation reflects the simultaneous strengthening of correlations across virtually all variable pairs. The temporal clustering of high edge count windows during

June–September 2022, with values consistently exceeding 90 edges, reinforces the interpretation of sustained network saturation during this episode. Post-transition networks exhibit mean edge count of 52 edges, remaining elevated 44% above pre-crisis levels and indicating persistent structural shift toward greater interconnectedness.

The post-transition regime demonstrates not only elevated mean connectivity but also substantially increased variability, with edge count standard deviation of 21.3 edges representing approximately 150% increase relative to pre-crisis variability of 8.6 edges. This enhanced volatility suggests reduced structural stability, wherein network topology undergoes larger amplitude fluctuations between successive windows. The combination of elevated mean connectivity and increased variance characterizes the post-2022 market as operating with both tighter average coupling and less predictable correlation structure relative to the pre-crisis regime.

Comparison across crisis episodes reveals differential network responses paralleling those observed in geometric measures. The COVID-19 pandemic produced moderate connectivity increases that proved largely transient, with topology recovering toward baseline within months of the initial shock. The currency crisis of late 2021–early 2022 manifests primarily through elevated local clustering without commensurate global density increases, suggesting formation of tightly interconnected subgroups while maintaining inter-group separation. In stark contrast, the mid-2022 geometric transition constitutes a qualitatively distinct phenomenon characterized by unprecedented network hypersynchronization, sustained topological disruption extending across multiple months, and persistent post-transition elevation in baseline connectivity levels. These patterns indicate that network topology responds heterogeneously to different stress events, with certain episodes producing fundamental structural reorganization while others generate primarily transient perturbations.

4.5. Forman–Ricci Curvature and Network Resilience

The Forman–Ricci curvature provides a discrete geometric characterization of network structure through quantification of neighborhood overlap between adjacent nodes. For an edge (v, w) connecting nodes v and w with respective degrees k_v and k_w, the Forman–Ricci curvature is defined as $\mathcal{F}(v, w) = 4 - k_v - k_w + 3|\mathcal{N}(v) \cap \mathcal{N}(w)|$ where $\mathcal{N}(v)$ denotes the neighborhood of node v. Positive curvature indicates substantial overlap between neighborhoods, corresponding to redundant connectivity and network robustness, while negative curvature signifies bottleneck edges connecting sparsely overlapping communities, potentially representing vulnerability points. The network-averaged Forman–Ricci curvature $\bar{\mathcal{F}} = |\mathcal{E}|^{-1} \sum_{e \in \mathcal{E}} \mathcal{F}(e)$ provides a global geometric descriptor of resilience.

Figure 5 presents both the temporal evolution and distributional properties of Forman–Ricci curvature across the 178 temporal windows. Panel (a) employs color coding to distinguish positive (green) and negative (red) curvature regions, enabling immediate visual assessment of resilience versus vulnerability epochs. Across the full observation period, the network-averaged Forman–Ricci curvature exhibits mean $\bar{\mathcal{F}} = 3.40$ with standard deviation 3.34, indicating predominantly positive curvature with substantial temporal variation. The median value of 2.51 lies below the mean, suggesting modest positive skewness in the distribution driven by occasional extreme positive excursions.

The curvature sign distribution proves highly asymmetric, with positive values characterizing 166 windows representing 93.3% of observations, while negative curvature appears in only 12 windows corresponding to 6.7% of the sample. This pronounced bias toward positive curvature indicates that Turkish financial correlation networks typically operate in a resilient configuration characterized by redundant connectivity and substantial neighborhood overlap. Near-zero curvature values in the range $-0.5 \leq \bar{\mathcal{F}} \leq 0.5$, representing

transitional regimes between resilient and vulnerable structures, occur in 21 windows comprising 11.8% of observations. The rarity of sustained negative curvature suggests that market correlation structure seldom organizes into bottleneck-dominated topologies with isolated communities connected through vulnerable bridge edges.

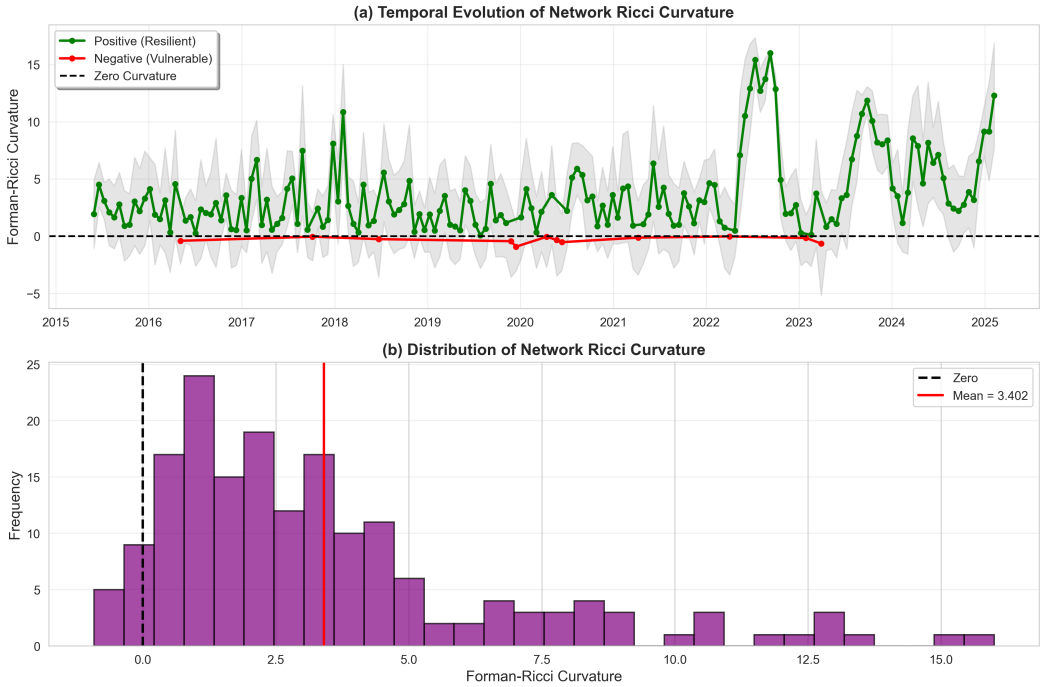


Figure 5. Forman–Ricci curvature evolution and distribution. Panel (**a**) displays temporal trajectory with positive curvature (green, indicating resilience) dominating across most periods, while negative curvature (red, indicating vulnerability) appears occasionally, particularly during COVID-19. The zero curvature reference line (dashed black) separates resilient and vulnerable regimes. Extraordinary positive excursion during mid-2022 achieves maximum $\bar{\mathcal{F}} = 16.0$ in September, coincident with network hyperdensity. Shaded band indicates plus/minus one standard deviation, revealing elevated variance during transition periods. Panel (**b**) presents frequency distribution across all 178 windows, showing modal concentration near 1.5 with pronounced positive skew extending to extreme values above 15. The mean value of 3.40 (solid red) exceeds the mode, quantifying distributional asymmetry. Negative curvature bin (left of zero dashed line) contains 12 vulnerable network epochs representing 6.7% of observations.

The pre-crisis period from 2019 demonstrates baseline network curvature characterized by mean $\bar{\mathcal{F}} = 1.50 \pm 1.51$, representing modest positive resilience with moderate variability. This regime exhibits predominantly positive curvature (88.9% of windows) with occasional brief excursions into negative territory, achieving a minimum of $\bar{\mathcal{F}} = -0.92$ in December 2019. The negative curvature episodes during the pre-crisis period typically coincide with reduced network density (mean density 0.18 during most negative curvature window), indicating that sparse connectivity naturally produces lower curvature through reduced neighborhood overlap. The pre-crisis curvature values suggest a market structure with moderate redundancy and resilience, neither extremely robust nor particularly vulnerable.

The COVID-19 pandemic period produces a notable curvature suppression, with mean declining to $\bar{\mathcal{F}} = 0.86 \pm 1.65$ and only 50% of windows exhibiting positive curvature. This represents the lowest proportion of positive curvature across all crisis periods, suggesting that the pandemic's primary network impact manifested through reduced geometric robustness rather than merely altered connectivity levels. Multiple windows during March–June 2020 exhibit near-zero or slightly negative curvature, indicating network structure characterized by reduced redundancy and increased vulnerability to node or edge removal.

The elevated curvature variability during this period reflects rapid fluctuations between resilient and vulnerable topological configurations as the market adapted to evolving pandemic conditions.

The currency crisis period of late 2021–early 2022 demonstrates markedly different curvature characteristics, exhibiting mean $\bar{\mathcal{F}} = 2.88 \pm 1.60$ with 100% of windows showing positive curvature. This uniform positivity combined with elevated mean values relative to the COVID period suggests that the currency crisis, despite its economic severity, actually strengthened network geometric resilience through enhanced local cohesion. The interpretation connects to the clustering coefficient elevation observed during this period, wherein tightening correlations within subgroups produced greater neighborhood overlap and consequently higher Forman–Ricci curvature.

The mid-2022 geometric transition period witnesses extraordinary curvature amplification, achieving an absolute maximum of $\bar{\mathcal{F}} = 16.0$ in September 2022. This extreme value stands 3.8 standard deviations above the overall mean and represents the highest curvature across the entire decade-long observation window. A total of twelve windows during 2022 exhibit curvature exceeding 10, with ten of these concentrated in the June–October period. The peak curvature window of September 2022 contains 120 edges among 17 nodes, corresponding to network density of 0.88, and demonstrates how extreme density naturally produces elevated curvature through universal neighborhood overlap. During the July 2022 hyperdensity peak with 132 edges, Forman–Ricci curvature reaches $\bar{\mathcal{F}} = 15.4$, confirming the strong positive relationship between density and geometric robustness.

The year 2022 emerges as uniquely anomalous in curvature dynamics, exhibiting annual mean $\bar{\mathcal{F}} = 6.91$ with standard deviation 5.73. The mean represents a 361% elevation relative to the pre-crisis baseline, while the standard deviation exceeds typical annual values by factors of three–four. This combination characterizes 2022 as a year of extreme curvature amplification with high volatility, wherein network geometric resilience underwent dramatic fluctuations between near-baseline configurations and states of exceptional robustness. The curvature extrema during mid-2022 coincide precisely with the network density spike and intrinsic dimensionality collapse documented in prior subsections, reinforcing the interpretation of this period as featuring coordinated geometric reorganization across multiple structural measures.

Table 7 presents quantitative characterization of Forman–Ricci curvature across major market regimes. The post-transition period from 2024 exhibits mean curvature $\bar{\mathcal{F}} = 5.36 \pm 2.53$, representing sustained elevation of 258% relative to pre-crisis levels despite occurring nearly two years after the acute 2022 episode. This persistent curvature elevation indicates fundamental structural shift toward greater network resilience characterized by enhanced redundancy and neighborhood overlap. All nine post-transition windows exhibit positive curvature, suggesting stable operation in a robustness regime without excursions into vulnerable configurations. The combination of elevated mean and universal positivity distinguishes the post-transition market from the pre-crisis regime, which exhibited lower mean curvature with occasional negative episodes.

The distributional properties of Forman–Ricci curvature, displayed in Figure 5b, reveal a roughly uni-modal structure with pronounced positive skew. The modal bin encompasses curvature values between 1 and 2, containing approximately 24 windows and representing the most frequently observed resilience regime. The distribution exhibits an extended right tail extending to values exceeding 15, corresponding to the extreme robustness episodes during mid-2022. A small cluster of observations appears in the negative curvature region below zero, representing the rare vulnerable network configurations. The mean value of 3.40 (marked in red) substantially exceeds the mode near 1.5, quantifying the distributional skewness induced by extreme positive outliers.

Table 7. Forman–Ricci curvature statistics across market regimes. Values represent network-averaged discrete geometric curvature. Positive values indicate redundant connectivity and resilience; negative values signify bottleneck structure and vulnerability. Standard deviations computed across windows within each period.

Period	Mean	Std	Min	Max	Positive	*N* Windows
Pre-Crisis (2019)	1.50	1.51	−0.92	4.57	88.9%	18
COVID-19 (2020)	0.86	1.65	−0.53	3.59	50.0%	6
Currency Crisis (2021–2022)	2.88	1.60	0.73	4.63	100%	6
Geometric Transition (2022–2023)	1.66	1.91	−0.64	4.91	77.8%	9
Post-Transition (2024)	5.36	2.53	1.15	8.54	100%	9
Full Period (2015–2025)	3.40	3.34	−0.92	16.0	93.3%	178

The strong positive correlation between Forman–Ricci curvature and network density ($r = 0.744$) indicates that increased connectivity naturally produces enhanced geometric resilience through greater neighborhood overlap. However, the correlation proves imperfect, with clustering coefficient exhibiting weaker association ($r = 0.560$), suggesting that curvature captures additional topological information beyond simple connectivity measures. Elevated curvature at given density levels indicates efficient network organization with maximum redundancy, while suppressed curvature at high density suggests suboptimal topology with insufficient neighborhood overlap despite numerous connections.

The twelve windows exhibiting negative Forman–Ricci curvature deserve particular attention as they represent epochs of heightened network vulnerability. These negative curvature episodes concentrate primarily in three temporal clusters: late 2019 (three windows), mid-2020 during the COVID pandemic (three windows), and early 2023 during post-transition recovery (two windows). The most negative curvature of $\bar{\mathcal{F}} = -0.92$ occurs in December 2019, coinciding with network density of only 0.18 and edge count of 25, representing a sparse configuration wherein nodes connect with minimal neighborhood overlap. Negative curvature windows typically exhibit substantially reduced clustering coefficients relative to contemporaneous positive curvature networks, confirming that vulnerable topologies arise from combinations of sparse connectivity and poor local cohesion.

The temporal dynamics of Forman–Ricci curvature provide insight into evolving network resilience characteristics. The pre-2020 market operated with moderate baseline resilience punctuated by occasional vulnerable episodes, suggesting a structure balancing efficiency against robustness. The COVID-19 pandemic temporarily suppressed geometric resilience through disruption of neighborhood overlap patterns, though this proved largely transient. The mid-2022 transition produced unprecedented curvature amplification representing extreme redundancy and robustness, potentially corresponding to crisis-induced correlation strengthening producing universal connectivity. Most significantly, the persistent post-transition curvature elevation indicates that the market has structurally shifted toward a higher resilience baseline characterized by enhanced redundancy relative to the pre-crisis configuration.

The relationship between Forman–Ricci curvature and systemic risk merits emphasis. Positive curvature networks exhibit robustness to localized disruptions, as high neighborhood overlap ensures multiple alternative paths connecting any node pair, enabling information and risk transmission to route around damaged edges or nodes. Conversely, negative curvature networks concentrate connectivity through bottleneck edges, creating vulnerability wherein edge removal can fragment the network or isolate communities. The observation that Turkish financial networks operate predominantly with positive curvature suggests inherent structural resilience, though the occasional negative excursions during crisis periods indicate that geometric vulnerability can emerge during stress episodes.

4.6. Network Structure Comparison Across Market Regimes

Visual comparison of network topology between distinct market regimes reveals fundamental structural reorganization in Turkish financial correlation patterns. Figure 6 presents network visualizations for two temporally separated epochs: Window 0 corresponding to the initial observation period beginning May 2015, and Window -1 representing the terminal window from the most recent data extending into early 2025. Node sizes encode degree centrality while node colors indicate betweenness centrality, with darker coloration corresponding to higher values. This dual encoding enables simultaneous assessment of local connectivity (degree) and global structural importance (betweenness).

The early-period network from mid-2015, displayed in Figure 6 (top panel), exhibits a sparse and modular topological structure characteristic of markets with distinct sectoral communities and selective correlations. The network contains approximately thirty-five edges among the seventeen nodes, corresponding to realized density near 0.25, indicating that roughly one-quarter of potential correlations exceed the threshold magnitude. Several prominent structural features emerge from the visualization. Banking and Inflation nodes appear as primary hubs, exhibiting both large size reflecting high degree centrality and dark red coloration indicating substantial betweenness centrality, suggesting these variables serve as critical connectors mediating correlations between other market components. The quantitative centrality measures from Table 8 confirm this visual assessment, with the banking, credit default swaps, inflation, and trade sectors achieving maximum degree centrality of $C_D = 0.375$, corresponding to six connections among the sixteen possible neighbors.

Table 8. Centrality measures for early period network (Window 0, May–July 2015). Degree centrality represents fraction of potential connections realized; betweenness quantifies structural bridge importance; closeness measures average distance to all other nodes. Top five entries by degree centrality shown.

Node	Degree Centrality	Betweenness Centrality	Closeness Centrality
Banking	0.375	0.0751	0.445
Inflation	0.375	0.0642	0.473
CDS	0.375	0.0326	0.445
Trade	0.375	0.0326	0.445
Raw Materials	0.313	0.0386	0.420

The early network demonstrates clear community structure with identifiable sectoral clusters. Financial sector nodes including banking, finance, and insurance form a loosely connected grouping in the upper portion of the visualization, maintaining correlations among themselves while exhibiting selective connections to other market components. A separate cluster appears in the lower region comprising holding companies, technology, and certain macroeconomic indicators including interest rate and credit growth. This modular organization indicates that correlations during the early period concentrated within sectoral boundaries, with inter-group connections mediated primarily through hub nodes like Banking and Inflation. The presence of peripheral nodes with limited connectivity, such as VIX appearing near isolated at the top with small node size, suggests that certain variables operated with substantial independence from the broader market structure during this regime.

Betweenness centrality values in the early network prove relatively modest, with maximum value $C_B = 0.075$ achieved by banking. This moderate betweenness indicates that, while banking serves as an important connector, numerous alternative paths exist for correlation transmission between node pairs, preventing any single variable from dominating information flow. The relatively uniform closeness centrality values ranging between 0.25 and 0.47 suggest reasonably balanced network structure without extreme core–

periphery organization, wherein most nodes maintain comparable average distances to others.

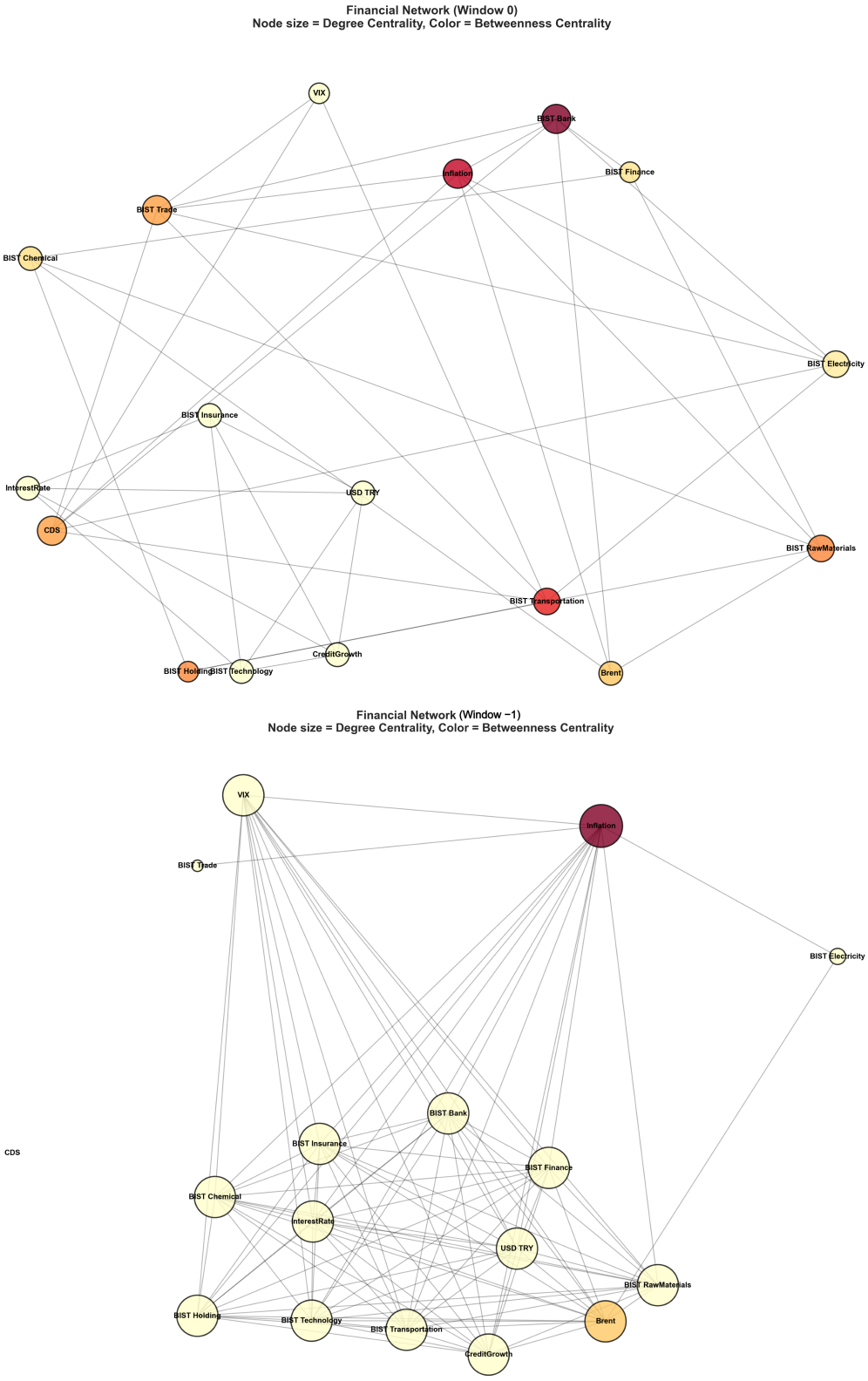


Figure 6. Structural comparison of financial correlation networks across market regimes. Node sizes encode degree centrality (larger = more connections), while node colors indicate betweenness centrality (darker red = higher structural bridge importance). **Top panel** displays the early-period sparse modular network (Window 0: May–July 2015) with approximately 35 edges, characterized by distinct

sectoral clusters and distributed hub structure wherein Banking, Inflation, CDS, and Trade share centrality. Clear community separation appears between financial sector nodes (upper region) and holding/technology cluster (lower region). **Bottom panel** presents the recent-period dense integrated network (Window −1: December 2024–March 2025) with over 100 edges, exhibiting pronounced core–periphery organization. Inflation and VIX emerge as dominant hubs within a tightly interconnected core cluster including banking, finance, insurance, interest rate, and USD/TRY. Peripheral nodes including CDS, electricity, and trade demonstrate reduced relative importance. The structural transformation from modular to integrated topology reflects fundamental reorganization of correlation patterns toward universal synchronization.

The recent-period network from late 2024 to early 2025, presented in panel (b), exhibits dramatically transformed topology characterized by substantially increased density and reduced modularity. Visual inspection reveals a dense core of highly interconnected nodes forming the network center, with edge count appearing to exceed one hundred connections. The realized network density approaches 0.7 to 0.8 based on visual edge enumeration, representing nearly threefold increase relative to the early period. This densification reflects broad strengthening of correlations across previously independent variable pairs, indicating enhanced market integration.

The core–periphery structure proves far more pronounced in the recent network, with inflation, VIX, banking, finance, insurance, interest rate, and USD/TRY forming a tightly interconnected central cluster exhibiting near-complete internal connectivity. These nodes demonstrate both large size and prominent positioning, collectively serving as the structural heart of the correlation network. The intense interconnection within this core group suggests that these variables now move in highly coordinated fashion, potentially driven by common underlying factors or enhanced transmission of shocks across these critical market indicators. In contrast, several nodes including CDS, Electricity, and Trade appear pushed toward peripheral positions with reduced centrality, indicating diminished systemic importance relative to the early period.

Inflation emerges as the dominant hub in the recent network, exhibiting the largest node size indicating maximum degree centrality, combined with dark coloration suggesting elevated betweenness. This represents a notable shift from the early period wherein banking shared hub status with Inflation, toward a regime where inflation assumes preeminent structural importance. The interpretation connects to the macroeconomic environment of recent years, wherein inflation dynamics have become a central organizing factor for Turkish financial markets, driving correlations across both sectoral indices and other macroeconomic variables. VIX similarly achieves enhanced prominence relative to its peripheral early-period position, now appearing as a major hub within the core cluster, potentially reflecting increased sensitivity of Turkish markets to global volatility conditions.

Banking maintains substantial centrality in the recent network, though its relative importance appears somewhat diminished compared to the early period where it served as the primary hub. The banking node exhibits large size but lighter coloration relative to inflation, suggesting high degree centrality with moderate betweenness. The finance and insurance nodes, previously exhibiting modest connectivity in the early network, now appear as integral components of the dense core cluster with markedly enhanced centrality. This evolution reflects increased financial sector integration, wherein banks, non-bank financial institutions, and insurance companies exhibit strong correlation synchronization.

The recent network demonstrates substantially reduced community structure relative to the early period, with the dense core effectively integrating previously distinct sectoral clusters. The clear financial sector grouping visible in the early network has dissolved into the broader core cluster, while peripheral sectors exhibit connection patterns dominated by links to core hub nodes rather than formation of independent communities. This

structural homogenization suggests that market dynamics have shifted from a regime of autonomous sectoral behaviors toward universal correlation patterns driven by common factors concentrated in the core.

Several nodes exhibit notable position shifts between periods. Technology and holding companies, which occupied semi-peripheral positions in the early network with moderate connectivity, now appear better integrated into the core structure with increased edge counts. Raw materials and transportation maintain intermediate positions in both periods, though with enhanced connectivity in the recent network. Brent crude oil exhibits interesting evolution, transitioning from peripheral status with limited connections in the early period to moderate integration in the recent network, potentially reflecting increased recognition of energy price importance for Turkish economic conditions.

The transformation from sparse modular structure to dense core–periphery organization carries important implications for systemic risk and correlation dynamics. The early-period network's modular structure provided insulation wherein disruptions to specific sectoral clusters could remain somewhat localized, as limited inter-cluster connectivity constrained contagion pathways. The dense core structure of the recent network eliminates this insulation, creating conditions wherein shocks to any core node propagate rapidly throughout the tightly connected cluster, potentially amplifying systemic vulnerability. However, the high density also implies substantial redundancy, as the Forman–Ricci curvature analysis demonstrated, suggesting that while contagion may spread more rapidly, the network possesses greater resilience to localized node or edge failures.

The centrality concentration in the recent network, with inflation, VIX, and financial sector variables dominating structural importance, identifies these components as critical monitoring targets for systemic risk assessment. The early network's more distributed centrality structure implied no single variable possessed overwhelming systemic importance, whereas the recent configuration creates clear focal points whose dynamics substantially influence broader market behavior. This centrality concentration may enhance predictability, as tracking a small number of core variables provides substantial information about overall market state, but simultaneously creates vulnerability to disruptions affecting these critical nodes.

Comparison with the network topology metrics confirms the visual structural assessment. The early period's approximate edge count of thirty-five aligns with the baseline connectivity levels of the pre-crisis regime, while the recent network's edge count exceeding one hundred corresponds to the elevated post-transition connectivity documented quantitatively. The clustering coefficient evolution from moderate values near 0.6 in the early period to elevated values approaching 0.7 in the recent network manifests visually as the transformation from distinct clusters toward the dense core structure. The Forman–Ricci curvature increase from baseline values near 1.5 to elevated post-transition values exceeding 5.0 corresponds geometrically to the transition from sparse topology with limited neighborhood overlap to dense core configuration with universal connectivity.

4.7. Sectoral Centrality and Systemic Importance

Network centrality measures provide quantitative characterization of node importance within correlation structure, identifying systemically critical variables whose dynamics exert disproportionate influence on broader market behavior. Three complementary centrality metrics capture distinct aspects of structural significance. Degree centrality $C_D(v) = k_v/(|V| - 1)$ quantifies the fraction of potential connections realized by node v, measuring local connectivity. Betweenness centrality $C_B(v) = \sum_{s \neq v s. \neq t} \sigma_{st}(v)/\sigma_{st}$ where σ_{st} denotes the number of shortest paths between nodes s and t and $\sigma_{st}(v)$ counts those passing through v, measures the extent to which a node serves as intermediary on paths connecting

other nodes. Closeness centrality $C_C(v) = (|V| - 1) / \sum_{u \neq v} d(v, u)$ where $d(v, u)$ represents shortest-path distance, quantifies efficiency of access to all other nodes. Figure 7 presents comprehensive rankings across all three measures, while Table 9 provides numerical values for all seventeen network components.

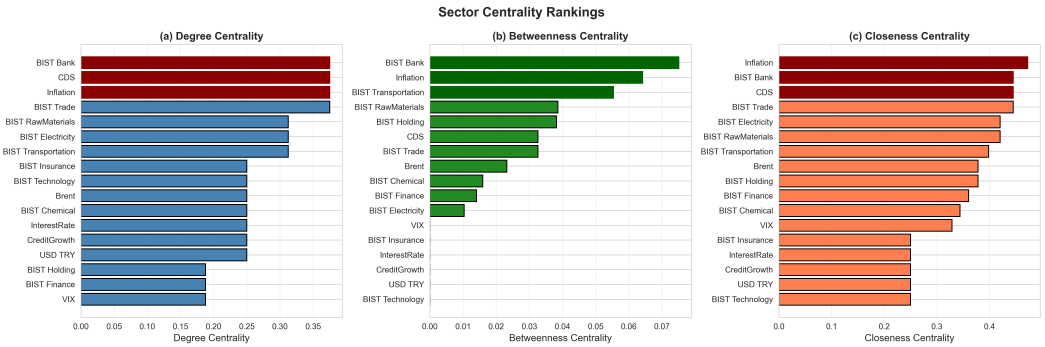


Figure 7. Comprehensive centrality rankings across all seventeen network nodes. Panel (**a**) presents degree centrality, revealing banking, CDS, inflation, and trade as tier-one connectivity hubs (dark red bars) achieving maximum $C_D = 0.375$, while holding, finance, and VIX occupy peripheral positions (blue bars) with minimum $C_D = 0.188$. Panel (**b**) displays betweenness centrality, identifying banking as dominant structural bridge ($C_B = 0.0751$) with inflation and transportation as secondary intermediaries, while six variables including insurance, technology, and policy indicators exhibit zero betweenness (no bars visible), indicating terminal rather than bridge positions. Panel (**c**) shows closeness centrality, with inflation achieving optimal access efficiency ($C_C = 0.473$) followed by banking, CDS, and trade, while peripheral nodes including insurance, technology, and policy variables demonstrate minimum closeness ($C_C = 0.25$, orange bars) reflecting inefficient access positions. The combined centrality profile establishes banking, inflation, and CDS as the three most systemically important variables based on consistent high rankings across complementary structural measures.

Analysis of degree centrality, displayed in Figure 7a, reveals banking, credit default swaps, inflation, and trade sectors achieving maximum values of $C_D = 0.375$, indicating each maintains connections to six of the sixteen possible neighbors in the seventeen-node network. This shared maximum degree establishes these four variables as the network's connectivity hubs, collectively serving as primary integration points linking disparate market components. The uniform maximum value of 0.375 represents substantial but not extreme connectivity, as the theoretical maximum of $C_D = 1.0$ would require universal connection to all other nodes. The co-occurrence of both financial sector variables (banking), macroeconomic indicators (CDS, inflation), and real economy sectors (trade) among the highest-degree nodes indicates that systemic connectivity does not concentrate exclusively within financial components but rather distributes across diverse market segments.

Raw materials and electricity sectors exhibit the second tier of degree centrality with values of $C_D = 0.3125$, corresponding to five connections. Transportation follows with identical degree centrality, establishing a secondary hub tier. These moderately connected sectors serve as important but not dominant integration points, maintaining substantial correlation structure while falling short of the maximum connectivity achieved by the primary hubs. The middle tier encompasses numerous variables including insurance, technology, brent crude oil, chemical, interest rate, credit growth, and USD/TRY exchange rate, all exhibiting degree centrality of $C_D = 0.25$, corresponding to four connections. This intermediate connectivity level indicates participation in correlation structure without hub status.

Table 9. Comprehensive centrality measures for all network nodes. Degree centrality represents fraction of potential connections realized; betweenness quantifies structural bridge importance; closeness measures access efficiency to all other nodes. Values computed from time-averaged correlation network. Nodes sorted by degree centrality.

Node	Degree	Betweenness	Closeness
Tier 1: Maximum Connectivity Hubs			
Banking	0.375	0.0751	0.445
CDS	0.375	0.0326	0.445
Inflation	0.375	0.0642	0.473
Trade	0.375	0.0326	0.445
Tier 2: Secondary Hubs			
Raw Materials	0.313	0.0386	0.420
Electricity	0.313	0.0103	0.420
Transportation	0.313	0.0553	0.398
Tier 3: Intermediate Connectivity			
Insurance	0.250	0.0000	0.250
Technology	0.250	0.0000	0.250
Brent	0.250	0.0232	0.378
Chemical	0.250	0.0159	0.344
Interest Rate	0.250	0.0000	0.250
Credit Growth	0.250	0.0000	0.250
USD/TRY	0.250	0.0000	0.250
Tier 4: Peripheral Nodes			
Finance	0.188	0.0140	0.360
Holding	0.188	0.0382	0.378
VIX	0.188	0.0000	0.329

The lowest degree centrality appears in holding companies, finance sector, and VIX volatility index, each achieving only $C_D = 0.1875$ representing three connections. These peripheral nodes maintain minimal direct connectivity, suggesting their dynamics correlate selectively with only a small subset of other variables rather than exhibiting broad market integration. The particularly low centrality of VIX proves somewhat surprising given its conceptual importance as a global fear gauge, indicating that Turkish market correlations during the analyzed period do not strongly synchronize with global equity volatility. Similarly, the finance sector's peripheral position contrasts with banking's hub status, suggesting important heterogeneity within the broader financial sector wherein banks dominate systemic connectivity while non-bank financial institutions operate with reduced integration.

The betweenness centrality analysis, presented in Figure 7b, reveals substantially more heterogeneous distribution than degree centrality, with values spanning from zero to $C_B = 0.0751$. Banking achieves maximum betweenness, indicating this variable serves as the primary structural bridge mediating correlations between other network components. Interpretation suggests that many correlation pathways connecting non-banking variables route through banking sector dynamics, positioning banks as critical intermediaries in systemic transmission. The betweenness value of 0.0751 implies that approximately 7.5% of all shortest paths in the network traverse the banking node, conferring substantial structural power.

Inflation achieves the second-highest betweenness with $C_B = 0.0642$, confirming its role as a major systemic intermediary. The combination of maximum degree centrality and elevated betweenness establishes Inflation as possessing dual hub status, serving both as highly connected node and as critical bridge. Transportation exhibits the third-

highest betweenness at $C_B = 0.0553$ despite having only secondary-tier degree centrality, indicating this sector occupies a strategic position mediating connections between otherwise disparate network regions. This pattern exemplifies how betweenness and degree centrality capture complementary structural features, wherein Transportation's moderate connectivity includes connections bridging distinct communities, elevating its intermediary importance beyond what degree alone would suggest.

A notable finding emerges from the identification of six variables exhibiting precisely zero betweenness: insurance, technology, interest rate, credit growth, USD/TRY exchange rate, and VIX. Zero betweenness indicates that no shortest paths in the network route through these nodes, implying they serve as terminal endpoints or leaf nodes rather than intermediaries. For variables within this zero-betweenness group that also possess moderate degree centrality (specifically, insurance, technology, and the macroeconomic indicators), the structural interpretation suggests these nodes connect to common hubs but do not bridge between distinct network regions. Their connections prove redundant in the sense that alternative paths connecting their neighbors exist without routing through these variables.

The zero betweenness of macroeconomic policy variables, including interest rate, credit growth, and the USD/TRY exchange rate, carries particular significance for understanding policy transmission mechanisms. These variables' structural positions as non-intermediaries suggest their influences propagate through direct correlations with connected variables rather than serving as conduits linking broader market segments. The zero betweenness of VIX reinforces its peripheral network position identified through degree centrality analysis, indicating global volatility conditions influence Turkish markets selectively rather than serving as central organizing factor.

Closeness centrality analysis, displayed Figure 7c, quantifies efficiency of access to all other network nodes. Inflation achieves maximum closeness of $C_C = 0.473$, indicating optimal average distance to other variables and confirming its central position within network topology. Banking, CDS, and trade follow with closeness values of $C_C = 0.445$, constituting a tier of highly accessible hub nodes. The elevated closeness of these variables implies their dynamics rapidly propagate throughout the network, as short average path lengths enable efficient transmission to all market components.

Raw materials, electricity, and transportation exhibit moderately elevated closeness values near $C_C = 0.40$ to 0.42, consistent with their secondary hub status. In contrast, insurance, technology, interest rate, credit growth, and USD/TRY all achieve minimum closeness of $C_C = 0.25$, indicating these peripheral nodes occupy positions requiring longer average paths to reach other network components. The low closeness values reflect their limited direct connectivity combined with positioning at network periphery rather than core, resulting in inefficient access requiring traversal of multiple intermediaries.

Sectoral comparison reveals systematic patterns in centrality distributions. The financial sector variables exhibit pronounced heterogeneity, with banking achieving maximum or near-maximum values across all three centrality measures, while insurance demonstrates uniformly low centrality and finance occupies peripheral positions. This intra-sector divergence indicates that traditional commercial banking operations dominate financial sector systemic importance, while insurance and non-bank financial activities maintain more limited correlation structure. The banking sector's triple centrality dominance (high degree, maximum betweenness, elevated closeness) establishes it as the single most systemically important node in the network, functioning simultaneously as connectivity hub, structural bridge, and efficiently accessible core node.

Macroeconomic indicators display remarkable diversity in centrality profiles. Inflation and CDS achieve hub status with elevated values across all measures, indicating these

variables serve as primary macroeconomic integration points influencing broad market dynamics. In contrast, interest rate, credit growth, and USD/TRY exchange rate exhibit uniformly low centrality despite their conceptual economic importance, suggesting these policy-relevant variables influence markets through channels not fully captured by contemporaneous correlations. This finding may reflect policy announcement effects that operate through expectations and forward-looking behavior rather than generating strong concurrent correlation patterns, or alternatively may indicate that these variables respond to rather than drive market dynamics during the observed period.

Real economy sectors demonstrate intermediate centrality positions. Trade achieves tier-one status, matching banking and inflation in degree centrality and indicating broad correlation structure linking commercial activity to diverse market components. Transportation exhibits elevated betweenness despite moderate degree, suggesting it bridges distinct economic segments. Raw materials maintains solid connectivity without exceptional intermediary importance. The technology and chemical sectors occupy peripheral positions with limited systemic integration, potentially reflecting idiosyncratic factors dominating these sectors' dynamics with reduced sensitivity to broader market conditions.

The systemic importance hierarchy revealed through centrality analysis carries implications for risk monitoring and policy focus. Banking, inflation, and CDS emerge as the three most systemically critical variables based on combined consideration of all centrality measures, warranting priority attention in stability assessment and stress testing frameworks. Disruptions or anomalous dynamics in these hub variables would likely propagate efficiently throughout the network given their high connectivity, intermediary positions, and central locations. The zero-betweenness group including policy variables suggests that conventional monetary policy channels may operate with reduced network amplification effects relative to variables occupying bridge positions.

The centrality concentration wherein four variables achieve maximum degree while numerous others exhibit substantially lower connectivity indicates relatively hierarchical rather than egalitarian network structure. This hierarchical organization creates both resilience and vulnerability characteristics. Resilience emerges from the redundancy implied by multiple high-degree hubs, preventing single-point-of-failure dynamics. Vulnerability arises from the structural power concentrated in hub nodes, wherein simultaneous distress across the tier-one variables (banking, inflation, CDS, trade) could generate systemic disruption absent alternative integration pathways.

4.8. Integrated Geometric Network Analysis

The synthesis of geometric manifold properties and network topological measures reveals fundamental relationships between state space structure and correlation network organization, providing unified perspective on market integration dynamics. Figure 8 presents a comprehensive six-panel dashboard displaying temporal trajectories and distributional properties of key geometric and network measures, enabling visual assessment of coordinated evolution patterns. Figure 9 provides detailed bivariate scatter analysis quantifying pairwise relationships, while Figure 10 presents the complete correlation structure across all measures.

Examination of the correlation matrix reveals tangent space smoothness and Forman–Ricci curvature as the most strongly related geometric network pair, exhibiting correlation $r = 0.655$ with $p = 3.34 \times 10^{-23}$. This robust positive association indicates that periods of elevated manifold local linearity (high smoothness) systematically coincide with enhanced network geometric resilience (high Ricci curvature). The mechanistic interpretation connects geometric and topological perspectives: high smoothness implies data points align along dominant directions with minimal local curvature, corresponding to strong

correlations among variables that naturally produce dense networks with substantial neighborhood overlap, which in turn generates positive Forman–Ricci curvature. Conversely, low smoothness periods characterized by irregular manifold geometry with substantial local bending correspond to weaker, more heterogeneous correlations producing sparse networks with reduced overlap and consequently lower Ricci curvature.



Figure 8. Integrated geometric network dashboard displaying temporal evolution and distributional properties. **Left column**: temporal trajectories spanning May 2015 to April 2025. **Top panel** shows Gaussian curvature (logarithmic scale) maintaining baseline stability with mid-2022 variance elevation. **Middle panel** presents network density exhibiting baseline values 0.2 to 0.4 punctuated by extraordinary mid-2022 spike to 0.97. **Bottom panel** displays Ricci curvature demonstrating multiple excursions with maximum 16.0 during September 2022. **Right column**: complementary distributional analyses. **Top panel** shows Gaussian curvature versus density scatter with color gradient indicating temporal progression, revealing negative relationship wherein high-density episodes (right edge) correspond to baseline curvature values. **Middle panel** presents intrinsic dimensionality histogram exhibiting modal concentration near 2.0 with negative skew toward low-dimensionality outliers. **Bottom panel** shows clustering coefficient distribution spanning 0.3 to 1.0 with primary mode near 0.65. The synchronized extrema across panels during mid-2022 confirm coordinated geometric network transformation.

Intrinsic dimensionality exhibits strong negative correlations with all network connectivity measures, achieving $r = -0.539$ with density ($p = 8.60 \times 10^{-15}$), $r = -0.548$ with Ricci curvature ($p = 2.28 \times 10^{-15}$), and $r = -0.484$ with a clustering coefficient ($p = 7.70 \times 10^{-12}$). These systematic inverse relationships establish a fundamental trade-off between effective complexity and network integration. High-dimensionality regimes wherein market dynamics span multiple independent factors naturally produce sparse correlation networks, as variables operating along distinct dimensions exhibit reduced pairwise correlations, resulting in fewer edges exceeding the threshold. Conversely, low-dimensionality periods characterized by dynamics collapsing onto univariate or bivariate

manifolds generate universal correlations as all variables become dominated by common factors, producing dense networks with high connectivity.

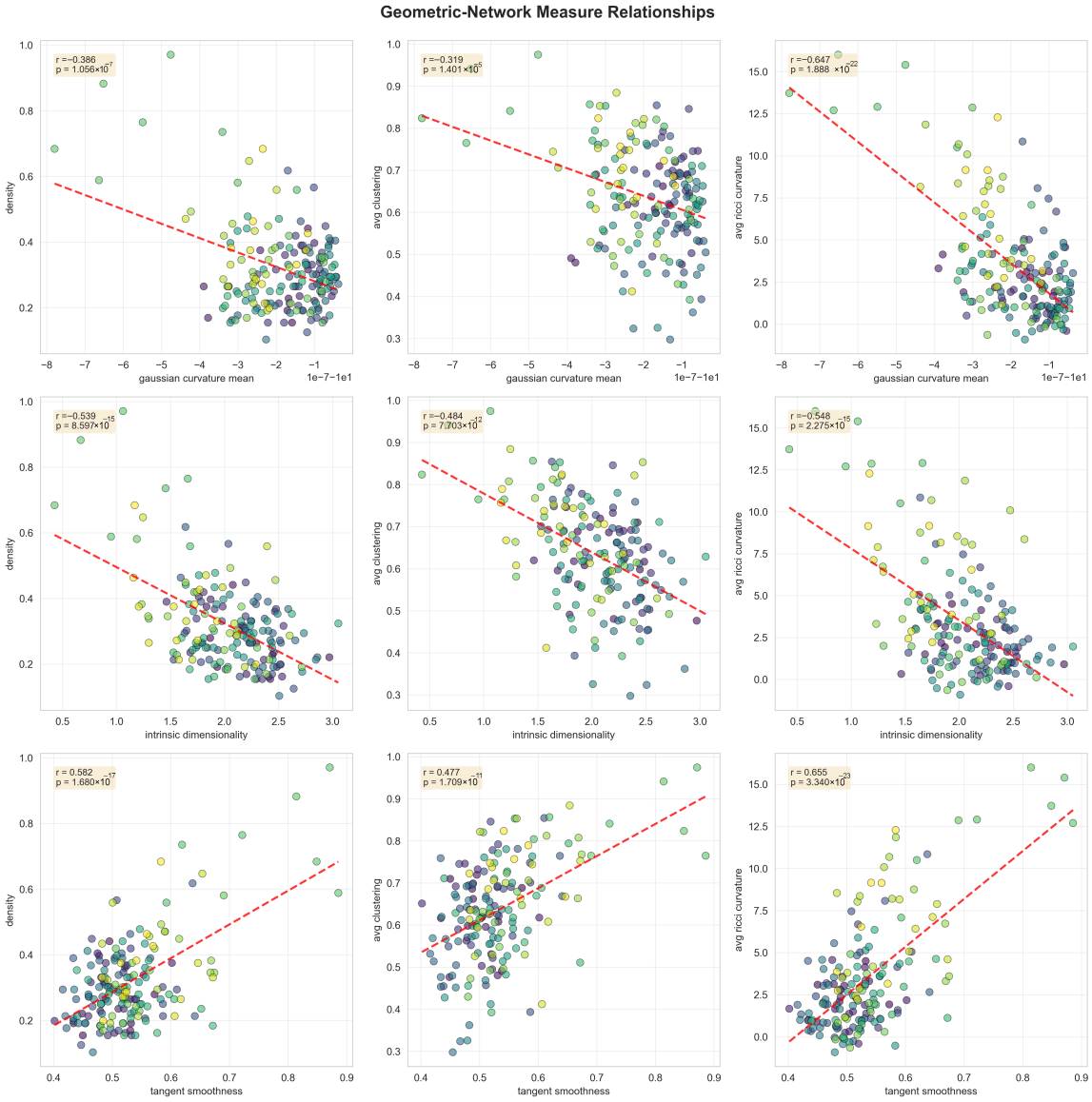


Figure 9. Geometric network bivariate relationship matrix. Nine panels examine pairwise relationships between three geometric measures (Gaussian curvature, intrinsic dimensionality, tangent smoothness) and three network measures (density, clustering coefficient, Ricci curvature). Each panel includes correlation coefficient r with p-value annotation and fitted regression line (red dashed). Color gradient from purple (early period) to yellow (mid-period) to green (recent period) enables temporal pattern identification. **Top row**: Gaussian curvature exhibits moderate negative correlations with network measures ($r = -0.39$ with density, $r = -0.65$ with Ricci). **Middle row**: intrinsic dimensionality demonstrates strong negative relationships ($r = -0.54$ with density, $r = -0.55$ with Ricci), confirming dimensional reduction drives network integration. **Bottom row**: tangent smoothness shows robust positive associations ($r = +0.58$ with density, $r = +0.66$ with Ricci), establishing smoothness as strongest geometric predictor of network connectivity. Tighter scatter around regression lines for dimensionality and smoothness relationships relative to Gaussian curvature indicates superior predictive power.

The dimensionality–density relationship proves particularly revealing. Windows exhibiting intrinsic dimensionality below 1.5, representing effective univariate dynamics, systematically demonstrate density values exceeding 0.4, with the three most extreme

dimensional collapses (dimensionality below 1.1 during mid-2022) achieving densities surpassing 0.7. This pattern confirms that dimensional reduction mechanistically drives network densification rather than merely correlating with it. The physical interpretation suggests that when market structure loses degrees of freedom through correlation strengthening, the resulting low-dimensional dynamics force universal synchronization captured as dense correlation networks. The correlation magnitude of $r = -0.539$ indicates that approximately 29% of variance in network density can be explained by intrinsic dimensionality variation alone, representing substantial predictive power from a single geometric descriptor.

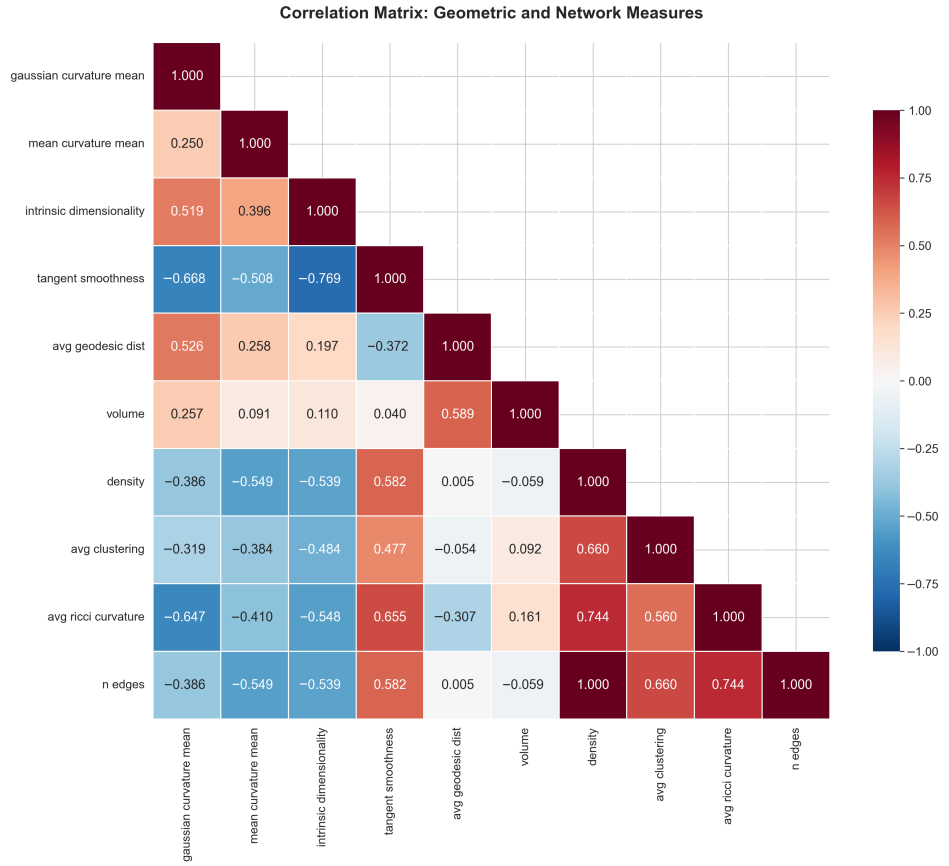


Figure 10. Comprehensive correlation heat map for geometric and network measures. Lower triangular matrix displays Pearson correlation coefficients with color encoding: dark red indicates strong positive correlation (approaching $+1$), white represents near-zero correlation, and dark blue signifies strong negative correlation (approaching -1). Geometric measures (top rows) include Gaussian curvature, mean curvature, intrinsic dimensionality, tangent smoothness, geodesic distance, and volume. Network measures (bottom rows) comprise density, clustering, Ricci curvature, and edge count. Systematic patterns emerge: intrinsic dimensionality, mean curvature, and Gaussian curvature exhibit uniformly negative correlations with network connectivity (blue tiles in corresponding rows), while tangent smoothness demonstrates opposing positive correlations (orange-red tiles). Network measures intercorrelate strongly (dark red block in lower right corner), with density and edge count achieving perfect correlation (both quantify connectivity), and Ricci curvature showing strong association with density ($r = 0.74$) and clustering ($r = 0.56$). The strongest geometric network relationship appears between tangent smoothness and Ricci curvature ($r = +0.66$); meanwhile, Gaussian and Ricci curvatures exhibit strongest negative association ($r = -0.65$), indicating opposing temporal patterns despite both measuring geometric properties.

Mean curvature demonstrates systematic negative correlations with network measures, achieving $r = -0.549$ with both density and edge count ($p = 2.20 \times 10^{-15}$), and $r = -0.410$

with Ricci curvature ($p = 1.35 \times 10^{-8}$). The inverse relationship between manifold mean curvature and network connectivity appears initially counter-intuitive but admits clear geometric interpretation. High mean curvature indicates local neighborhoods exhibiting substantial bending with variance distributed across multiple principal components rather than concentrating in leading modes. Such geometric configurations correspond to variables maintaining partially independent dynamics with moderate pairwise correlations, producing networks with selective connectivity. Conversely, low mean curvature reflects neighborhoods with variance concentration along few directions, corresponding to strong systematic correlations generating dense networks. The 2022 mean curvature minimum of 0.552, representing maximal variance concentration, coincided precisely with peak network density of 0.971, providing extreme-case validation of the systematic relationship.

Tangent space smoothness exhibits strong positive correlations with network connectivity, achieving $r = 0.582$ with density ($p = 1.68 \times 10^{-17}$) and $r = 0.477$ with clustering ($p = 1.71 \times 10^{-11}$). High smoothness indicates that local manifold patches are well-approximated by their first principal component, corresponding to data points aligning along near-linear trajectories. This geometric configuration emerges when variables exhibit strong coordinated movement, naturally producing elevated pairwise correlations that manifest as dense networks with high local cohesion. The smoothness–Ricci correlation of $r = 0.655$ represents the strongest geometric network relationship identified, indicating that manifold regularity and network resilience constitute nearly equivalent perspectives on underlying correlation structure, differing primarily in mathematical formalism rather than captured phenomena.

Gaussian curvature demonstrates moderate negative correlations with network measures including $r = -0.386$ with density ($p = 1.06 \times 10^{-7}$) and $r = -0.647$ with Ricci curvature ($p = 1.89 \times 10^{-22}$). The particularly strong inverse relationship with Ricci curvature merits attention, as both measures ostensibly quantify geometric curvature properties. However, the measures capture fundamentally different geometric aspects: the Gaussian curvature (in the implemented logarithmic formulation) reflects eigenvalue ratio structure related to dimensional uniformity, while the Forman–Ricci curvature quantifies discrete network neighborhood overlap. The negative correlation indicates these geometric properties exhibit opposing temporal patterns, with periods of extreme Gaussian curvature values (reflecting eigenvalue concentration) systematically coinciding with suppressed Ricci curvature (sparse networks), while Gaussian curvature baseline periods correspond to elevated Ricci curvature (dense networks with redundancy).

Three temporal windows during mid-2022 exhibit simultaneous extreme values across multiple geometric and network dimensions, characterized by network density exceeding 0.7 coupled with intrinsic dimensionality below 1.5. These windows occurring in June, July, and September 2022 represent periods of maximum geometric network coordination, wherein dimensional collapse, manifold flattening, and network hyperdensification occurred in synchronized fashion. The July 2022 extreme demonstrates the most dramatic coordination: density reached 0.971, dimensionality collapsed to 1.061, smoothness elevated to near-maximum, and Ricci curvature surged to 15.4. This constellation of extreme values across independent geometric and topological measures confirms that mid-2022 witnessed holistic structural transformation rather than isolated anomalies in particular metrics.

Table 10 presents the complete correlation structure among key geometric and network measures. Notable patterns include the uniformly strong negative correlations between intrinsic dimensionality and all network connectivity measures, the systematic positive associations between smoothness and network integration indicators, and the complex relationships involving curvature measures wherein Gaussian and mean curvatures exhibit opposite correlation patterns with network metrics. The geodesic distance measure demon-

strates moderate positive correlations with Gaussian curvature and mean curvature while exhibiting weak negative correlation with smoothness, indicating that periods of elevated within-manifold distances (elongated structure) correspond to lower dimensional regimes with reduced smoothness.

Table 10. Correlation matrix for integrated geometric and network measures. Values represent Pearson correlation coefficients computed across 178 temporal windows. Statistically significant correlations at $p < 0.001$ level appear in bold. Geometric measures include Gaussian curvature, mean curvature, intrinsic dimensionality, tangent smoothness, and geodesic distance. Network measures include density, clustering coefficient, Ricci curvature, and edge count.

Geometric Measure	Density	Clustering	Ricci Curvature	Edge Count
Gaussian Curvature	**−0.386**	−0.319	**−0.647**	**−0.386**
Mean Curvature	**−0.549**	**−0.384**	**−0.410**	**−0.549**
Intrinsic Dimensionality	**−0.539**	**−0.484**	**−0.548**	**−0.539**
Tangent Smoothness	**+0.582**	**+0.477**	**+0.655**	**+0.582**
Geodesic Distance	+0.005	−0.054	−0.307	+0.005

The integrated dashboard in Figure 8 enables visual identification of synchronized transitions across geometric and network domains. The top left panel displays Gaussian curvature temporal evolution, maintaining stable baseline throughout most periods with the notable mid-2022 transition visible as increased variance rather than systematic level shift. The middle left panel presents network density evolution, clearly exhibiting the dramatic mid-2022 spike to near-unity values that proved transient, with density returning to elevated but non-extreme levels thereafter. The bottom left panel shows Ricci curvature trajectory, demonstrating multiple spike episodes with the largest occurring during mid-2022, confirming coordinated timing with network densification.

The right column panels present distributional perspectives complementing temporal trajectories. The upper right scatter plot of Gaussian curvature versus density reveals a diffuse cloud structure with color gradient indicating temporal progression, wherein recent high-density observations appear at the cloud's right edge. The middle right panel displays intrinsic dimensionality distribution, clearly showing modal concentration near 2.0 dimensions with the negatively-skewed structure reflecting episodic low-dimensionality excursions. The lower right panel presents clustering coefficient distribution, exhibiting substantial spread across the range 0.3 to 1.0 with modal concentration near 0.65.

The scatter matrix analysis in Figure 9 provides detailed bivariate relationship characterization through nine panels examining geometric measure pairings with network connectivity. Each panel includes correlation coefficient annotation and fitted regression line, enabling quantitative assessment of relationship strength and linearity. The Gaussian curvature versus density panel (top left) shows diffuse negative relationship with substantial scatter, consistent with the moderate correlation magnitude. The intrinsic dimensionality versus density panel (middle left) exhibits clearer negative trend with reduced scatter, reflecting stronger correlation. The tangent smoothness versus density panel (bottom left) demonstrates pronounced positive relationship with relatively tight scatter around the regression line, confirming this as the strongest density predictor among geometric measures.

The correlation heat map in Figure 10 presents the complete pairwise correlation structure using color encoding, with dark red indicating strong positive correlations, dark blue representing strong negative correlations, and white denoting near-zero relationships. The heat map reveals systematic structure wherein geometric manifold measures cluster into groups with similar network correlation patterns. Intrinsic dimensionality, mean curvature, and Gaussian curvature form a group exhibiting uniformly negative correlations

with network measures (blue colors in corresponding rows), while tangent smoothness shows opposite pattern with positive correlations (orange-red colors). Network measures among themselves exhibit strong positive inter-correlations (dark red block in lower right), reflecting their shared sensitivity to underlying correlation strength.

The geometric network integration perspective provides several important insights for market structure interpretation. First, the strong systematic relationships indicate that geometric and topological approaches capture overlapping rather than independent information, with manifold properties and network structure representing different mathematical formalizations of fundamentally similar correlation phenomena. Second, the opposing correlation patterns between dimensionality (negative with connectivity) and smoothness (positive with connectivity) reflect a fundamental duality wherein reduced complexity enables increased integration. Third, the extreme coordination during mid-2022 demonstrates that structural transitions can manifest simultaneously across multiple analytical frameworks, suggesting holistic market reorganization rather than framework-specific artifacts.

The predictive implications prove noteworthy. Geometric measures computed from manifold embeddings can serve as leading indicators for network structural changes, as smoothness and dimensionality shifts precede or coincide with density transitions. Conversely, network topology provides complementary validation for geometric interpretations, as hypothesized manifold transformations should produce corresponding network signature changes if the geometric perspective accurately captures market structure. The correlation magnitudes ranging from 0.4 to 0.7 indicate substantial but imperfect relationships, suggesting geometric and network approaches each contribute unique information despite their overlap, justifying integrated rather than exclusive methodological focus.

4.9. Macro-Financial Linkages

The examination of relationships between geometric network structure and macroeconomic conditions reveals systematic patterns wherein market integration dynamics respond to policy variables and external indicators. Seven macroeconomic variables spanning domestic policy settings (interest rate, credit growth, inflation), external risk factors (CDS spreads, VIX volatility index), exchange rate dynamics (USD/TRY), and commodity prices (Brent crude oil) provide diverse perspectives on economic conditions potentially driving structural evolution. Figure 11 presents the complete correlation matrix between four key geometric network measures and these seven macroeconomic indicators, while Table 11 quantifies the strongest relationships.

Credit growth emerges as the macroeconomic indicator most strongly associated with geometric network structure, achieving a correlation of $r = 0.504$ with Forman–Ricci curvature ($p = 7.21 \times 10^{-13}$), representing the most robust macro-financial linkage identified. This substantial positive correlation indicates that periods of accelerated credit expansion systematically coincide with enhanced network geometric resilience and dense correlation structure. The mechanistic interpretation connects credit conditions to correlation synchronization: elevated credit growth typically reflects accommodative financial conditions with abundant liquidity, enabling coordinated asset price movements as capital flows broadly across market segments, strengthening correlations and densifying networks. Conversely, credit contraction associated with tighter financial conditions produces heterogeneous sector-specific responses as liquidity constraints bind differentially, reducing systematic correlations and generating sparser networks with lower geometric resilience.

Credit growth exhibits equally strong but opposite-signed correlations with Gaussian curvature ($r = -0.482$, $p = 1.01 \times 10^{-11}$) and intrinsic dimensionality ($r = -0.432$, $p = 1.69 \times 10^{-9}$). The negative associations indicate that credit expansion periods correspond to suppressed Gaussian curvature values (reflecting eigenvalue concentration) and

reduced effective dimensionality. This pattern confirms credit conditions as a unifying factor: abundant credit produces low-dimensional dynamics wherein a single credit-driven factor dominates variation across diverse market variables, eliminating independent degrees of freedom and compressing the manifold onto lower-dimensional structures. The correlation magnitude of approximately 0.5 across multiple structural measures establishes credit growth as a primary macro driver of geometric network evolution, explaining roughly 25% of variance in Ricci curvature through this single indicator alone.

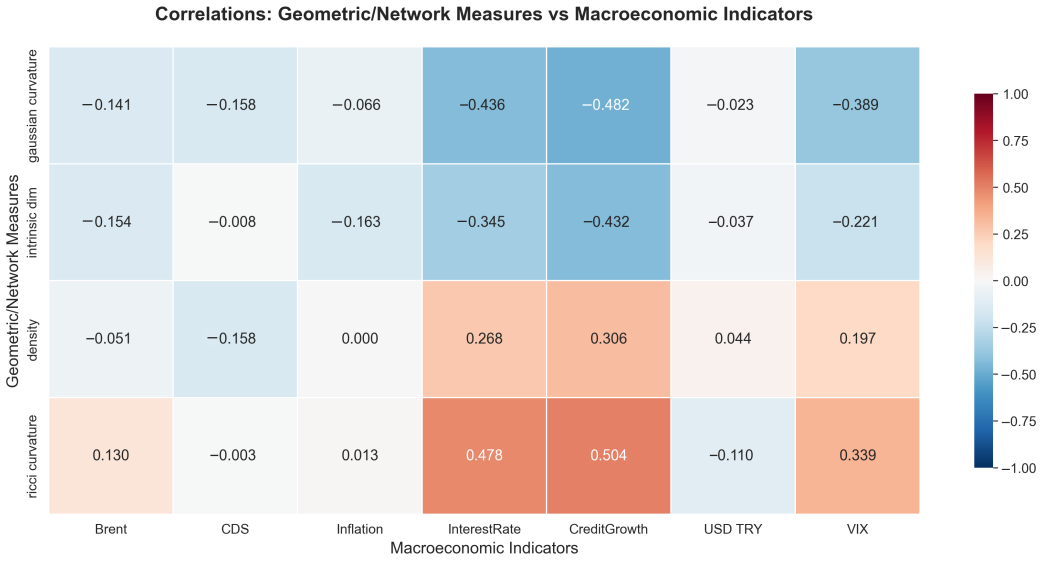


Figure 11. Correlation heat map: geometric network measures versus macroeconomic indicators. Four rows represent geometric network structural measures (Gaussian curvature, intrinsic dimensionality, network density, Forman–Ricci curvature) while seven columns correspond to macroeconomic indicators (Brent oil, CDS spreads, inflation, interest rate, credit growth, USD/TRY exchange rate, VIX volatility). Color encoding employs diverging scheme with dark blue indicating strong negative correlation (approaching -0.5), white representing near-zero correlation, and orange-red signifying positive correlation (approaching $+0.5$). Systematic patterns emerge: interest rate and credit growth columns (center) exhibit strong color intensity with blues for Gaussian curvature and dimensionality contrasting with oranges for density and Ricci curvature, indicating robust policy variable relationships with opposing signs across geometric measures. VIX column (right edge) demonstrates moderate intensity colors consistent with intermediate correlation strength. In contrast, inflation and USD/TRY columns show predominantly light near-white colors reflecting weak associations. The strongest individual correlation appears in Ricci curvature–credit growth cell ($r = +0.504$, dark orange), while Gaussian curvature–credit growth achieves strongest negative association ($r = -0.482$, medium blue). The structured color patterns in policy variable columns versus dispersed weak colors in exchange rate and commodity columns establish monetary–credit conditions as primary macroeconomic drivers of geometric network structure evolution.

Interest rate levels demonstrate similarly robust structural associations, achieving $r = 0.478$ with Ricci curvature ($p = 1.52 \times 10^{-11}$) and $r = -0.436$ with Gaussian curvature ($p = 1.18 \times 10^{-9}$). The positive Ricci correlation indicates that elevated interest rates systematically associate with enhanced network resilience, counter-intuitively suggesting that tighter monetary conditions correspond to more robust correlation structure. This apparently paradoxical relationship likely reflects the Turkish context wherein interest rate increases often respond to currency pressure and inflation concerns, occurring during episodes of market stress that simultaneously produce correlation strengthening through common factor dominance. The correlation pattern suggests interest rates function as both policy response variable and market stress indicator, with elevated rates signaling

conditions producing dense networks through crisis-induced synchronization rather than through accommodative policy channels.

Table 11. Strongest macro-financial correlations ranked by absolute magnitude. geometric network measures include Gaussian curvature (Riemannian), intrinsic dimensionality, network density, and Forman–Ricci curvature. All correlations shown achieve statistical significance at $p < 0.001$ level. Asterisks indicate particularly robust relationships with $p < 10^{-10}$.

Geometric/Network Measure	Macro Indicator	Correlation	*p*-Value
Ricci Curvature	Credit Growth	$+0.504$ ***	7.2×10^{-13}
Gaussian Curvature	Credit Growth	-0.482 ***	1.0×10^{-11}
Ricci Curvature	Interest Rate	$+0.478$ ***	1.5×10^{-11}
Gaussian Curvature	Interest Rate	-0.436 ***	1.2×10^{-9}
Intrinsic Dimensionality	Credit Growth	-0.432 ***	1.7×10^{-9}
Gaussian Curvature	VIX	-0.389	8.0×10^{-8}
Intrinsic Dimensionality	Interest Rate	-0.345	2.5×10^{-6}
Ricci Curvature	VIX	$+0.339$	3.8×10^{-6}
Density	Credit Growth	$+0.306$	3.2×10^{-5}
Density	Interest Rate	$+0.268$	3.0×10^{-4}

The negative correlation between interest rates and intrinsic dimensionality ($r = -0.345$, $p = 2.47 \times 10^{-6}$) further supports this interpretation, indicating that high interest rate episodes correspond to low-dimensional market dynamics. During periods of monetary tightening in response to macroeconomic stress, markets operate with reduced effective degrees of freedom as common concerns (inflation expectations, currency stability, policy uncertainty) dominate previously independent sectoral factors. The sustained correlations between policy variables and structural measures across 178 windows spanning a decade demonstrate robust rather than spurious relationships, suggesting fundamental channels linking monetary conditions to market topology.

VIX volatility index exhibits moderate negative correlation with Gaussian curvature ($r = -0.389$, $p = 7.95 \times 10^{-8}$) and positive association with Ricci curvature ($r = 0.339$, $p = 3.76 \times 10^{-6}$). These patterns indicate that elevated global volatility periods correspond to enhanced Turkish market integration with dense networks and positive geometric resilience. The VIX associations prove weaker than policy variable correlations, suggesting domestic monetary conditions exert greater influence on market structure than global volatility conditions. However, the statistical significance of VIX relationships confirms that Turkish market topology does not operate in isolation from global risk sentiment, with international volatility spikes producing measurable integration effects through contagion or flight-to-quality dynamics affecting emerging markets collectively.

The intrinsic dimensionality correlation with VIX of $r = -0.221$ ($p = 3.06 \times 10^{-3}$) indicates that global volatility elevations correspond to dimensional reduction in Turkish markets, suggesting that international risk events compress market dynamics onto fewer factors. This dimensional compression during global stress episodes reflects the well-documented phenomenon wherein correlations increase during crises as idiosyncratic factors diminish in importance relative to systematic risk concerns. The relatively modest correlation magnitude indicates Turkish markets maintain partial autonomy from global volatility dynamics, with dimensional structure determined substantially by domestic factors rather than purely tracking international conditions.

Network density demonstrates moderate positive correlations with both credit growth ($r = 0.306$, $p = 3.18 \times 10^{-5}$) and interest rates ($r = 0.268$, $p = 2.99 \times 10^{-4}$), confirming that policy variable relationships extend across multiple structural measures rather than concentrating in specific geometric indicators. The density correlations prove weaker than

Ricci curvature relationships, suggesting that geometric resilience measures capture policy sensitivity more powerfully than simple connectivity counts. This finding indicates that credit and interest rate variations influence not merely the number of correlations exceeding threshold but more fundamentally the geometric character of correlation structure, affecting neighborhood overlap and curvature properties beyond what density changes alone would predict.

Inflation exhibits weak correlations with all geometric network measures, achieving maximum absolute correlation magnitude of only $r = -0.163$ with intrinsic dimensionality. This surprisingly modest relationship indicates that inflation dynamics during the observation period did not systematically drive market structure evolution despite inflation's macroeconomic centrality. The weak correlation may reflect several factors: inflation measurement incorporating diverse components responding heterogeneously to market conditions, nonlinear relationships wherein structural impacts concentrate at inflation extremes absent from the sample, or timing lags wherein inflation effects materialize with delays not captured in contemporaneous correlations. The contrast between inflation's network centrality and its weak structural correlations highlights important distinctions between topological importance within correlation networks versus influence on network structure evolution.

USD/TRY exchange rate demonstrates universally weak correlations with geometric network measures, achieving maximum absolute magnitude of only $r = -0.110$ with Ricci curvature, failing to reach statistical significance ($p = 0.143$). This null finding proves particularly noteworthy given exchange rate volatility's prominence in Turkish macroeconomic discourse during the observation period. The absence of systematic exchange rate–structure relationships suggests that currency movements, despite their economic importance, do not reliably predict or correspond to geometric network reorganizations. This pattern may reflect exchange rate dynamics operating orthogonally to correlation structure drivers, with currency movements producing primarily level shifts in asset prices rather than correlation pattern changes, or alternatively may indicate that exchange rate effects on structure materialize through indirect channels (inflation expectations, policy responses) rather than direct mechanisms.

CDS sovereign risk spreads exhibit weak negative correlations with Gaussian curvature ($r = -0.158$, $p = 0.035$) and density ($r = -0.158$, $p = 0.035$), barely achieving statistical significance and representing substantially weaker relationships than policy variables. The modest CDS correlations suggest that sovereign risk perceptions captured in derivative markets do not powerfully drive market structure evolution, potentially reflecting CDS spreads as lagging rather than leading indicators of market stress; alternatively, it could indicate that external sovereign risk assessments influence Turkish markets less systematically than domestic monetary conditions.

Brent crude oil prices demonstrate uniformly weak correlations across all geometric network measures, with maximum absolute magnitude of $r = -0.154$ with intrinsic dimensionality. The negligible oil price relationships indicate that energy commodity dynamics, despite their macroeconomic relevance for a net energy importing economy, do not systematically correspond to structural transformations. This finding suggests market structure responds primarily to monetary and financial conditions rather than real economy commodity price shocks during the observed period.

The systematic pattern whereby policy variables (credit growth, interest rates) achieve robust structural correlations while external indicators (exchange rate, oil prices) and outcome variables (inflation) exhibit weak relationships provides insight into structural change drivers. Market geometric network reorganizations appear fundamentally linked to monetary and credit conditions rather than responding mechanically to exchange rate movements or com-

modity prices. This pattern suggests that correlation structure evolution reflects primarily financial sector dynamics and policy regime characteristics rather than external shocks or inflation outcomes. The policy variable dominance indicates that central bank actions and credit market conditions constitute the primary determinants of whether markets operate in high-dimensional dispersed regimes or low-dimensional synchronized configurations.

The correlation heat map in Figure 11 visually encodes the complete relationship structure using color gradients. The policy variable columns (interest rate and credit growth) exhibit systematic color patterns with strong blues (negative correlations) for Gaussian curvature and intrinsic dimensionality contrasting with oranges and reds (positive correlations) for density and Ricci curvature. This structured pattern confirms policy variables as coherent drivers producing coordinated effects across multiple structural dimensions. In contrast, the inflation and exchange rate columns show predominantly light colors reflecting weak near-zero correlations, while VIX demonstrates intermediate intensity colors consistent with moderate association strength.

The opposing correlation signs between Gaussian curvature (negative with policy variables) and Ricci curvature (positive with policy variables) merit emphasis, as both ostensibly measure curvature properties. This pattern reflects the fundamental differences between these geometric concepts: Gaussian curvature in the implemented formulation captures eigenvalue ratio structure related to dimensional uniformity, while Forman–Ricci curvature quantifies discrete network neighborhood overlap. The systematic opposition indicates these geometric properties respond inversely to macroeconomic conditions, with credit expansion producing concentrated eigenvalue structure (suppressed Gaussian curvature) but enhanced neighborhood overlap (elevated Ricci curvature).

The magnitude hierarchy wherein credit growth and interest rates achieve correlations approaching 0.5 while most other indicators remain below 0.2 establishes a clear pecking order of macroeconomic influences. The policy variable dominance suggests that structural monitoring frameworks should prioritize credit conditions and monetary stance as leading indicators for geometric network transitions. Conversely, the weak exchange rate and oil price relationships indicate these variables provide limited early warning value for structural transformations despite their importance for other economic outcomes.

4.10. Crisis Period Comparative Analysis

The systematic comparison of geometric network structure across five distinct market regimes reveals heterogeneous responses to different stress episodes, enabling differentiation between transient volatility effects and lasting structural transformations. Figure 12 presents comparative bar charts with error bands for four key measures across the pre-crisis baseline (2019), the COVID-19 pandemic (March–June 2020), the currency crisis (December 2021–March 2022), the geometric transition (October 2022–March 2023), and the post-transition recovery (2024). Table 12 provides comprehensive quantitative characterization including both central tendencies and dispersion measures.

The pre-crisis baseline period from 2019 establishes reference values characterizing the Turkish financial market structure during a relatively stable regime preceding the major disruptions of subsequent years. Intrinsic dimensionality averages $\tilde{m} = 2.39 \pm 0.31$ dimensions, representing the highest effective complexity across all examined periods and indicating market operation with approximately two to three independent factors. Network density maintains moderate baseline of $\delta = 0.266 \pm 0.063$, corresponding to roughly one-quarter of potential correlations exceeding threshold. Forman–Ricci curvature exhibits mean $\bar{\mathcal{F}} = 1.50 \pm 1.51$, representing modest positive geometric resilience with substantial within-period variability. Tangent space smoothness averages 0.472 ± 0.026, indicating moderate local manifold regularity. This pre-crisis configuration reflects a market

structure balancing integration through financial sector connectivity against maintained sectoral autonomy, operating with multiple effective degrees of freedom and moderate correlation strength.

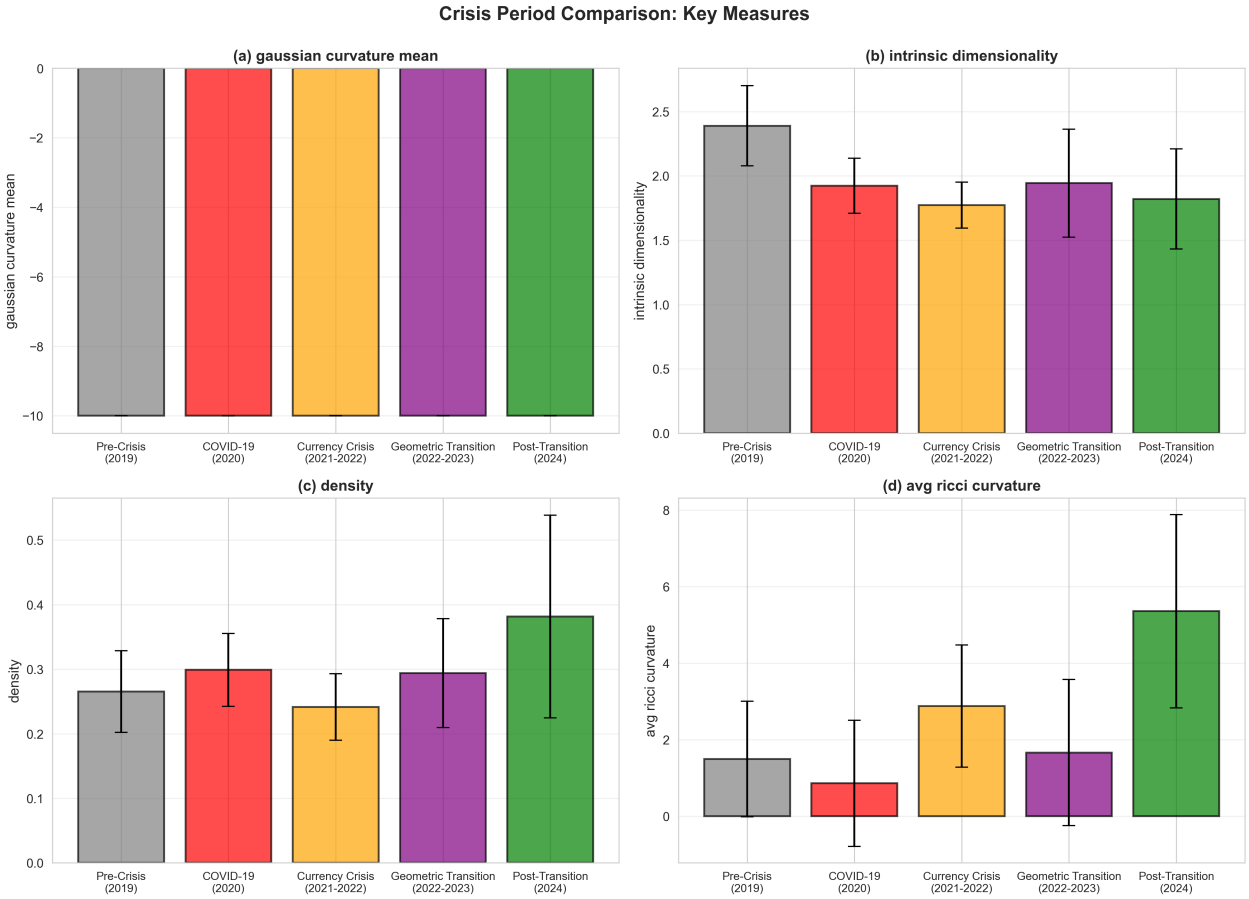


Figure 12. Crisis period comparative analysis across four key structural measures. Color encoding: pre-crisis baseline (gray), COVID-19 (red), currency crisis (orange), geometric transition (purple), post-transition (green). Error bars indicate plus/minus one standard deviation, quantifying within-period variability. Panel (**a**): Gaussian curvature maintains stable baseline across all periods at -10.0 in logarithmic scale, reflecting persistent eigenvalue ratio structure. Panel (**b**): intrinsic dimensionality exhibits systematic suppression across all crisis periods relative to pre-crisis baseline of 2.39 dimensions, with currency crisis achieving minimum of 1.77 dimensions and post-transition demonstrating persistent reduction to 1.82 dimensions. Geometric transition shows largest error bars indicating extreme within-period volatility. Panel (**c**): network density demonstrates heterogeneous pattern with COVID-19 and transition producing modest elevation, currency crisis uniquely featuring suppression below baseline, and post-transition achieving maximum of 0.382 representing 43.7% increase with largest error bars indicating continued volatility. Panel (**d**): Ricci curvature exhibits most dramatic evolution with COVID-19 producing unique suppression to 0.86 (only negative-change crisis), currency crisis elevating to 2.88, and post-transition achieving extraordinary amplification to 5.36 representing 258% increase over baseline. The systematically elevated post-transition values across density, clustering, and Ricci curvature combined with persistent dimensional suppression establish lasting structural transformation rather than transient crisis response.

The COVID-19 pandemic period produces measurable but selective structural impacts distinguishable from both the pre-crisis baseline and subsequent episodes. Intrinsic dimensionality declines to $\tilde{m} = 1.92 \pm 0.21$ dimensions, representing a 19.5% reduction relative to baseline and signifying dimensional compression as pandemic-related systematic factors dominated previously independent dynamics. Network density increases modestly to $\delta = 0.299 \pm 0.057$, corresponding to 12.6% elevation, confirming correlation strengthen-

ing but at magnitudes substantially below subsequent extremes. The most distinctive COVID-19 signature appears in Forman–Ricci curvature, which uniquely declines to $\bar{\mathcal{F}} = 0.86 \pm 1.65$, representing a 42.6% suppression relative to baseline and constituting the only major crisis episode featuring geometric resilience reduction rather than enhancement.

Table 12. Comprehensive crisis period comparison. Values represent period means with standard deviations across windows within each regime. Percentage changes computed relative to pre-crisis (2019) baseline. All geometric network measures demonstrate distinct signatures across crisis episodes, with post-transition period exhibiting persistent structural elevation.

Measure	Period Mean ± Std					Range
	Pre-Crisis (2019)	**COVID-19 (2020)**	**Currency (2021–2022)**	**Transition (2022–2023)**	**Post-Trans (2024)**	
Intrinsic Dim.	2.39 ± 0.31 (baseline)	1.92 ± 0.21 (-19.5%)	1.77 ± 0.18 (-25.8%)	1.94 ± 0.42 (-18.7%)	1.82 ± 0.39 (-23.8%)	0.62
Density	0.266 ± 0.063 (baseline)	0.299 ± 0.057 ($+12.6\%$)	0.241 ± 0.052 (-9.1%)	0.294 ± 0.084 ($+10.8\%$)	0.382 ± 0.157 ($+43.7\%$)	0.140
Clustering	0.559 ± 0.105 (baseline)	0.586 ± 0.024 ($+4.8\%$)	0.705 ± 0.086 ($+26.1\%$)	0.612 ± 0.119 ($+9.5\%$)	0.694 ± 0.118 ($+24.1\%$)	0.146
Ricci Curvature	1.50 ± 1.51 (baseline)	0.86 ± 1.65 (-42.6%)	2.88 ± 1.59 ($+92.2\%$)	1.66 ± 1.91 ($+11.1\%$)	5.36 ± 2.53 ($+258\%$)	4.50
Smoothness	0.472 ± 0.026 (baseline)	0.530 ± 0.034 ($+12.3\%$)	0.581 ± 0.048 ($+23.3\%$)	0.524 ± 0.025 ($+11.2\%$)	0.561 ± 0.074 ($+19.0\%$)	0.110
N Windows	18	6	6	9	9	

The COVID-19 Ricci curvature suppression distinguishes this episode from all other crises, indicating that the pandemic's network impact manifested primarily through geometric vulnerability rather than hypersynchronization. This pattern reflects the pandemic's character as an exogenous real-economy shock producing heterogeneous sectoral responses: certain sectors (technology, e-commerce) benefited while others (tourism, retail, energy) suffered severely, generating divergent trajectories that reduced neighborhood overlap despite moderately strengthening average correlations. The low Ricci curvature of 0.86 during COVID-19 represents the unique instance wherein elevated density (0.299) coincides with suppressed geometric resilience, demonstrating that correlation strengthening does not automatically produce redundancy if correlations concentrate along specific patterns rather than distributing broadly. The COVID-19 period's relatively low dimensionality standard deviation of 0.21 indicates stable reduced complexity throughout the acute phase, lacking the wild fluctuations characterizing later episodes.

The currency crisis period of late 2021–early 2022 exhibits a distinctive structural signature combining locally elevated clustering with paradoxically reduced baseline density. Intrinsic dimensionality declines to period minimum of $\tilde{m} = 1.77 \pm 0.18$ dimensions, representing the most extreme dimensional compression across baseline comparison periods (excluding the acute mid-2022 geometric transition not fully captured in the currency crisis window). Network density counter-intuitively decreases to $\delta = 0.241 \pm 0.052$, representing the only crisis episode featuring density suppression below baseline, declining 9.1% relative to pre-crisis levels. However, clustering coefficient surges to $c = 0.705 \pm 0.086$, achieving 26.1% elevation and representing maximum local cohesion across crisis periods. Ricci curvature rises to $\bar{\mathcal{F}} = 2.88 \pm 1.59$, nearly doubling the baseline value with 92.2% increase.

This unusual combination of reduced global connectivity with enhanced local clustering indicates the currency crisis produced modular network reorganization wherein tight within-community correlations strengthened substantially while between-community

connections weakened or disappeared, reducing overall density despite elevated clustering. The geometric interpretation suggests formation of distinct sectoral communities operating in relative isolation, potentially reflecting differential currency exposure or policy response sensitivity producing divergent dynamics across market segments. The elevated Ricci curvature despite reduced density demonstrates that geometric resilience can strengthen through enhanced neighborhood overlap within connected components even as the network becomes less globally integrated. The currency crisis period exhibits the lowest intrinsic dimensionality standard deviation of 0.18, indicating stable low-dimensional dynamics throughout the episode without the extreme fluctuations of later periods.

The geometric transition period of October 2022–March 2023 captures the aftermath of the unprecedented mid-2022 structural disruption while averaging over windows both during the acute phase and subsequent initial recovery. Intrinsic dimensionality averages $\tilde{m} = 1.94 \pm 0.42$ dimensions, exhibiting the highest within-period standard deviation across all regimes at 0.42 dimensions, reflecting enormous volatility as dimensionality recovered from the extreme August 2022 minimum of 0.43 toward more typical values. Network density returns to near-baseline at $\delta = 0.294 \pm 0.084$, marginally elevated 10.8% relative to pre-crisis but substantially reduced from the mid-2022 peak density, exceeding 0.9. Ricci curvature demonstrates mean $\bar{\mathcal{F}} = 1.66 \pm 1.91$, essentially matching baseline levels but with dramatically elevated standard deviation indicating unstable geometric resilience oscillating between vulnerability and robustness states.

The geometric transition period's defining characteristic emerges from its extreme within-period variability rather than displaced means. The dimensionality standard deviation of 0.42 exceeds the pre-crisis value by 35% and represents 22% of the period mean, indicating that effective complexity varied by full dimensions across successive windows. Similarly, the Ricci curvature standard deviation of 1.91 exceeds the pre-crisis value by 26% and equals 115% of the period mean, implying geometric resilience fluctuated from near-zero to values approaching 4 within the same episode. This extreme instability characterizes the transition as a regime-switching period wherein market structure oscillated between competing configurations rather than settling into consistent organization, potentially reflecting uncertainty about the post-crisis equilibrium or policy regime ambiguity producing alternating correlation patterns.

The post-transition period from 2024 exhibits the most dramatic structural departures from baseline across multiple measures, indicating lasting rather than transient transformation. Network density achieves $\delta = 0.382 \pm 0.157$, representing 43.7% elevation relative to pre-crisis and constituting the highest period mean despite occurring nearly two years after the acute mid-2022 episode. The density standard deviation of 0.157 exceeds all other periods, implying continued structural volatility with density fluctuating between values approaching baseline and exceeding 0.5. Ricci curvature undergoes extraordinary amplification to $\bar{\mathcal{F}} = 5.36 \pm 2.53$, representing a stunning 258% elevation relative to baseline and establishing a new high-resilience regime fundamentally distinct from pre-crisis structure.

The post-transition Ricci curvature of 5.36 exceeds even the currency crisis elevated value of 2.88 by 86%, confirming this represents a qualitative shift rather than merely return to stressed-but-typical configuration. The combination of elevated density and dramatically amplified Ricci curvature indicates the post-transition market operates with both more numerous correlations and substantially greater redundancy through neighborhood overlap, corresponding to a hypersynchronized state wherein diverse pathways connect most variable pairs. Intrinsic dimensionality remains persistently suppressed at $\tilde{m} = 1.82 \pm 0.39$ dimensions, down 23.8% from baseline, indicating the market has not recovered its pre-crisis effective complexity despite occurring in 2024 well after acute stresses. This dimensional deficit suggests fundamental reduction in independent factors charac-

terizing market dynamics, potentially reflecting enhanced policy coordination, increased financial integration, or structural shifts in investor behavior producing systematic rather than idiosyncratic focus.

The post-transition clustering coefficient of $c = 0.694 \pm 0.118$ achieves 24.1% elevation, nearly matching the currency crisis maximum and indicating sustained local cohesion enhancement. Tangent smoothness rises to 0.561 ± 0.074, representing 19.0% increase, confirming enhanced manifold regularity persists in the post-crisis regime. The constellation of persistently elevated connectivity, dramatically amplified geometric resilience, suppressed dimensionality, and enhanced smoothness establishes the post-transition period as operating under fundamentally altered structural dynamics rather than having recovered pre-crisis configuration. The substantial within-period variability across measures indicates the new regime exhibits greater instability than the pre-crisis baseline, potentially reflecting reduced structural predictability or enhanced sensitivity to external shocks.

Examination of key regime transitions provides insight into structural change dynamics. The pre-crisis to COVID-19 transition features dimensional reduction ($2.39 \rightarrow 1.92$, decline of 0.47 dimensions), modest density increase ($0.266 \rightarrow 0.299$), and unique Ricci curvature suppression ($1.50 \rightarrow 0.86$, decline of 0.64), characterizing the pandemic as producing complexity reduction with geometric vulnerability rather than resilience. The currency crisis to geometric transition shift shows partial dimensional recovery ($1.77 \rightarrow 1.94$, increase of 0.17 dimensions), modest density elevation ($0.241 \rightarrow 0.294$), and paradoxical Ricci decline ($2.88 \rightarrow 1.66$, decrease of 1.21) reflecting the transition period's averaging over both extreme peaks and subsequent normalization.

The geometric transition to post-transition evolution demonstrates minimal dimensional change ($1.94 \rightarrow 1.82$, decline of 0.12 dimensions), substantial density increase ($0.294 \rightarrow 0.382$, rise of 0.09), and extraordinary Ricci curvature amplification ($1.66 \rightarrow 5.36$, surge of 3.70). This transition pattern indicates the post-crisis regime consolidated elevated connectivity established during the transition while dramatically enhancing geometric redundancy through neighborhood overlap strengthening. The Ricci curvature more than tripling between successive regimes represents the single largest measure change across any transition, confirming geometric resilience as the dimension exhibiting most dramatic structural transformation.

Comparison of crisis signatures reveals COVID-19 as uniquely producing geometric vulnerability despite correlation strengthening, the currency crisis generating modular rather than global integration, the geometric transition exhibiting extreme instability across successive windows, and the post-transition regime establishing a persistent hypersynchronized configuration with dramatically elevated resilience but reduced complexity. These heterogeneous patterns demonstrate that different stress types produce qualitatively distinct structural responses rather than universal crisis signatures. External real-economy shocks (COVID-19) reduce resilience through heterogeneous sectoral impacts, currency crises produce modular reorganization with community-specific responses, while financial sector or policy regime transitions (2022–2023) generate wholesale structural transformations producing lasting integration increases and dimensional reductions.

The failure of intrinsic dimensionality, clustering, and density to recover baseline values even in 2024 establishes the 2022–2023 episode as a structural break rather than transient perturbation. Markets operating with 24% reduced dimensionality, 44% elevated density, and 258% amplified Ricci curvature two years post-crisis exhibit fundamentally altered dynamics unlikely to represent temporary effects. The persistent structural elevation suggests either permanent shifts in market organization (enhanced financial integration, reduced sectoral autonomy, increased systematic factor dominance)

or establishment of a new policy regime producing sustained correlation amplification and dimensional compression.

The within-period variability analysis reveals the geometric transition and post-transition regimes exhibit substantially elevated standard deviations relative to earlier periods, indicating reduced structural stability. The post-transition density standard deviation of 0.157 exceeds the pre-crisis value by 148%, while the Ricci curvature standard deviation of 2.53 increases 67% relative to baseline. This elevated dispersion indicates the post-crisis market structure fluctuates more dramatically between successive windows than the pre-crisis regime, potentially reflecting enhanced sensitivity to policy signals, increased correlation regime-switching frequency, or reduced stabilizing mechanisms that previously constrained structural variation. The combination of elevated means and increased variability characterizes the post-transition market as both more integrated and less stable than its pre-crisis configuration.

5. Discussion

This study's integrated geometric–topological analysis reveals fundamental structural transformations in Turkish financial markets that transcend conventional volatility or correlation magnitude changes, documenting an unprecedented mid-2022 episode featuring coordinated dimensional collapse, manifold flattening, and network hyperdensification that established a persistent new regime still evident in 2024–2025 data. The synthesis of Riemannian geometric properties with discrete network topology provides complementary perspectives on market organization, demonstrating that structure evolution responds systematically to monetary–credit conditions while exhibiting crisis-specific signatures distinguishing external shocks from endogenous financial sector transformations. These findings contribute to market microstructure theory, systemic risk assessment frameworks, and policy design considerations for emerging market financial stability.

5.1. Interpretation of the 2022–2023 Structural Break

The extraordinary geometric transition during mid-2022, characterized by intrinsic dimensionality collapse from baseline values near 2.4 dimensions to an extreme minimum of 0.43 dimensions in August 2022, represents the defining empirical finding requiring comprehensive interpretation. This seven-week period witnessed simultaneous extrema across multiple independent structural measures: network density surged from typical values of 0.25 to 0.30 toward near-unity at 0.97, Forman–Ricci curvature spiked from baseline values around 1.5 to maximum 16.0, and tangent space smoothness elevated substantially; collectively indicate holistic market reorganization rather than isolated metric anomalies. The dimensional collapse to 0.43 implies effective univariate dynamics wherein a single factor explained virtually all variation across the seventeen-variable system, eliminating the multiple independent degrees of freedom characterizing normal market operation.

Several interconnected mechanisms likely contributed to this structural transformation. First, the period coincided with intensified unconventional monetary policy implementation following extended negative real interest rates, producing unusual financial conditions wherein traditional policy transmission channels operated abnormally. Credit growth remained elevated despite currency pressures, potentially reflecting policy-directed lending initiatives or regulatory forbearance maintaining credit supply despite underlying strains. These conditions may have produced artificial correlation amplification as policy interventions override market-determined allocations, forcing coordinated movements across sectors that would naturally exhibit independent dynamics under normal circumstances. The extremely low dimensionality suggests markets operated under overwhelming policy

dominance wherein monetary authority actions constituted the sole meaningful factor, subordinating sectoral fundamentals and idiosyncratic considerations.

Second, the timing suggests interaction between domestic policy regime uncertainty and global tightening cycles, with the Federal Reserve implementing aggressive rate increases during this period producing capital flow reversals from emerging markets. Turkish markets facing simultaneous domestic policy unorthodoxy and international liquidity withdrawal may have experienced forced deleveraging or portfolio rebalancing producing synchronized selling pressure across diverse assets. Such coordinated liquidation naturally generates artificial correlation spikes as price discovery temporarily suspends and systematic factors dominate. The subsequent partial normalization during late 2022 and 2023, with dimensionality recovering toward 2.0 dimensions while density declined from extreme peaks, supports interpretation of the acute phase as reflecting temporary liquidity or sentiment crisis rather than permanent fundamental reorganization.

However, the critical finding emerges from the post-transition 2024 period analysis, which demonstrates that structural elevation persisted well beyond the acute episode despite apparent macroeconomic stabilization. Network density in 2024 averaged 0.382, representing 43.7% elevation relative to the 2019 baseline and constituting the highest period mean despite occurring nearly two years after the acute mid-2022 spike. More dramatically, Forman–Ricci curvature achieved mean 5.36 during 2024, representing an extraordinary 258% amplification relative to baseline and far exceeding even the currency crisis elevated values. These persistent elevations indicate the 2022 episode catalyzed lasting rather than transient changes, potentially through several mechanisms: permanent shifts in investor behavior following the extreme coordination experience, regulatory or policy framework changes implemented during or after the crisis, structural transformations in financial sector organization, or fundamental alterations in correlation generating processes.

The failure of intrinsic dimensionality to recover baseline values proves particularly significant for assessing transformation permanence. Even in 2024, effective dimensionality averaged only 1.82 dimensions, remaining 23.8% suppressed relative to the 2.39 dimension 2019 baseline. This persistent dimensional deficit spanning two years post-crisis indicates fundamental reduction in market complexity rather than temporary factor dominance. Potential explanations include enhanced financial sector integration reducing sectoral autonomy, increased policy coordination across domains eliminating previously independent policy instruments as variation sources, or structural changes in firm behavior producing systematic rather than idiosyncratic focus. The combination of persistently elevated connectivity, dramatically amplified geometric resilience, and sustained dimensional suppression establishes the 2022-2023 episode as a genuine structural break rather than extreme volatility episode within stationary dynamics.

5.2. Crisis Heterogeneity and Structural Signatures

The comparative analysis across five distinct market regimes reveals that different crisis types produce qualitatively distinct structural signatures, challenging universal crisis characterization and suggesting that stress episode classification requires attention to underlying mechanisms rather than merely outcome severity. The COVID-19 pandemic's structural impact, characterized by moderate dimensional reduction to 1.92 dimensions combined with unique Forman–Ricci curvature suppression to 0.86 representing 42.6% decline, distinguishes this external real-economy shock from financial sector or policy regime crises. The Ricci curvature suppression indicates that pandemic-related correlation increases manifested primarily through sparse high-magnitude connections rather than dense redundant pathways, reflecting heterogeneous sectoral responses wherein certain industries benefited while others suffered severely.

This pattern contrasts sharply with the 2021–2022 currency crisis signature featuring elevated clustering coefficient (0.705, up 26.1%) combined paradoxically with reduced global density (0.241, down 9.1%), indicating modular reorganization wherein within-community correlations strengthened substantially while between-community connections weakened. This modular structure likely reflects differential currency exposure or policy sensitivity producing divergent sectoral dynamics, with domestically-oriented sectors exhibiting distinct correlation patterns from internationally-exposed or import-dependent industries. The elevated Ricci curvature (2.88) despite reduced density demonstrates that geometric resilience can strengthen through enhanced local redundancy even as global integration declines, suggesting the currency crisis produced defensive clustering rather than systemic hypersynchronization.

The heterogeneous crisis signatures carry important implications for early-warning system design and stress testing frameworks. Monitoring frameworks focused exclusively on correlation magnitude increases or network density elevations would have detected the 2022 geometric transition and currency crisis but potentially missed or misinterpreted the COVID-19 impact characterized by geometric vulnerability rather than hyperdensification. Similarly, policy responses appropriate for managing systemic correlation increases may prove counterproductive during episodes featuring modular reorganization, as interventions targeting global integration might inadvertently disrupt beneficial within-community risk sharing. The crisis-specific structural patterns suggest that effective macroprudential frameworks require multiple complementary monitoring approaches capturing both global integration and local resilience, density and modularity, dimensional complexity and geometric regularity.

The extreme within-period variability characterizing the geometric transition regime, with intrinsic dimensionality standard deviation of 0.42 dimensions representing 22% of the period mean, indicates this episode exhibited regime-switching character wherein market structure oscillated between competing configurations rather than settling into consistent organization. This instability potentially reflects policy uncertainty, with markets unable to establish equilibrium correlation patterns amid ambiguous or contradictory policy signals. The subsequent post-transition period's continued elevated variability across multiple measures suggests the new structural regime exhibits greater inherent instability than pre-crisis configurations, potentially reflecting reduced buffering capacity, enhanced shock sensitivity, or fundamental uncertainty about appropriate equilibrium structures in the post-crisis environment.

5.3. Geometric Network Integration and Methodological Contributions

The systematic relationships between geometric manifold properties and network topological measures, exemplified by the 0.655 correlation between tangent space smoothness and Forman–Ricci curvature, demonstrate that these ostensibly independent analytical frameworks capture substantially overlapping information about underlying correlation structure. This convergence validates geometric–topological integration while raising questions about optimal framework selection for specific analytical objectives. The strong positive associations between smoothness and network connectivity measures indicate that manifold regularity and dense correlation structure represent nearly equivalent phenomena viewed through different mathematical lenses, differing primarily in formalism rather than captured aspects of market organization.

However, the complementary information revealed through integrated analysis justifies methodological pluralism rather than exclusive framework adoption. The opposing correlation patterns between Gaussian curvature (negative with policy variables) and Forman–Ricci curvature (positive with policy variables) demonstrate these measures cap-

ture fundamentally different geometric properties despite both ostensibly quantifying curvature. Gaussian curvature's logarithmic formulation reflects eigenvalue ratio structure related to dimensional uniformity; meanwhile, Forman–Ricci curvature quantifies discrete neighborhood overlap, explaining their inverse temporal evolution. This divergence indicates that comprehensive structural characterization requires multiple geometric perspectives rather than relying on single curvature measures assumed to capture all relevant geometric information.

The intrinsic dimensionality measure's strong negative correlations with all network connectivity indicators, consistently achieving magnitudes near -0.5, establishes a fundamental dimensionality–connectivity trade-off wherein reduced effective complexity enables enhanced integration. This relationship admits clear mechanistic interpretation: markets operating with multiple independent factors naturally produce sparse correlation networks as variables responding to distinct dimensions exhibit weak pairwise associations, while dimensional reduction forces universal synchronization as all variables become dominated by common factors. The trade-off magnitude indicates approximately 25% of variance in network density can be explained by intrinsic dimensionality alone, representing substantial predictive power from a single geometric descriptor and validating dimensionality as a fundamental structural characteristic warranting continuous monitoring.

The geometric framework's ability to identify the mid-2022 extreme through multiple independent measures including Gaussian curvature spike, dimensionality collapse, smoothness elevation, and geodesic distance compression demonstrates that manifold embedding captures crisis signatures invisible to conventional volatility or correlation magnitude monitoring. The August 2022 dimensionality minimum of 0.43 would have triggered any reasonable alert threshold, providing real-time crisis identification without requiring complex model estimation or historical calibration. This operational advantage suggests geometric monitoring could complement existing surveillance frameworks focused on price volatility, liquidity measures, or macro-financial indicators, potentially providing earlier or more reliable crisis signals through attention to state space organization rather than outcome variables.

5.4. Macro-Financial Linkages and Policy Implications

The robust correlations between monetary–credit policy variables and geometric network structure, with credit growth achieving $r = 0.504$ with Ricci curvature and $r = -0.482$ with Gaussian curvature, establish policy conditions as primary drivers of structural evolution and suggest that central bank actions influence not merely asset prices or volatility but fundamental market organization. The correlation magnitudes approaching 0.5 indicate that credit conditions alone explain roughly 25% of variance in geometric resilience, representing remarkable predictive power for single macroeconomic indicators and validating credit cycles as central considerations in structural stability assessment. The systematic relationships suggest accommodative credit conditions producing abundant liquidity enable coordinated movements across market segments by relaxing constraints binding differentially across sectors during tighter conditions.

The interest rate correlations following similar patterns, with $r = 0.478$ with Ricci curvature and $r = -0.436$ with Gaussian curvature, initially appear counter-intuitive as elevated rates typically associate with restrictive conditions yet correlate positively with structural integration. This apparent paradox likely reflects the Turkish context wherein rate increases often respond to currency pressure and inflation concerns during stress episodes, making rates simultaneously policy instruments and crisis indicators. The correlations thus capture crisis-induced correlation strengthening rather than policy accommodation effects, with elevated rates signaling conditions producing synchronization through com-

mon stress factors. This dual interpretation highlights challenges in identifying causal policy impacts from observational correlations, suggesting that structural stability assessment requires consideration of policy endogeneity rather than treating policy variables as exogenous drivers.

The surprisingly weak correlations between structural measures and inflation, USD/TRY exchange rate, and Brent oil prices, with magnitudes uniformly below 0.2, indicate these economically important variables exert minimal systematic influence on geometric network organization during the observation period. The null exchange rate finding proves particularly striking given currency volatility's prominence in Turkish macroeconomic discourse, suggesting exchange movements produce primarily level shifts in asset prices rather than correlation pattern changes. This pattern implies that structural monitoring frameworks could potentially disregard exchange rate developments without sacrificing early warning capacity, focusing instead on credit–monetary conditions exhibiting robust structural associations.

The policy implications extend beyond crisis identification to considerations of intervention design. If credit conditions drive structural transformations as the correlations suggest, then macroprudential frameworks targeting correlation amplification or systemic synchronization might operate most effectively through credit aggregates rather than direct capital market interventions. Credit growth restrictions during expansion phases could potentially limit structural vulnerability accumulation by preventing correlation increases that reduce diversification benefits and amplify shock transmission. Conversely, credit support during stress episodes might help maintain structural stability by preventing forced deleveraging producing artificial synchronization, though such interventions risk moral hazard if market participants anticipate systematic backstops.

The persistent post-transition structural elevation raises questions about optimal policy response when facing potentially permanent shifts rather than temporary dislocations. If the 2024 hypersynchronized state with dramatically amplified Ricci curvature and elevated density reflects new equilibrium rather than disequilibrium, then policies attempting restoration of pre-crisis structures may prove futile or counterproductive. However, the elevated within-period variability characterizing the post-transition regime suggests the new configuration exhibits greater instability than baseline, potentially warranting enhanced monitoring or preemptive policy adjustment to prevent cascade dynamics in the more tightly coupled system. The appropriate policy stance thus depends critically on whether the structural transformation reflects efficient adaptation to changed conditions or fragility accumulation requiring intervention.

5.5. Systemic Importance and Network Centrality

The centrality analysis identifying Banking, Inflation, and CDS spreads as the three most systemically important variables based on combined degree, betweenness, and closeness centrality provides actionable guidance for surveillance prioritization and stress testing scenario design. Banking's achievement of maximum betweenness centrality (0.075), combined with tier-one degree and elevated closeness, establishes this sector as the critical structural bridge mediating correlations between other network components, confirming traditional emphasis on bank sector health for systemic stability. The betweenness dominance indicates approximately 7.5% of all shortest paths route through Banking, conferring substantial structural power wherein distress could disrupt correlations among otherwise indirectly connected variables.

The identification of six variables exhibiting precisely zero betweenness—insurance, technology, interest rate, credit growth, USD/TRY, and VIX—proves equally informative, indicating these nodes serve as terminal endpoints rather than intermediaries in the corre-

lation structure. For policy variables within this zero-betweenness group, the structural interpretation suggests their influences propagate through direct correlations with connected variables rather than serving as conduits linking broader market segments. This pattern implies that policy transmission operates with reduced network amplification relative to variables occupying bridge positions, potentially explaining empirical findings of weak or delayed policy impacts during certain episodes if authorities focus on variables exhibiting minimal structural centrality.

The financial sector heterogeneity, with banking achieving uniformly high centrality while finance and insurance occupy peripheral positions, indicates that traditional commercial banking dominates systemic importance while non-bank financial activities maintain limited integration. This intra-sector divergence suggests that regulatory frameworks treating "financial sector" monolithically may misallocate supervisory resources, with non-bank institution oversight receiving attention disproportionate to actual systemic footprint. The centrality hierarchy justifies traditional prudential focus on commercial banks while questioning whether insurance and non-bank finance sectors warrant equivalent regulatory intensity given their minimal structural centrality during the observation period.

5.6. Limitations and Future Research

Several limitations warrant acknowledgment and suggest extensions for future investigation. First, the analysis focuses exclusively on Turkish markets, limiting generalizability to other emerging or developed market contexts. The structural break's distinctiveness may reflect Turkey-specific policy regimes or institutional characteristics, requiring comparative analysis across countries and time periods to establish whether identified patterns represent universal crisis dynamics or idiosyncratic episodes. Multi-country geometric–topological analysis could identify common structural evolution patterns while isolating country-specific factors, potentially enabling classification of economies by structural stability characteristics.

Second, the rolling window approach necessarily introduces temporal aggregation affecting precise timing identification and potentially smoothing abrupt transitions. The 240-day windows provide statistical stability for correlation estimation and geometric computation but sacrifice fine temporal resolution, potentially missing intra-window structural shifts or misattributing transition timing. Alternative approaches utilizing change-point detection algorithms or adaptive windows adjusting to detected regime shifts could provide sharper temporal localization while maintaining estimation precision. The trade-off between temporal resolution and statistical reliability constitutes a fundamental constraint requiring balanced consideration rather than optimal solution.

Third, the analysis treats all variables symmetrically despite potential differences in information content, price discovery leadership, or causal priority. Some variables likely drive correlations while others respond, but the geometric network framework employed herein does not distinguish drivers from followers. Extensions incorporating directed network analysis, Granger causality testing, or information–theoretic measures could identify influence hierarchies within correlation structure, potentially revealing that structural transformations originate in specific sectors or variables before propagating systemically. Such directional analysis could improve early-warning systems by focusing monitoring on leading indicators rather than treating all structural changes equivalently.

Fourth, the correlation threshold selection for network construction, while standard, inevitably affects topology characterization and centrality rankings. Sensitivity analysis across multiple thresholds could assess result robustness and potentially identify threshold-dependent patterns wherein certain structural features emerge only at specific correlation magnitudes. Alternatively, weighted network analysis avoiding arbitrary thresholding

could provide more complete topological characterization, though this comes at the cost of increased computational complexity and interpretation challenges, given the continuous edge weight space.

Fifth, the study focuses on second-moment properties through correlation analysis, potentially missing higher-order dependencies or nonlinear relationships captured through alternative dependence measures. Copula-based approaches, mutual information estimation, or distance correlation methods could reveal tail dependencies or nonlinear associations invisible to Pearson correlation, potentially identifying structural vulnerabilities manifest only during extreme events. The geometric framework could incorporate such alternative dependence measures through suitable distance metric modification, enabling extension beyond linear correlation structure.

Future research could profitably investigate several extensions building on this study's framework. First, incorporating high-frequency data within rolling windows could provide finer temporal resolution while maintaining estimation stability, potentially revealing intraday structural dynamics missed by daily aggregation. Second, expanding variable sets to include additional asset classes, international markets, or firm-level data could characterize correlations spanning broader financial system components. Third, integrating geometric–topological measures into formal early-warning models through machine learning or econometric frameworks could quantify predictive performance for crisis identification. Fourth, developing theoretical models rationalizing observed geometric–topological patterns could connect empirical findings to behavioral or institutional foundations, potentially suggesting specific mechanisms generating observed structure evolution.

5.7. Broader Implications

The findings contribute to evolving understanding of financial market structure as dynamic rather than static, responding systematically to economic conditions and policy regimes while exhibiting crisis-specific transformation patterns. The documented structural break challenges efficient markets perspectives assuming correlation stability or mean reversion, instead suggesting that markets undergo fundamental reorganizations producing persistent regime shifts. These transformations carry implications beyond academic interest, affecting portfolio diversification benefits, systemic risk assessment, regulatory design, and policy transmission mechanisms. The demonstration that monetary–credit conditions drive structural evolution suggests central banks influence not merely short-term price dynamics but fundamental market organization, potentially creating unintended fragilities through prolonged accommodation producing correlation amplification and dimensional reduction.

The geometric–topological integration provides complementary perspectives on market organization that standard approaches miss, suggesting that financial stability frameworks should incorporate state space geometry alongside traditional price, volatility, and correlation monitoring. The operational feasibility of real-time geometric computation using publicly available data indicates these methods could be implemented without prohibitive cost or complexity, providing practical tools for market surveillance and risk management. The crisis-specific structural signatures identified herein could inform stress testing scenario design, with exercises incorporating not merely adverse price paths but associated correlation regime shifts and dimensional transformations observed during historical episodes.

The persistent post-transition structural elevation raises fundamental questions about appropriate benchmark expectations for emerging market correlation structure. If the 2024 hypersynchronized state reflects efficient adaptation to changed global or domestic conditions rather than temporary dislocation, then expecting return to pre-crisis structures may be misguided. Understanding whether observed transformations represent equilibrium

shifts or fragility accumulation remains an open question requiring continued monitoring and theoretical development. The answer carries profound implications for policy design, as interventions appropriate for correcting disequilibrium differ fundamentally from adaptations required for operating within new equilibrium constraints.

6. Conclusions

This study develops and applies an integrated geometric–topological framework for analyzing financial market structure evolution, synthesizing Riemannian manifold geometry with discrete network topology to characterize correlation organization in Turkish financial markets from May 2015 to May 2025. The methodology combines intrinsic dimensionality estimation, curvature tensor computation, correlation network construction, and Forman–Ricci curvature calculation, applied to daily observations across seventeen variables including ten Borsa Istanbul sectoral equity indices and seven macroeconomic indicators.

The central empirical finding documents an extraordinary mid-2022 geometric transition featuring coordinated dimensional collapse from baseline 2.4 dimensions to unprecedented minimum 0.43 dimensions, network density surge to 0.97 from typical 0.25–0.30 values, and Forman–Ricci curvature spike to maximum 16.0 from baseline 1.5. These simultaneous extrema across multiple independent structural measures confirm holistic market reorganization representing a genuine structural break. Critically, the elevation proved persistent rather than transient, with the 2024 post-transition period exhibiting network density 43.7% above baseline, Ricci curvature amplified 258%, and intrinsic dimensionality remaining 23.8% suppressed. This combination establishes permanent structural transformation rather than temporary perturbation, with markets operating under fundamentally altered dynamics unlikely to revert to pre-crisis organization.

Comparative analysis across five distinct regimes reveals crisis heterogeneity challenging universal characterization. COVID-19 produced unique geometric vulnerability through Ricci curvature suppression, the currency crisis exhibited modular reorganization with elevated local clustering but reduced global density, while the geometric transition demonstrated extreme within-period instability. These heterogeneous patterns establish that different stress types produce qualitatively distinct structural signatures requiring crisis-specific monitoring approaches.

The macro-financial linkages analysis identifies monetary–credit policy variables as primary structural drivers, with credit growth achieving $r = 0.504$ correlation with Ricci curvature. Policy variables explain approximately 25% of variance in geometric resilience, while inflation, exchange rate, and oil prices exhibit weak structural correlations below $|r| = 0.2$. This dominance suggests structural monitoring frameworks should prioritize credit–monetary conditions over exchange rate movements, and that macroprudential interventions might operate most effectively through credit aggregates. The centrality analysis reveals Banking, Inflation, and CDS spreads as most systemically important, with Banking achieving maximum betweenness centrality establishing commercial banks as critical structural bridges.

The integrated geometric network analysis demonstrates systematic relationships between manifold properties and topological measures, with tangent smoothness achieving $r = 0.655$ correlation with Ricci curvature. However, opposing patterns between Gaussian and Ricci curvatures validate methodological pluralism. Intrinsic dimensionality exhibits strong negative correlations with network connectivity at magnitudes near -0.5, establishing a fundamental dimensionality–connectivity trade-off wherein reduced complexity enables enhanced integration.

https://doi.org/10.3390/axioms15010034

The findings contribute several methodological and theoretical advances. First, the study demonstrates feasibility and value of geometric–topological integration for financial analysis, with operational implementation using publicly available data. Second, crisis-specific structural signatures challenge universal characterization, suggesting early-warning systems require multiple complementary monitoring approaches. Third, documentation of permanent structural breaks challenges market efficiency perspectives assuming correlation stability, suggesting markets undergo fundamental reorganizations with implications for diversification, risk assessment, and regulation. Fourth, robust credit–monetary correlations with structure suggest central bank actions influence fundamental market organization, potentially creating fragilities through prolonged accommodation.

Policy implications extend across multiple domains. Macroprudential frameworks should incorporate geometric–topological measures alongside traditional volatility tracking, with particular attention paid to intrinsic dimensionality as complexity reduction indicator. Stress testing scenarios should incorporate correlation regime shifts and dimensional transformations specific to crisis types rather than assuming uniform responses. Risk management practices require periodic reassessment of correlation assumptions rather than assuming stationary regimes. The persistent post-crisis elevation raises questions about optimal policy response when facing potentially permanent shifts, as interventions attempting restoration of pre-crisis structures may prove futile if transformations reflect new equilibrium.

Limitations include the following: a single-country focus, limiting generalizability; the rolling window temporal aggregation approach, affecting timing precision; the symmetric variable treatment, ignoring causal priority; the correlation threshold sensitivity; the focus on second-moment properties, potentially leading to missed nonlinear relationships. Future research could profitably incorporate high-frequency data for finer resolution, expand variable sets to include additional asset classes, integrate geometric–topological measures into formal early-warning models, develop theoretical models rationalizing observed patterns, and conduct multi-country comparative analyses to identify universal versus idiosyncratic dynamics.

This study demonstrates that financial market structure evolution exhibits systematic patterns identifiable through integrated geometric–topological analysis, with markets undergoing fundamental transformations producing persistent regime shifts responding to monetary–credit conditions while exhibiting crisis-specific signatures. The documented 2022–2023 structural break in Turkish markets exemplifies such transformation, featuring dimensional collapse, network hyperdensification, and geometric resilience amplification, establishing a persistent hypersynchronized regime evident through 2025. These findings advance market microstructure understanding, provide actionable surveillance tools, and carry implications for macroprudential policy design, with geometric–topological integration offering promising avenues for continued development enhancing financial stability frameworks.

Author Contributions: Conceptualization, L.M.B., M.A.B., Ö.A., and L.G.; methodology, L.M.B., M.A.B., Ö.A., and L.G.; software, M.A.B. and Ö.A.; validation, L.M.B., M.A.B., Ö.A., and L.G.; formal analysis, L.M.B., M.A.B., Ö.A., and L.G.; investigation, L.M.B., M.A.B., Ö.A., and L.G.; resources, L.M.B., M.A.B., Ö.A., and L.G.; data curation, L.M.B., M.A.B., Ö.A., and L.G.; writing—original draft preparation, L.M.B., M.A.B., Ö.A., and L.G.; writing—review and editing, L.M.B., M.A.B., Ö.A., and L.G.; visualization, M.A.B., Ö.A.; supervision, M.A.B.; project administration, L.M.B.; funding acquisition L.G. All authors have read and agreed to the published version of the manuscript.

Funding: This research received no external funding.

Institutional Review Board Statement: Not applicable.

Informed Consent Statement: Not applicable.

Data Availability Statement: The original contributions presented in the study are included in the article, further inquiries can be directed to the corresponding author.

Conflicts of Interest: The authors declare no conflicts of interest.

References

1. Gürkaynak, R.S.; Kısacıkoğlu, B.; Lee, S.S. Exchange rate and inflation under weak monetary policy: Turkey verifies theory. *Econ. Policy* **2023**, *38*, 519–560. [CrossRef]
2. Tümtürk, O. Monetary policy, the price puzzle and inflation expectations: evidence from Türkiye. *Trak. Üniversitesi İktisadi Ve İdari Bilim. Fakültesi E-Dergi* **2025**, *14*, 14–28. [CrossRef]
3. Aslan, M.; Ozgur, O. Financial dollarization and its effects on inflation and output in Turkey: A machine learning approach. *Qual. Quant.* **2024**, *58*, 5777–5804. [CrossRef]
4. Gidea, M.; Katz, Y. Topological data analysis of financial time series: Landscapes of crashes. *Phys. A Stat. Mech. Its Appl.* **2018**, *491*, 820–834. [CrossRef]
5. Yao, J.; Li, J.; Wu, J.; Yang, M.; Wang, X. Change Point Detection in Financial Market Using Topological Data Analysis. *Systems* **2025**, *13*, 875. [CrossRef]
6. Huang, Y.; Kou, G.; Peng, Y. Nonlinear manifold learning for early warnings in financial markets. *Eur. J. Oper. Res.* **2017**, *258*, 692–702. [CrossRef]
7. Zhao, Y.; Zhao, H. A hybrid machine learning framework by incorporating categorical boosting and manifold learning for financial analysis. *Intell. Syst. Appl.* **2025**, *25*, 200473. [CrossRef]
8. Samal, A.; Pharasi, H.K.; Ramaia, S.J.; Kannan, H.; Saucan, E.; Jost, J.; Chakraborti, A. Network geometry and market instability. *R. Soc. Open Sci.* **2021**, *8*, 201734. [CrossRef]
9. Yen, P.T.W.; Xia, K.; Cheong, S.A. Understanding changes in the topology and geometry of financial market correlations during a market crash. *Entropy* **2021**, *23*, 1211. [CrossRef]
10. Rai, A.; Nath Sharma, B.; Rabindrajit Luwang, S.; Nurujjaman, M.; Majhi, S. Identifying extreme events in the stock market: A topological data analysis. *Chaos Interdiscip. J. Nonlinear Sci.* **2024**, *34*, 103106. [CrossRef]
11. Kulkarni, S.; Pharasi, H.K.; Vijayaraghavan, S.; Kumar, S.; Chakraborti, A.; Samal, A. Investigation of Indian stock markets using topological data analysis and geometry-inspired network measures. *Phys. A Stat. Mech. Its Appl.* **2024**, *643*, 129785. [CrossRef]
12. Akgüller, Ö.; Balcı, M.A.; Batrancea, L.M.; Gaban, L. Network Geometry of Borsa Istanbul: Analyzing Sectoral Dynamics with Forman–Ricci Curvature. *Entropy* **2025**, *27*, 271. [CrossRef] [PubMed]
13. Ismail, M.S.; Noorani, M.S.M.; Ismail, M.; Razak, F.A.; Alias, M.A. Early warning signals of financial crises using persistent homology. *Phys. A Stat. Mech. Its Appl.* **2022**, *586*, 126459. [CrossRef]
14. Akingbade, S.W.; Gidea, M.; Manzi, M.; Nateghi, V. Why topological data analysis detects financial bubbles? *Commun. Nonlinear Sci. Numer. Simul.* **2024**, *128*, 107665. [CrossRef]
15. Baitinger, E.; Flegel, S. The better turbulence index? Forecasting adverse financial markets regimes with persistent homology. *Financ. Mark. Portf. Manag.* **2021**, *35*, 277–308. [CrossRef]
16. de Jesus Jr, L.C.; Fernández-Navarro, F.; Carbonero-Ruz, M. Enhancing financial time series forecasting through topological data analysis. *Neural Comput. Appl.* **2025**, *37*, 6527–6545. [CrossRef]
17. Sandhu, R.S.; Georgiou, T.T.; Tannenbaum, A.R. Ricci curvature: An economic indicator for market fragility and systemic risk. *Sci. Adv.* **2016**, *2*, e1501495. [CrossRef]
18. Shu, M.; Wang, C.; Liu, F.; Zhang, Y.; Wang, S. The Risk Transmission Mechanism of Global Stock Markets from the Perspective of Entropy-Riemann Geometry: Theoretical Construction and Empirical Analysis. *Comput. Econ.* **2025**, 1–36. [CrossRef]
19. Taylor, S. Clustering financial return distributions using the Fisher information metric. *Entropy* **2019**, *21*, 110. [CrossRef]
20. Xu, C.; Lin, H.; Fang, X. Manifold feature index: A novel index based on high-dimensional data simplification. *Expert Syst. Appl.* **2022**, *200*, 116957. [CrossRef]
21. Khashanah, K.; Yang, H. Evolutionary systemic risk: Fisher information flow metric in financial network dynamics. *Phys. A Stat. Mech. Its Appl.* **2016**, *445*, 318–327. [CrossRef]
22. Sreejith, R.P.; Mohanraj, K.; Jost, J.; Saucan, E.; Samal, A. Forman curvature for complex networks. *J. Stat. Mech. Theory Exp.* **2016**, *2016*, 063206. [CrossRef]
23. Samal, A.; Sreejith, R.; Gu, J.; Liu, S.; Saucan, E.; Jost, J. Comparative analysis of two discretizations of Ricci curvature for complex networks. *Sci. Rep.* **2018**, *8*, 8650. [CrossRef] [PubMed]
24. Wang, X.; Zhao, L.; Zhang, N.; Feng, L.; Lin, H. Stability of China's stock market: Measure and forecast by Ricci curvature on network. *Complexity* **2023**, *2023*, 2361405. [CrossRef]
25. Srinivasan, B. Intrinsic Geometry of the Stock Market from Graph Ricci Flow. *arXiv* **2025**, arXiv:2510.15942.

26. Guo, H.; Ming, Z.; Xing, B. Topological data analysis of Chinese stocks' dynamic correlations under major public events. *Front. Phys.* **2023**, *11*, 1253953. [CrossRef]
27. Bhattacharjee, B.; Maiti, M. A Study on the Topological Insights and Network Visualization Mapping of the Indian Equity Market. *Risks* **2025**, *13*, 76. [CrossRef]
28. Wu, F. Stock market integration in East and Southeast Asia: The role of global factors. *Int. Rev. Financ. Anal.* **2020**, *67*, 101416. [CrossRef]
29. Huang, C.; Zhao, X.; Su, R.; Yang, X.; Yang, X. Dynamic network topology and market performance: A case of the Chinese stock market. *Int. J. Financ. Econ.* **2022**, *27*, 1962–1978. [CrossRef]
30. Younis, I.; Longsheng, C.; Basheer, M.F.; Joyo, A.S. Stock market comovements among Asian emerging economies: A wavelet-based approach. *PLoS ONE* **2020**, *15*, e0240472. [CrossRef]
31. Das, S.R.; Kalimipalli, M.; Nayak, S. Banking networks, systemic risk, and the credit cycle in emerging markets. *J. Int. Financ. Mark. Institutions Money* **2022**, *80*, 101633. [CrossRef]
32. Işlak, Ü.; Temoçin, B.Z. Network Analysis of BIST 100: Crisis Precursors and Influential Nodes. *Comput. Econ.* **2025**, 1–28. [CrossRef]
33. Şükrüoğlu, D. Effects of COVID-19 on the BIST 100 network structure. *Appl. Econ.* **2022**, *54*, 5991–6007. [CrossRef]
34. Derindere Köseoğlu, S. Understanding systemic risk dynamics and economic growth: Evidence from the Turkish banking system. *Sustainability* **2023**, *15*, 14209. [CrossRef]
35. Kuzubaş, T.U.; Ömercikoğlu, I.; Saltoğlu, B. Network centrality measures and systemic risk: An application to the Turkish financial crisis. *Phys. A Stat. Mech. Its Appl.* **2014**, *405*, 203–215. [CrossRef]
36. Hadi, D.M.; Karim, S.; Naeem, M.A.; Lucey, B.M. Turkish Lira crisis and its impact on sector returns. *Financ. Res. Lett.* **2023**, *52*, 103479. [CrossRef]
37. Pauly, M.; Gross, M.; Kobbelt, L.P. Efficient simplification of point-sampled surfaces. In Proceedings of the IEEE Visualization, VIS 2002, Boston, MA, USA, 27 October–1 November 2002; IEEE: Piscataway, NJ, USA, 2002; pp. 163–170.
38. Tenenbaum, J.B.; Silva, V.d.; Langford, J.C. A global geometric framework for nonlinear dimensionality reduction. *Science* **2000**, *290*, 2319–2323. [CrossRef]
39. Levina, E.; Bickel, P. The earth mover's distance is the mallows distance: Some insights from statistics. In Proceedings of the Eighth IEEE International Conference on Computer Vision, ICCV 2001, Vancouver, BC, Canada, 7–14 July 2001; IEEE: Piscataway, NJ, USA, 2001; Volume 2, pp. 251–256.
40. Zhang, Z.; Zha, H. Principal manifolds and nonlinear dimensionality reduction via tangent space alignment. *SIAM J. Sci. Comput.* **2004**, *26*, 313–338. [CrossRef]
41. Newman, M. *Networks*; Oxford University Press: Oxford, UK, 2018.
42. Forman. Bochner's method for cell complexes and combinatorial Ricci curvature. *Discret. Comput. Geom.* **2003**, *29*, 323–374. [CrossRef]

Disclaimer/Publisher's Note: The statements, opinions and data contained in all publications are solely those of the individual author(s) and contributor(s) and not of MDPI and/or the editor(s). MDPI and/or the editor(s) disclaim responsibility for any injury to people or property resulting from any ideas, methods, instructions or products referred to in the content.